Conowingo Pond Mass Balance Model

Exelon Generation Company, LLC
300 Exelon Way
Kennett Square, Pennsylvania

June 2017

Authorship and Acknowledgements

The primary author of this report is James Fitzpatrick (HDR). Other contributors include Nataliya Kogan, Mark Velleux, James Hallden, and Carmen Santos (HDR). Sediment nutrient flux, sediment nutrient composition, and sediment diagenesis data were provided by Dr. Jeffrey Cornwell and Mike Owens (UMCES) with funding support from Exelon. HSPF simulation results were provided by Dr. Gopal Bhatt (Pennsylvania State University and Chesapeake Bay Program). Data analysis and modeling efforts benefited from discussions with Drs. Jeffrey Cornwell and Jeremy Testa (UMCES), Dr. James Martin (University of Mississippi), Dr. Damian Brady (University of Maine), and Dr. Carl Cerco (USACE-ERDC).

The author gratefully acknowledges review comments from Drs. James Martin and Damian Brady.

Contents

Tables

Figures

1 Introduction

The deeper regions of the mainstem Chesapeake Bay (the Bay) have experienced persistent summer hypoxia (less than 2 mg O_2/L) or anoxia (0 mg O_2/L) for several decades that has been attributed to a combination of excessive nutrients (Hagy et al., 2004, Kemp et al., 2005) and vertical stratification of the water column arising from density driven flows (Boicourt, 1992; Pritchard and Schubel, 2001; Murphy et al., 2011). In order to limit the temporal and spatial extent of this hypoxia and anoxia, the USEPA Chesapeake Bay Program, a collective state-federal partnership, has been implementing one of the nation's most extensive total maximum daily load (TMDL) program, since 2010 (USEPA, 2010; Linker et al., 2013). Efforts have been made to reduce watershed-wide excess loadings of nutrients and sediments from wastewater facilities, urban and suburban stormwater runoff, agricultural operations, atmospheric deposition, septic systems, and other sources.

The Susquehanna River is the largest of the nine major tributaries that discharge to the Bay (Hagy et al., 2004; Murphy et al., 2011) and drains portions of New York, Pennsylvania, and Maryland. The river empties into the northern most portion of the Bay and provides more than half of the freshwater flow to the estuarine system (Schubel and Pritchard, 1986). It also provides a significant fraction of the non-tidal total nitrogen (TN), total phosphorus (TP) and suspended sediments (SS) load to the Bay. The lower portion of the Susquehanna River includes a three reservoir system (Figure 1), which was constructed in the early 20th century to generate hydroelectric power. These reservoirs include, from upstream to downstream, Lake Clarke (impounded by the Safe Harbor Dam), Lake Aldred (impounded by the Holtwood Dam), and Conowingo Pond (impounded by Conowingo Dam). Recently, it has been suggested that this reservoir system is not trapping nutrients and sediments as effectively as it had in the past as it approaches its sediment storage capacity (Langland, 1998; Zhang et al., 2013; Langland, 2015; Zhang et al., 2016). It has also been suggested that additional sediment and phosphorus loadings, associated with high flow events such as Tropical Storm Lee, are being delivered to Chesapeake Bay (Hirsch, 2012). These additional scour loadings, when combined with loadings based on the 2010 TMDL, have been estimated to result in the non-attainment of Chesapeake Bay water quality standards (WQS) for dissolved oxygen (USACE, 2015; Cerco and Noel, 2016; Linker et al., 2016).

However, the estimated dissolved oxygen non-attainment due to sediment and nutrient scour may not be correct due to uncertainty in the bio-available fraction of the nutrients that are scoured. The Bay modeling framework, Water Quality and Sediment Transport Model (WQSTM) (Cerco et al., 2010), used in the WQS attainment assessment (USACE, 2015), includes particulate and dissolved organic and inorganic nutrient (carbon, nitrogen and phosphorus) forms as well as a sediment nutrient diagenesis and sediment flux model (DiToro, 2001). The sediment diagenesis and nutrient flux model (SFM) considers three pools or classes of reactivity for particulate organic nutrients in the sediment bed. The distinction between the pools represents a discretization to estimate the actual continuity of diagenesis, similar to the "G-model" of Westrich and Berner (1984).

Historically, these three pools of reactivity in the SFM included: labile or G_1 (with a reaction rate of 0.01 day^{-1} at 20 °C), refractory or G_2 (with a reaction rate of 0.0018 day^{-1} at 20 °C) and inert or G_3. The water column also includes labile (with a reaction rate of 0.12 day^{-1} at 20 °C) and refractory (with a reaction rate of 0.005 day^{-1} at 20 °C) particulate organic pools. The model framework further assumed that when non-algal labile particulate organic nutrients settle to the sediment bed they are split between the labile (65%), refractory (20%), and inert (15%) pools and that when non-algal refractory particulate organic nutrients settle to the sediment bed they are split between the refractory (57%) and inert (43%) pools. For the 2010 TMDL, the Chesapeake Bay Program took a relatively simple approach with respect to the composition of non-algal particulate organic nutrients and assumed that all above fall-line non-algal particulate organic nutrients, including scoured particulate organic nutrients, were refractory in form.

The question arises, "What is the real reactivity of the material being scoured from the sediment bed?" This is a valid question, since depending upon the time intervals between storms and the depth of scour or erosion it may be that a significant portion of the scoured material may be inert (G_3) or less reactive than the refractory or G_2 pool. For example, if the time interval between major flow events, which result in sediment scour, is say five years, and the burial rate of organic nutrients is 2 cm/year, then only about 4% of the organic nutrients below a 10 cm depth would be refractory or G_2 with no labile or G_1 matter; in other words, 96% of the organic nutrients below 10 cm would be inert or G_3. If the scour event resulted in greater than 10 cm of erosion, then the scoured inert material found below this depth would be treated as refractory while in the water column and 57% of this material would be put into the refractory pool of the SFM once it settles to the sediment bed; thus transforming inert organic nutrients into bio-available nutrients.

In the development and calibration of the original sediment flux model (DiToro and Fitzpatrick, 1993), it was assumed that the G_3 organic nutrients in the sediment bed were inert. This assumption appeared to provide a favorable calibration to the observed sediment oxygen demand, inorganic nutrient fluxes and particulate organic nutrient concentrations in the sediment bed. However, with the issue of sediment and nutrient scour from the Lower Susquehanna River Reservoir System, the assumption concerning the reactivity or bio-availability of the G_3 pool of sediment organic nutrients has been called into question. In addition, the assumption concerning the composition (G_1, G_2, and G_3 carbon, nitrogen and phosphorus) of the scoured nutrients entering the water column in Conowingo Pond and being transported out of Conowingo Pond into Chesapeake Bay has been called into question.

2 Methods

In order to investigate these questions, the Exelon Generation Company (Exelon) provided funding to support field and laboratory studies of Conowingo Pond sediments, including measurements of sediment oxygen demand and nutrient fluxes, sediment bed solid-phase composition, pore water concentrations and nutrient diagenesis and the development of a Conowingo Pond Mass Balance Model (CPMBM). Data from field and laboratory studies were provided by Dr. Jeffrey Cornwell and Mr. Michael Owens

(pers.comm.) from the University of Maryland Center for Environmental Science (UMCES). The details of the field and laboratory methodologies are documented elsewhere (Cornwell et al., 2014).

2.1 Conowingo Pond Mass Balance Model (CPMBM)

The CPMBM is comprised of two separate, but coupled models: ECOMSED, which is a hydrodynamic/sediment transport model and RCA, a generalized water quality model developed by HDR, Inc. (Isleib and Thuman, 2011; Zhang and Li, 2011; Testa et al., 2014). The RCA water quality model includes a two-layer sediment diagenesis and nutrient flux submodel (SFM) and is described in detail elsewhere (DiToro, 2001; Brady et al., 2013; Testa et al., 2013).

The SFM considers a 10 cm active depth that includes two layers, which represent the near-surface aerobic and underlying anaerobic environments and simulates the cycling of carbon, dissolved oxygen, nitrogen, phosphorus, silica, and sulfur. In this application, the SFM was modified so that under the 10 cm active depth, there is an archive stack that is comprised of another one-hundred-forty 1 cm slices for a depth of 1.5 meter. Below the 1.5 meter active and archive stack is a completely mixed deep bed layer that is 3 meters in depth for a total sediment depth of 4.5 m. The SFM was also modified to account for changes in the depth of the active layer and the exchange of nutrients between the active layer and the archive stack and deep bed layer based on deposition and erosion of sediments as determined from the ECOMSED hydrodynamic/sediment transport model. If the deposition of solids results in the depth of the active layer equaling or exceeding 10.5 cm, then 1 cm of mass of nutrients (G_1, G_2, and G_3 particulate organic, and dissolved inorganic nutrients) and oxygen demanding end-products (hydrogen sulfide and methane) are removed from the active layer and placed at the top of the archive stack (layer 1). The remaining layers are then moved down one-level in the archive stack. The bottom layer of the stack (layer 140) is then moved down into the deep bed layer, using a mass balance approach. The active layer is then reduced by 1 cm. This process continues as long as deposition from the water column to the sediment bed persists.

Erosion is the reverse of deposition. If erosion results in the active layer being reduced to 9.5 cm or less, then the mass of nutrients (G_1, G_2, and G_3 particulate organic, and dissolved inorganic nutrients) and oxygen demanding end-products (hydrogen sulfide and methane) in the surface 1 cm layer of the archive stack are moved into the active layer, using a mass balance approach and the depth of the active layer is increased by 1 cm. The remaining layers of the archive stack are moved upwards and 1 cm of mass of nutrients and oxygen demanding end-products are moved from the deep bed into the bottom layer of the archive stack. This process also continues as long as erosion occurs. The deep bed layer provides a reserve of organic and inorganic nutrients to allow the model to continue running should more than 1.5 meters of erosion (the 10 cm active layer and the one- hundred-forty 1 cm layers of the archive stack) occur within a model grid cell. Diagenesis also continues to occur in each layer of the archive stack, reducing the concentrations of particulate organic matter and increasing the concentrations of inorganic nutrients and oxygen-demanding end-products. Diagenesis

is assumed not to occur in the deep bed (i.e., the organic nutrients are treated as conservative variables in the deep bed). This is a conservative assumption and, in part , allows a G3 pool to remain at depth and available to be re-introduced into the archive stack if needed and, in part, recognizes that additional less reactive G-pools might be present at depth and prevents the model from computing unrealistically low values of particulate organic matter (POM) at depth.

The water column portion of the CPMBM is driven by changes in water elevation, advective flows and mixing as determined by the ECOMSED hydrodynamic model. Nutrient loadings entering Conowingo Pond from Lake Aldred, via the Holtwood Dam, and from Muddy Creek and Broad Creek are provided by the USEPA Chesapeake Bay Program Office (CBPO) watershed model (Phase 6, Beta 2, Gopal Bhatt, pers.comm.); an estimate of nutrients loadings for the ungauged portion of the Conowingo Pond watershed was made using information from Muddy Creek and Broad Creek. A conceptual diagram of the CPMBM is shown in Figure 2.

2.2 Data Sources and Analysis

2.2.1 Early Studies – 1981-1984

While there have been numerous studies concerning sediment transport around the three reservoir system, there have been relatively few programs that have sampled water column nutrients, sediment nutrient composition, sediment oxygen demand, sediment nutrient flux, and sediment nutrient deposition within the reservoir system. Some of the earliest studies were performed by researchers from the Academy of Natural Sciences and the University of Maryland. These studies provided estimates of plankton metabolism (water column photosynthesis and respiration), sediment oxygen demand, using darkened plexiglass chambers and corrected for phytoplankton respiration, and particulate carbon, nitrogen and phosphorus during the summers of 1981 and 1982. Station mean SOD rates ranged from 1.08 gm O_2/m^2-day in August 1981 to 2.75 gm O_2/m^2-day in June 1981 and averaged 2.17 gm O_2/m^2-day across all stations over the sampling period June 23, 1981 to September 1, 1981 (Sanders et al., 1982a). Average carbon, nitrogen, and phosphorus content of the sediments (expressed as a percentage of sediment dry weight) were 4.01%, 0.34%, and 0.14%, respectively (Sanders et al., 1982a). Estimates of mean SOD were 1.71 gm O_2/m^2-day and 1.62 g O_2/m^2-day for the two stations sampled in August 1982 (Sanders et al., 1982b). The latter study also made estimates of oxygen transfer across the air/water interface using a floating dome device. Reported values of the diffusion coefficient ranged from 0.19-3.12 g O_2/m^2-hr, averaged 1.31 gm O_2/m^2-hr, and were found to vary with wind speed. Sanders et al. (1982b) reported that their values were low compared to a previous study, but noted that maximum average wind velocities in 1982 did not exceed 5 m/sec in 1982.

Boynton et al. (1984) studied seston dynamics, using sediment trap arrays, in the three reservoir system in late September-early October of 1983 and in June of 1984. They note in their report that the estimates from the sediment trap experiments are vertical fluxes of particulates to the depth beneath the water surface at which the collecting cup(s) were suspended, rather than the estimates of flux to the sediment surface.

However, they did make deposition rate estimates by assuming that the surface and mid-depth collecting cups on each array collected newly depositing material rather than locally resuspended material undergoing resuspension-depositional cycling. Based on this assumption, their reported values of deposition within the reservoir ranged from 1.4-2.6 gm C/m^2-day, 0.158-0.251 gm N/m^2-day, and 0.0496-0.0847 gm P/m^2-day of carbon, nitrogen, and phosphorus, respectively in September of 1983 and 0.24-0.78 gm C/m^2-day, 0.038-0.080 gm N/m^2-day, and 0.0088-0.0143 gm P/m^2-day of carbon, nitrogen, and phosphorus, respectively in June 1984.

2.2.2 Maryland Department of Natural Resources – 1989

In 1989 researchers from Oak Ridge National Laboratory, Maryland Department of Natural Resources and Versar, Inc. took several cores within Conowingo Pond. Using these cores, they developed estimates of rates of sediment accretion in Conowingo Pond from vertical profiles of weapons-test Cs-137, nuclear power plant-related Cs-134, and naturally derived PB-210 (McLean et al., 1991). Net accretion rates ranged from about 2 cm/yr downstream of a nuclear power plant cooling tower, just below the mid-point of the Pond, to a high of 7 cm/year at the mouth of Broad Creek, in the lower third of the reservoir.

2.2.3 Susquehanna River Basin Commission - 2000

With funding provided by the Chesapeake Bay Commission and the Pennsylvania Department of Environmental Protection, the Susquehanna River Basin Commission (SRBC) conducted a study of the sediments behind the three dams on the Lower Susquehanna River (Edwards, 2006). Sampling and analyses were conducted as part of a multi-disciplinary effort in cooperation with the U.S. Geological Survey (USGS), Maryland Geological Survey (MGS), and UMCES.

Sediment samples were collected from 34 cores in the reservoirs behind the three lower Susquehanna River dams (Figure 3); 22 of the cores were collected in Conowingo Pond. The cores were then partitioned into surface, middle, and bottom portions. Shallow box cores, of about 20 centimeters (8 inches) deep, were collected and analyzed for phosphate associations and mobility in and out of the sediments. Of interest to this project, the deeper cores were analyzed for particle size (sand-silt-clay and coal fractions), X-rayed for composition of the various layers, and tested for nutrients (total carbon, total nitrogen and total phosphorus). Initially, we planned on utilizing these sediment bed carbon (C), nitrogen (N) and phosphorus (P) data to calibrate the CPMBM. However, after performing data analysis, we concluded that we would only be able to use the N and P data. The fact that the three reservoirs have large pools or lenses of coal within the sediment bed did not allow us to develop a consistent picture of the organic carbon content of the sediment despite the estimates of sediment bed coal content made by the MGS and UMCES team.

Figure 4 presents plots of the percent coal, % total C:% total N, % total C:% total P, and %total N:% total P ratios versus percent total C for each of the three reservoirs. These plots also show a general trend line of the data as well as the standard Redfield ratios on

a weight basis. The top panel of Figure 4 shows that, in general, the percent coal increases with the percent of bed carbon. However, there is considerable variation around the trend line, with the percent coal often varying by factors of 10-20 for a given percent carbon. For Lake Clarke and Conowingo Pond, % TC:% TN ratios generally exceed the Redfield ratio of 5.68 by factor of 5-10 at high percent C values (>10 %C), but are generally close to the Redfield ratio value for percent C values of 5 or less. Similarly, the % TC:% TP ratios observed in Lake Clarke and Conowingo Pond exceed the Redfield ratio by factors of 5-10 for % C greater than 15, but are in the Redfield range for % C less than 10. The % TN:% TP ratios for Lake Clarke and Conowingo Pond are generally less than the Redfield ratio across the range of bed carbon, but the variability is considerably less than observed in % TC:% TN and % TC:% TP ratios. A potential reason for values less than the Redfield ratio for %TN:%TP is due to processes of nitrification and denitrification that occur in the sediment bed that produces N_2 gas, which escapes from the sediment, and lowers bed nitrogen content. No such pathway exists for phosphorus.

Interestingly, the sediment nutrient content of Lake Aldred differs from that observed in Lake Clarke and Conowingo Pond. This is more clearly illustrated in Figure 5, which presents plots of % TN, Total P (ug/g), % iron (Fe) versus sediment bulk density and Total P versus % Fe for near surface sediments (< 20 cm) and all depths, together with trend lines of the data. In all three reservoirs there is a clear trend between increasing bulk density and decreasing % TN, Total P and % Fe. One can also note that bulk densities range from 1.33-1.97 gm/cm^3 in Lake Clark, to 1.58-2.38 gm/cm^3 in Lake Aldred, to 1.25-1.83 gm/cm^3 in Conowingo Pond. Also of interest is the high correlation between Total P and % Fe. This relationship suggests that phosphorus is retained in the sediment bed under conditions of high concentrations of iron. This is likely due to either precipitation of phosphate containing minerals (Troup, 1974), such as vivianite, $Fe_3(PO_4)_2$(s), or by partitioning to phosphate sorption sites.

The data were also reviewed to determine if there were consistent vertical patterns observed in the nutrients. The data do not appear to have a consistent vertical pattern, i.e., constant in the vertical or monotonically increasing or decreasing, as shown in Figure 6 (for sediment cores 1, 2, 3, and 36). This may be due to the layering of coal within the cores or due to non-consistent patterns of deposition and erosion.

2.2.4 University of Maryland Center for Environmental Science – 2015-2016

The next large source of data has been made available by researchers from UMCES with funding provided by Exelon and under management of Gomez and Sullivan Engineers, D.P.C. These data included field and laboratory measurements of sediment bed solid-phase composition, sediment oxygen demand and nutrient fluxes (ammonium (NH_4), nitrate+nitrite (NO_x), denitrification (N_2), and soluble reactive phosphorus (SRP), pore water (NH_4), SRP concentrations and nutrient diagenesis (Cornwell and Owens, pers.comm.).

Similar to what was observed in the SRBC field data, vertical profiles of nutrients collected and analyzed by UMCES did not show a consistent vertical pattern. This is

illustrated in Figure 7 for PIP and TP. Similar irregular vertical patterns were also observed for carbon and nitrogen.

Flux measurements using sediment box cores were made at thirteen sites (with duplicate cores at three of the sites) in Conowingo Pond in May of 2015. In July and September, 2015 eight of the original sites were revisited and duplicate cores were taken at each site, in December of 2015 six sites were revisited with duplicate cores taken at each site. Finally, in April 2016 the eight sites that were visited in July and September, 2015 were re-occupied and duplicate cores were taken as each site. In addition, in April 2016, three sites (with duplicate cores) each in Lakes Clarke and Aldred were sampled. A summary of the observed data are presented in Table 1. Profiles (six depths) of near surface pore water NH_4, SRP and Fe were obtained from four of the cores collected for the flux measurements during the May, July, December 2015 and April 2016 surveys and for two of the cores from the September survey. Generally, the concentrations of pore water NH_4, SRP and Fe increased going down core. The greatest increases on a percent basis were observed for SRP and Fe. This is likely due to the formation of iron oxides in the aerobic layer and enhanced partitioning of SRP to these iron oxides.

Measurements of solid phase C and N were obtained for the surface (0-1 cm) from the flux cores. Not every flux core was analyzed for every survey. The fewest cores analyzed were for the December 2015 survey, while the remaining cores had measurements from twelve or thirteen cores. Lake Clarke and Lake Aldred also had measurements of the surface (0-1 cm) from the cores used to determine fluxes for April 2016. Survey averaged surface TC ranged from a low of 4.56 % to a maximum of 5.51 %, with an average of 5.13 %, while survey averaged surface TN ranged from a low of 0.29 % to a maximum of 0.35 %, with an average of 0.32 %. The TN were 0.31 % and 0.28 %, respectively. In August 2015, five long cores (≥ 300 cm) were analyzed for C and N. Ten centimeter subcores were draw from the long cores (5-15, 25-35, 45-55, 75-85, 95-105, 145-155, 205-215, and 265-275 cm). Survey average TC ranged from 5.76 to 8.28 %, while TN ranged from 0.25 to 0.38 %.

UMCES performed diagenesis experiments on five long cores, in order to obtain estimates of the reactivity of C, N and P in the long cores. These diagenesis experiments were conducted over a period of 252 days and generally provided six data points over the course of the experiments from which linear regression analysis was performed. However, after discussions with Dr. Cornwell (pers.comm.) it was concluded that the P diagenesis results were not useful. Apparently, the formation of SRP from the diagenesis of organic P was quickly partitioned onto the solids within the sample vial and there was virtually no increase in pore water SRP. Also, there are some reservations about the carbon diagenesis data as well. The TCO_2 observed during the time-course of the diagenesis experiments was extremely variable and resulted in negative regression slopes (Figure 8) for about half of the time-series. We assumed that all negative slopes were equivalent to zero when generating average diagenesis for G_3 carbon. Diagenesis results for organic nitrogen were much better behaved (Figure 9). Only four out of the twenty-two experiments resulted in negative slopes for NH_4 production. The overall average diagenesis rate from the organic nitogen-NH_4 production is 6.4×10^{-5} umol/g-day, while for organic carbon-TCO_2 it is 2.9×10^{-4} umol/g-day (Table 2). However, if one

removes two of the carbon regression estimates that exceed the G_2 diagenesis rate of $1.8x10^{-3}$, umol/g-day the rate would be $7.0x10^{-5}$ umol/g-day. Based on this data analysis, we have chosen a value of $6.5x10^{-5}$ umol/g-day, which lies between the estimates of G3-diagenesis for organic nitrogen and organic carbon, going forward in the modeling effort.

UMCES also conducted diagenesis experiments on four of the flux cores taken in September 2015. The diagenesis experiments utilized the top two centimeters from each core and would be thought to include G_1, G_2 fractions or organic matter as well as a fraction of G_3. However, given the limited number of samples (5-6) it would not be able to discern the three fractions nor their reactivity rates. Rather, we used a non-linear optimization model to estimate an average reaction rate for the surface layer and a fraction of the total C or total nitrogen that was metabolized during the course of the 249 diagenesis experiments. The non-linear model is similar to that used by Burdige (1991):

$$\frac{dC_i}{dt} = \frac{k_i f_i POM_i}{1+K_i} \quad (1)$$

Where:

C_i = is the concentration of TCO_2 or NH_4 in solution,

T = is time,

k_i = is the first order reaction rate,

f_i = is the fraction metabolizable carbon or nitrogen, and

POM_i = is the concentration of carbon or nitrogen in the sediment.

This equation can be solved by assuming $C_i = C_{0,I}$ at t=0., yielding

$$C_c = C_{0,c} + f_i POC(1 - e^{-k_C t}) \quad (2)$$

for carbon ($K_i = K_C$ = zero for carbon) and

$$C_{cN} = C_{0,N} + \frac{f_i PON}{1+K_N}(1 - e^{-k_C t}) \quad (3)$$

for nitrogen ($K_i = K_N$ = 1 for ammonium). For PON we utilized the observed TN reported by UMCES from the flux cores (0-1 cm); due to concerns of the presence of coal in the surface sediments, for POC we multiplied the observed TN reported by UMCES from the flux cores (0-1 cm) by 8. We then used a non-linear pattern search routine to fit two parameters, f_i and k_i. We also used variable initial parameter estimates for the pattern search routine to see if the routine found a "universal" solution or to see if the initial estimates resulted in finding different local minima. In only three of the sixteen parameter fits for C were the solutions relatively close to one another (fraction metabolizable and reaction rates were within a factor of two or less), while in ten of the sixteen parameter fits for N, the solutions were virtually the same (Figure 10 as an example) and two others the parameters were within a factor of two (Figure 11 as an example). For many of those cases where the pattern search routine failed to converge

on a single solution, the pattern search traded off between the fraction metabolizable nitrogen versus the reaction rate. Table 3 reports the means and standard deviations of those cores for which the parameter fits were relatively close together.

Interestingly, the fraction metabolizable for carbon was much smaller than that for nitrogen and the reaction rate for carbon was larger than the reaction rate for nitrogen. This is opposite to what was found by Burdige (1991) for lower Chesapeake Bay surface (0-2 cm) sediments. Burdige found an average diagenesis rate of 2.7 /yr for carbon (range 0.51-8.1 /yr) and an average fraction metabolizable of 16.5 % (range 2-44%) for carbon. For nitrogen Burdige found an average diagenesis rate of 7.9 /yr (range 3.4-14.6 /yr) versus an average of 2.5 /yr (range 0.8-4.1 /yr) for Conowingo Pond nitrogen. Burdige also found an average fraction metabolizable of 17.2 % (range 4-38 %) versus an average of 15.8 % (range 3.9-35.9 %) for Conowingo Pond. Burdige's nitrogen diagenesis rate of 7.9 /yr corresponds to a reaction rate of 0.022 /day, which lies between the G_1 and G_2 diagenesis rates of 0.035 /day and 0.0018 /day, respectively, developed by DiToro and Fitzpatrick (1993) for the Chesapeake Bay SFM, while the Conowingo diagenesis rate of 2.5 /yr corresponds to a value of 0.0064 /day. The Conowingo Pond rate likely represents a blend of G1 and G2 material and since it is closer to the G2 rate estimated by DiToro and Fitzpatrick may suggest a slightly greater percentage of G2 in Conowingo Pond sediments, hence the lower blended rate.

Given that only three of sixteen parameter fits for carbon were found to be "acceptable", we cannot make a statement of how Conowingo Pond sediment carbon might differ or be similar to Chesapeake Bay sediment carbon. For nitrogen, however, with fourteen out of sixteen parameter fits being "acceptable", it appears that the fraction of nitrogen that is metabolized appears similar. However, it appears as if the Conowingo diagenesis rate is lower than the Chesapeake Bay rate. Since, the diagenesis experiments are estimating a blended reactivity rate (i.e., a mix of G_1 and G_2), these results may imply that there is a slightly greater percentage of G_2 material in Conowingo Pond sediments, hence the lower blended rate.

2.3 Application of the Stand-Alone SFM

While awaiting the development and calibration of the hydrodynamic/sediment transport model, it was decided to conduct some initial water quality simulations on Conowingo Pond using a stand-alone version of SFM. The stand-alone SFM treats the Conowingo Pond sediment bed as one model cell or segment and only includes the 10 cm active layer. The SFM does not consider erosional events, but rather treats Conowingo Pond as net depositional. As described elsewhere (DiToro, 2001; Brady et al., 2013; Testa et al., 2013), the SFM considers the deposition of organic matter from the water column to the sediment bed, the decomposition or diagenesis of the deposited organic matter and the flux of resulting end-products (SOD, NH_4, NO_x and SRP) back to the overlying water column. The SFM utilizes overlying water column temperature and concentrations of DO, NH_4, NO_x, and SRP as a boundary condition to the sediment bed and concentration gradients between the water column and pore water in the bed help to determine the flux of SOD and nutrients between the water column and the sediment bed.

To set up the stand-alone SFM it was necessary to develop water column concentrations of DO, NH_4, NO_x, and SRP and overlying water column temperature and to determine the fluxes of organic matter (C, N, and P) to the bed. For the water column concentrations, we used observed data from the USGS gaging station at Conowingo Dam (station 1578310) for the period 1996-2014. We averaged all January data (1996-2014) to obtain a long-term monthly average for January and repeated the process for each month of the year, February through December. Figure 12 presents the overlying water column temperature, nutrients and DO used as boundary conditions for the stand-alone SFM. We used the following procedure to determine fluxes of particulate organic matter (POM) from the water column to the sediment bed:

1. The USEPA provided output from the Chesapeake Bay watershed model (Phase 6, Beta 2) for Holtwood Dam (Lake Aldred), Muddy Creek, Broad Creek and Conowingo Dam (Conowingo Pond) for flow, NH_4, NO_x, SRP (or PO_4), particulate inorganic phosphorus (PIP), organic nitrogen (ORGN), organic phosphorus (ORGP), and phytoplankton carbon.

2. Using a protocol developed for the Chesapeake Bay Program by Carl Cerco (USACE, ERDC, pers.comm.) the water quality variables of interest were determined as follows:

    a. Correct ORGN and ORGP for the phytoplankton component, so as to compute detrital ORGN and ORGP:

        ORGN = ORGN – Phytoplankton carbon/5.67

        ORGP = ORGP - Phytoplankton carbon/40

    b. 60% of remaining ORGN is assigned to the dissolved pool (DORGN) and 40% of the remaining ORGN is then assigned to the particulate pool (PORGN)

    c. Dissolved organic carbon (DORGC) and particulate organic carbon (PORGC) are determined by multiplying the DORGN and PORGN pools by 8, i.e.,

        DORGC = 8 x DORGN

        PORGC = 8 x PORGN

    d. Compute a new phosphorus variable, P^*, as the sum of ORGP and PIP. Dissolved organic phosphorus (DORGP) is then assumed to be 22.6 % of P^* or

        $DORGP = 0.226 \times P^* = 0.226 \times (ORGP + PIP)$

    e. The remaining fraction, 0.774, is particulate and 58% is apportioned to PIP and 42% is apportioned to particulate organic phosphorus (POPGP) or

$$PIP = 0.58 \times 0.774 \times P^{*} = 0.58 \times 0.774 \times (ORGP + PIP)$$

$$PORGP = 0.42 \times 0.774 \times P^{*} = 0.42 \times 0.774 \times (ORGP + PIP)$$

3. We performed 90-day block average mass balances for POM (phytoplankton plus C, N, and P) and PIP around Conowingo Pond for each year of the simulation period (1996-2014) as follows:

   $$POM_{i,net} = POM_{i,Holtwood} + POM_{i,MuddyCreek} + POM_{i,BroadCreek} - POM_{i,Conowingo}$$

   where $POM_{i,net}$ = is the net mass balance for water quality variable i (phytoplankton, C, N, P and PIP) and Holtwood, Muddy Creek, and Broad Creek are the inputs and Conowingo is the export. If $POM_{i,net}$ is positive then that implies that there was more POM or PIP coming into Conowingo Pond than being exported and the assumption is that the excess POM or PIP was deposited to the sediment bed. This excess POM and PIP was then divided by the bottom surface area of the reservoir to obtain a flux of POM or PIP as gm/m^2-day.

4. With the water column boundary conditions and fluxes determined now all that remained was to assign the fractions of G_1, G_2, and G_3 to the non-phytoplankton POM and calibrate the model. The G_1, G_2 and G_3 fractions for detrital C, N, and P were calibrating variables. The G_1, G_2, and G_3 splits for phytoplankton were as developed for the SFM by DiToro and Fitzpatrick (1993):

	G_1	G_2	G_3
Carbon	0.65	0.20	0.15
Nitrogen	0.65	0.25	0.10
Phosphorus	0.65	0.20	0.15

A number of calibration runs were performed varying the non-phytoplankton POM G_1, G_2, and G_3 fractions before arriving at a reasonable calibration. However, given the lack of a multi-year calibration flux data set, there was some uncertainty as to which of the calibrated G-fractions provided the best calibration. Three sets of results will be presented below.

2.3.1 Calibration Results

We arrived at three sets of G-fraction coefficients that appeared to provide a good calibration to the available data. They are as follows:

Run 01		G_1	G_2	G_3
	Carbon	0.10	0.40	0.50
	Nitrogen	0.10	0.50	0.40
	Phosphorus	0.25	0.45	0.30

Run 02		G_1	G_2	G_3
	Carbon	0.15	0.35	0.50
	Nitrogen	0.15	0.45	0.40
	Phosphorus	0.30	0.40	0.30

Run 03		G_1	G_2	G_3
	Carbon	0.15	0.50	0.35
	Nitrogen	0.15	0.55	0.30
	Phosphorus	0.30	0.50	0.20

Essentially, the difference between the first two runs (Run 01 and Run 02) was to shift a little (5 %) G_2 POM into the G_1 POM pool. In the third run (Run 03), we shifted 10-15% of the G_3 pool to the G_2 pool. As will be shown below, there was not a significant difference between the results for Runs 01 and 02. First, the results for Run 01 will be presented in Figures 13-15. Figure 13 presents results for carbon and SOD for Run 01. Shown on the upper left panel are the model computations of carbon (algal, detrital or non-algal carbon and total carbon) deposition to the sediment bed. Also shown are the mean and range of the settlement trap data observed by Boynton et al. (1984) between June and October 1984. As seen on the plot there is quite a bit of year-to-year variability. However, for a number of years, the summer deposition provided from the simple mass balance from the USEPA watershed model is within the range of deposition report by Boynton et al.

The center left panel (Figure 13) shows the time history of G_1, G_2, G_3 and total organic carbon in the sediment bed and can be compared to observations from 1981 (Sanders et al., 1981), 2000 (Edwards, 2006) and UMCES (Cornwell, pers.comm.). As can be seen, the model computation of POC is about 1 %, while the data range between 3.5 and 25% carbon with a mean of about 7%. However, it is important to note that the presence of coal in these sediments may be biasing the percent carbon high in the data. The bottom left panel presents the total and pore water hydrogen sulfide in oxygen equivalents and is meant to be a diagnostic plot. Similarly, the next two panels, upper right – carbon diagenesis (sum of the G-reaction rates times the G-carbon present) and middle right – depth of the aerobic layer are also diagnostic plots. High rates of diagenesis are usually associated with high rates of deposition and the aerobic layer depths vary between about 1 and 3 mm with minima during the summer period and maxima during the winter period. Finally, the bottom right panel presents a comparison between the SFM computed SOD versus data from 1981/1982 (Sanders et al., 1982a, 1982b) and 2015/2016 (Cornwell, pers.comm.).

The model computations show the various contributions to the total sediment oxygen demand, carbonaceous, and nitrogenous (oxidation of ammonia nitrogen, flux of dissolved methane and flux of methane gas). It is possible that some of the methane gas that is fluxed may be oxidized as part of the measurement of SOD, so we are

including it in the comparison to the observed SOD. However, it is unlikely that the flux of methane gas would be oxidized and, therefore, will not be included in our discussion of the comparison of observed and computed SOD. If one compares the maxima of the computed CSOD+NSOD+J_{CH4-AQ} to the Sanders et al. (1994a, 1994b) and UMCES (Cornwell, pers.comm.) they compare favorably to the means of the August and September 1981 data, but are low compared to the mean of the August 1984 data. They are also slightly low compared to the May 2015, but compare reasonably well to the remaining 2015 and 2016 SOD data. One point worth noting though is that the water temperature in Conowingo Pond in May 2015 and the temperature at which the core incubations were conducted was 25 °C as compared to the temperature of 21 °C which the SFM model sees at a corresponding time. Given the temperature correction factors used for diagenesis rates in SFM that could account for about a 40-50 percent change in the computed SOD.

Figure 14 presents the results for the nitrogen component of the model. Starting in the upper left panel the algal, detrital and total particulate organic nitrogen (PON) deposition to the sediment bed are shown. Also shown are the mean and range of the 1984 settlement trap data observed by Boynton et al. (1984). There are some years where the model computed depositional fluxes compare favorably to the data, while for other years the model appears biased high. The second panel from the top left presents the G_1, G_2, G_3 and total organic nitrogen in the sediment bed and can be compared against data collected in 1981, 2000, and 2015. The model total organic nitrogen is about 0.1 %, which is low compared to the observed means in 1981, 2000, and 2015, values for which lie between 0.2 and 0.3 %. The next panel down on the left shows the overlying water column, aerobic and anaerobic pore water concentrations for NO_3 and is for diagnostic purposes. The bottom panel on the left shows the time-series of computed nitrate flux (J_{NO3}) and can be compared to the UMCES 2015/2016 data. Model computations of J_{NO3} are always into the sediment and range from about 15 to 50 mg N/m^2-day. Generally, these are within the range of the observed data, except that they are low compared to the May 2015 data and perhaps a little high compared to the means of the December 2015 and April 2016 observed data, both of which also report a few flux measurements from the sediment to the overlying water column. The top right panel shows the time-series of diagenesis of the organic nitrogen and it is correlated to the depositional fluxes of PON to the sediment bed. The second panel from the top right shows a time-series of overlying water column and aerobic and anaerobic layer pore water NH_4, which can be compared against the 2015/2016 UMCES pore water data from the flux and long cores. The anaerobic layer pore water NH_4 compares favorably to the observed 0.5-9 cm short core data and the observed pore water data from the long core (depths > 25 cm). The model computed aerobic layer NH_4 pore water is low compared to the 0.0-0.5 cm pore water data from the short cores, but this is likely due to the fact that the model computed aerobic layer depth is only a few millimeters in depth and, therefore, the 0-0.5 cm slice represents a combination of aerobic and anaerobic water and thus has a higher concentration of NH_4 in the pore water. The next panel (third down on the right) presents time-series plots of ammonium flux (J_{NH4}) computed by SFM and may be compared to the 2015/2016 UMCES data. Generally, the comparison is favorable, except for under-estimating the observed May 2015 mean J_{NH4}. As was noted

above for SOD, the incubation temperatures for the May 2015 flux measurements was 25 °C as compared to the SFM overlying water temperature of 21 °C, which could account for a 40-50 percent change in the computed NH_4 flux. Finally, the bottom right panel presents a time-series of the computed denitrification flux (J_{N2}), which represents a loss of nitrogen from the system due to the flux of nitrogen gas from the sediment through the water to the atmosphere. Generally, the computed J_{N2} lies within the range of the observed data collected by UMCES in 2015 and 2016.

Figure 15 presents the calibration results for the phosphorus component of the SFM. The upper left panel presents the time-series computations of the depositional flux of particulate organic phosphorus (algal and detrital) and particulate inorganic phosphorus (PIP) as well as Boynton's 1984 sediment trap data. As can be seen, the algal POP is the smallest component of the phosphorus deposition, with PIP the next largest component and detrital POP being the largest component of the total P flux to the sediment bed. Generally, the computed P flux to the bed is larger than that observed by Boynton in 1984. The middle panel on the left shows the three G-components and the total POP in the sediment bed; the average POP is between 0.025 and 0.03 percent. The bottom left panel shows the time-series of total P in the sediment bed and available data for comparison. The model indicates that the inorganic P is the larger component of the total bed P at between 0.115 and 0.12 percent, with POP between 0.025 and 0.03 percent, for a total P of between 0.14 and 0.155 percent. This compares favorably to the Sanders et al. 1981 estimates of between 0.13 and 0.145 percent and, while above the 2000 SRBC mean of 0.10%, is well within the observed range of 0.03 and 0.17 percent. However, the model over-estimates the UMCES measurements of inorganic P and TP. The model inorganic P appears to be a factor of two greater than the observed 2015 inorganic P data. If one were to correct the model computed inorganic P to match the observed inorganic P, then the model computed TP would be very close to the observed TP. A potential source of the excess inorganic P might be attributed to the deposition of PIP based on the USEPA/USACE watershed model loadings. .

The panel on the upper right (Figure 15) shows the time-series of diagenesis of the POP and is for diagnostic purposes. The middle right panel shows a time-series of overlying water column SRP or PO_4 and the available UMCES 2015/2016 data for comparison. The model computed long-term PO_4 concentration for the anaerobic layer is about 1050 ug P/L as compared to the UMCES 0.5-9 cm short core data which range from a low of about 70 ug/L to a high of about 1050 ug P/L, but with an average of all of the data of about 400 ug P/L or about a factor of two and a half times below the computed values. The over-estimation of the anaerobic PO_4 appears to be consistent with the over-estimation of inorganic P described above. Correcting the over-estimation of inorganic P would also help improve the calibration of anaerobic pore water PO_4. The aerobic layer model PO_4 concentration averages about 5 ug P/L, which is well below the observed 0.0-0.5 cm values of between 15 and 300 ug P/L. However, it is important to remember that the aerobic layer depth computed by the model is between 2 and 3 millimeters, while the data are for the 0.0-0.5 cm depth and would include a significant anaerobic layer thickness, which would result in a reduced level of iron oxides with which to sorb PO_4 and would result in increased PO_4 in the pore water. Finally, the bottom right hand panel shows the time-series of inorganic phosphorus flux (J_{PO4}) between the water column and

the sediment bed. The model computations show that J_{PO4} is always from the water column into the sediment bed. The SFM computed J_{PO4} is between 0 and about 6 mg P/m^2-day from the water column to the sediment bed. The model computations lie within the range of J_{PO4} reported by UMCES, but it is interesting to note that there were a few observations of P flux from the sediment to the overlying water column, although the survey means either indicated a zero flux or fluxes from the water column into the bed consistent with the model.

Figure 16 presents a comparison of the SFM computed fluxes for the three stand-alone SFM runs. The plots present the 19-year averages and maxima and minima of the fluxes from 1996 through 2014. The upper left panel compares the computed SOD with and without including the contribution of gaseous CH_4 release from the sediment. If one ignores the contribution of gaseous CH_4 to the SOD there is virtually no difference in the mean, minima, and maxima SOD between the three runs. The model slightly under-estimates the May 2015 UMCES SOD data by about 1 gm O_2/m^2-day but is within 0.5 gm O_2/m^2-day or less of the remaining data. Similarly, the other fluxes (nitrate-J_{NO3}, SRP or PO4-J_{PO4}, ammonium-J_{NH4} and denitrification flux-J_{N2}) are quite similar for the three sets of model coefficients, although the nitrogen fluxes are very slightly higher for RUN03. Comparing model vs. data, it is not obvious, which if any, set of coefficients can be considered to provide a better calibration. The other factor that might indicate a preference for one set of coefficients over the others is noting that for Run 03 the computed concentrations of POC and PON are slightly less (~23 and ~19 percent, respectively) than are computed for Runs 01 and 02 and thus Run 03 under-estimates the observed data slightly more than Runs 01 or 02.

2.4 CPMBM Setup

As mentioned above information concerning water elevations, water temperature, advective transport, vertical mixing, and changes in bed elevation are provided to CPMBM from the hydrodynamic/sediment transport model ECOMSED. This information is provided on an hourly basis for each day of the 18-year simulation period. Note in the water quality model, we do not include an active sediment layer in the eight rows of the model. This is due to the very shallow and rocky or bedrock nature of the upper portion of the Pond located just below the Holtwood Dam. Initial sediment transport model computations suggested that any deposition in these upper segments would be of a short duration, as such we decided to exclude this area of the model domain to avoid any numerical issues within the water quality model.

Nutrient loadings entering Conowingo Pond from upstream at Holtwood Dam and from the Muddy Creek and Broad Creek tributaries comes from the USEPA watershed model (Phase 6, Beta 2). Besides nutrient loadings, the watershed model also provides estimates of flows entering and exiting the Pond. However, during the development and calibration of the hydrodynamic/ sediment transport model, it was determined that the EPA watershed estimates of flow were not detailed enough to develop a good hourly flow/water elevation calibration of the Pond. This is in part due to the daily timescale for flows and loads that the USEPA WSM and the Chesapeake Bay water quality model are calibrated for. Further, the EPA watershed model does not include detailed information

as to how Exelon manages flow releases at Conowingo Dam for power generation and for spilling water in advance of high flow events. To address this issue an independent estimate of the flow balance around the Pond was developed. Therefore, our estimates of flow entering the Pond via Holtwood differed from that provided by the USEPA. As a consequence, we developed slightly different estimates of nutrient loadings entering the Pond from Holtwood; loadings from Muddy Creek and Broad Creek were utilized directly as provided by the USEPA WSM. In developing the revised loadings from Holtwood, we back-calculated the concentrations of the various nutrient forms by dividing the USEPA WSM nutrient loads by the USEPA WSM Holtwood flows and then multiplying these concentrations by the flows we developed for the calibration of the hydrodynamic/sediment transport model.

We also assumed that all water column water quality variables, other than DO and oxygen demanding material (aqueous CH_4), were treated as conservative. The only processes that affected the concentrations of water column water quality variables were the settling of the particulate nutrients (C, N, and P) and phytoplankton and the exchange of dissolved nutrients (NH_4, NO_3, SRP or PO_4) between the water column and the sediment bed, as determined by the SFM. Particulate organic matter was assumed to settle based on a weighted-average of the clay and silt settling velocities and concentrations provided by the sediment transport model, as per equation 4:

$$v_{POM} = \frac{v_{sc} \cdot c_c + v_{ss} \cdot c_s}{c_c + c_s} \quad (4)$$

Where:

V_{POM} = settling rate of particulate organic matter (m/day),

V_{sc} = settling rate of clays = 0.35 (m/day),

C_c = concentration of clays (mg/L),

V_{ss} = settling rate of silts = 51.8 (m/day), and

C_s = concentration of silts (mg/L).

The only non-conservative variables were DO and aqueous CH_4. The processes that affected dissolved oxygen were SOD, reaeration with the atmosphere and oxygen loss as dissolved CH_4 was oxidized in the water column. The reason for treating DO as a non-conservative variable was to see if model computations of DO would help us to determine which set of model coefficients, especially the differences between Runs 01 and 02 versus 03 (discussed in the previous section), would provide a better fit to the observed DO data. The idea was that if we were over-estimating how much POM was in the G_2 pool then we might under-estimate the observed water column DO versus if we under-estimated the G_2 pool then we would over-estimate the water column DO.

In making DO a non-conservative variable, we then needed to estimate two additional model coefficients, the air-water reaeration coefficient and the oxidation rate of aqueous CH_4. Using the O'Connor-Dobbins (1958) reaeration formula, based on advective velocities and depths, in combination with the Banks and Herrera (1977) reaeration

formula, based on wind speed and depth and using average advective velocities, average wind speed corrected for direction and fetch and average Pond depth, we arrived at an estimated mass transfer coefficient (K_L, which in turn can be used to calculate the reaeration coefficient via $K_a = K_L/H$) of 0.25 m/day. We also assumed an oxidation rate of 0.1 /day for aqueous CH_4.

3 Results

The principal calibration goals were to:

1. Reproduce the observed water quality data at the USGS gaging station (USGS 01578310) located just downstream of the Conowingo Dam, and

2. Reproduce the observed sediment bed concentrations for nitrogen and phosphorus (carbon was not included due to the influence of coal in the carbon measurements).

3.1 Calibration to the USGS Conowingo Gage

Calibration results to the USGS gage will be presented using time-series figures and cross-correlation plots. Each of the time-series figures will show two panels. The upper panel will show the 18-year calibration of daily-averaged outflow from Conowingo Pond versus the observed USGS flow, while the lower panel will show the 18-year calibration of the water quality concentrations versus the observed data. Data reported as “less than” are also included on the figures. Again, it is important to mention that the nutrient loadings to the CPMBM were obtained from the USEPA WSM (Phase 6, Beta 2). This, as will be shown subsequently, has some bearing on the calibration of the CPMBM model.

3.1.1 Phosphorus

Figure 17 presents the time-series calibration of the CPMBM to the observed Conowingo flow (upper panel) and to the observed Conowingo total phosphorus (TP) (lower panel). The calibration to the observed flow is quite good, as is also evidenced by the cross-correlation plot (Figure 18). While there is some deviation from the one-to-one line at the mid-range flows (~300-1,500 m^3/sec), the slope of the regression line is 1.06 and the correlation coefficient is very high (0.975). The calibration to TP also appears favorable. While not as good as for flow, the cross-correlation plot for TP (Figure 19) shows a regression slope is 0.831 and a correlation coefficient off 0.799. It can be seen that there is scatter around the one-to-one line and that perhaps the model tends more often to over-estimate TP. In attempting to gain further insight into the model behavior, we plotted the time-series of the inflow concentrations, provided by the USEPA WSM entering the Pond from the upstream boundary at Holtwood (Figure 20). We noticed for some model vs. data pairs, and especially for those pairs that corresponded to high flows, that when the model over-estimated the outflow TP, the inflow TP concentrations also over-estimated the observed TP. Therefore, perhaps a potential reason for the

CPMBM mismatch with the data might result, in part, from the inflow concentration provided by the WSM. This is further illustrated in Figures 21-27, where we look at the calibration of the dissolved and particulate forms of phosphorus.

Figure 21 presents time-series plots of dissolved organic phosphorus (DOP). As can be observed in this figure, there is a wide-range of flows wherein the model over-estimates the observed DOP. This results in a poor cross-correlation (Figure 22), with a slope and correlation coefficient of almost zero. We plotted (Figure 23) the WSM inflow DOP concentration versus the observed data and also found that the WSM over-estimates DOP. We then plotted observed DOP, WSM inflow DOP and CPMBM outflow DOP versus flow (Figure 24). The panel on the left shows the raw observations and corresponding watershed model inflow concentration and CPMBM outflow concentration. The panel on the right also shows data and model concentrations, but binned by flow ranges and plotted as mean and maximum and minimum within the flow bin versus flow. While it may not be appropriate to make comparisons of WSM inflow concentrations versus observed Conowingo data due to time-of-travel, which may be as long as 10-20 days or longer, at low flows, we believe that such comparisons are appropriate at flows greater than 1,000-1,500 m^3/sec, which correspond to travel times of 1-2 days or less, which limit the time available to transform organic nutrient forms to inorganic nutrient forms. It can be seen that for flows greater than or equal to 1,000 m^3/sec the inflow DOP concentration is two to four times greater than the observed outflow. A similar pattern can be observed in the total dissolved phosphorus (DP) for flows greater than or equal to 2,500 m^3/sec (Figure 25). Since DP includes both DOP and dissolved inorganic or soluble reactive phosphorus (PO_4), whatever DOP was converted to PO_4 would still remain within the DP pool. This DOP and DP mismatch contributes then to the mismatch of TP.

Figure 26 presents the calibration results for particulate phosphorus (PP). In general, the calibration appears reasonable, as is borne out in the cross-correlation plot (Figure 27). The slope of the regression line is 0.958 and the correlation coefficient is 0.813.

3.1.2 Nitrogen

Figure 28 presents the calibration of the CPMBM to the observed total nitrogen (TN) data. For the most part, the calibration appears reasonable, but the cross-correlation plot shows that the calibration is less favorable (Figure 29), with a slope of 0.168 and a correlation coefficient of only 0.261. If one focuses in it can be observed that CPMBM appears to over-estimate TN during some high flow events. This is, in part, due to the inputs provided by the WSM (Figure 30). As can be observed in Figure 31, for flows greater than or equal to 2,500 m3/sec, the Holtwood boundary TN is generally a factor of two or greater than the exported TN. The following analysis provides an overview as to the causes of the over-estimation of TN. Total nitrogen is comprised of four constituents: particulate organic nitrogen (PON), dissolved organic nitrogen (DON), ammonium nitrogen (NH_4), and nitrate+nitrite (NO_x). Figures 32 through 35 provide time-series of the calibration of PON, DON, NH4 and NO_x, respectively. From a review of these figures, it appears that the model: over-estimates PON, primarily during the winter months; over-estimates DON, during the winter months in 1998 through 2000 and

appears to over-estimate DON during high flow events; over-estimates NH_4 most of the time, but particularly during the summer months; and appears to provide a reasonable calibration to the NO_x. Cross-correlation statistics for these variables (Figures 36-39) are as follows:

	Slope	Correlation Coefficient
PON	1.748	0.868
DON	0.052	0.064
NH4	0.047	0.260
NOx	0.080	0.279

Although PON has a high correlation coefficient, as seen from the estimate of the slope, the model over-estimates the observed data. This is, in part, due to the inputs provided by the WSM (Figures 40 and 41). As can be seen in Figure 40, the WSM tends to over-estimate PON during high flow events, when the time-of-travel is short. This is also observed in Figure 41, when flows are between 1,000 and 10,000 m^3/sec. Figure 42 suggests that the WSM model may be under-estimating DON at low flows (although "time-of-travel" should be kept in mind), while the WSM may be over-estimating DON at higher flows. Mean-binned DON concentrations lie between about 0.15 and about 0.3 mg N/L across the range of flows, while the WQM shows an increasing trend in DON as flow increases until a flow of about 2,000 m^3/sec. Figure 43 shows that the WQM model appears to do a good job of estimating the import of NH_4 into Conowingo Pond at low flows, while the CPMBM severely over-estimates the export of NH_4. This then is a flaw in the CPMBM, which will be discussed in further detail in the section on the calibration of the sediment bed to follow. It is, however, worth noting that the WSM may be over-estimating NH_4 at mid- to high flows by about a factor of two. The watershed model also appears to over-estimate NO_x at flows between about 400 and 5,000 m^3/sec (Figure 44).

3.1.3 Carbon

Unfortunately, the quantity of data with which to calibrate total carbon (TC) was limited to 1997 through 2003. As can be seen in Figure 45 the calibration results are mixed and the cross-correlation analysis (Figure 46) results in a regression slope of 0.188 and a correlation coefficient of 0.425. Again, it appears as if the WSM is in part responsible for the poor calibration, due to an under-estimation of TC at low flows and perhaps an over-estimation of TC in the mid-flow range (Figure 47).

3.2 Calibration to Storm Event Data

For the Lower Susquehanna River Watershed Assessment (LSRWA), Cerco and Noel (2014) developed a loading analysis for two erosional events that occurred in 2011, an un-named event in March and Tropical Storm Lee, in early September. They developed their analysis using data provided by Jeffrey Chanat (USGS MD-DE-DC Science Center). Chanat provided measurements of flow, particulate phosphorus, suspended

sediment, and percent nitrogen and total organic carbon composition of the suspended sediment. Based on the suspended sediment and percentage composition, one can estimate a concentration of particulate nitrogen and carbon. Figure 48 presents a comparison of the flow and concentration data provided by Chanat versus CPMBM computations. It should be noted that Chanat did not report data for September 9. The uppermost panel, indicates that the peak flows are within about 15% of one another with the CPMBM being the higher flow. Subsequently, the USGS flow data are higher than that estimated by the CPMBM. Similarly, the peak particulate phosphorus (PP) data and model are within about 15% of one another, with the CPMBM being greater on September 8, but with the USGS data being higher on subsequent days. With respect to particulate nitrogen (PN), again CPMBM has a greater concentration on September 8 (by about 25%), and the data and model being very similar after that. For particulate carbon (PC), the USGS data and extrapolated data are significantly greater on September 8 (almost a factor of 2) and the USGS remain greater for the next three days as well. In part, this is due to the methodology for making carbon loading and concentration estimates for CPMBM based on the USEPA WSM. The methodology, as described earlier, estimates POC eight times the WSM PON concentration. Since NO_x is between a third and half of the total organic nitrogen, this limits the estimated maximum value of TC to about half of the observed value and helps explain the discrepancy in CPMBM computed TC versus the observed data. Using the flows and concentration data presented on Figure 48, the following total loads were estimated for phosphorus, nitrogen, and carbon for Tropical Storm Lee:

	USGS/Chanat (kg)	CPMBM (kg)	Percent Difference
PP	6.96×10^6	6.76×10^6	2.9
PN	1.58×10^7	1.04×10^7	35
PC	1.94×10^8	8.67×10^7	55

Again, note that the big discrepancy in carbon is likely due to the methodology for computing the inflow concentration of carbon to Conowingo Pond from the WSM, but may also be influenced by potential coal content from resuspended sediments from the three reservoir system.

Cerco and Noel also looked at the Conowingo load for the spring 2011 event. However, data for that period were limited to two surveys conducted on March 8 before the storm peak and March 12 the day of the peak USGS gage flow. Based on these two days of data, the USGS and CPMBM loads were as follows:

	USGS/Chanat (kg)	CPMBM (kg)	Percent Difference
PP	1.37×10^6	1.15×10^6	16
PN	8.36×10^6	2.40×10^6	71

PC	5.56×10^7	2.07×10^7	63

Differences in PN for the March event increase, in part, due to a higher percent nitrogen content on the March solids (0.375%) versus the September solids (0.21%). Again, we believe that some of the model versus data differences may be attributed to the methodology used for estimating particulate and dissolved organic nitrogen fractions, which assumes a constant fractional split irrespective of flow. However, we also acknowledge that while the differences between observed and computed PP loads are encouraging, the differences for PN and PC are larger than desired.

3.3 Sediment Composition Calibration

Calibration of the sediment bed composition of the CPMBM focused on near surface (3-19 cm) data from the SRBC field program (Edwards, 2006) and surface (0-1 cm) data from the UMCES field studies (Cornwell, pers.comm.).

Figure 49 presents the calibration results for sediment composition for particulate organic carbon (POC), total nitrogen (TN) and total phosphorus (TP) for the year 2000 SRBC data. The model results represent the active layer of the sediment nutrient flux model (SFM), which varies between 9.5 and 10.5 cm, while the data come from a near surface slice of 10 cm thickness that may lie between 3 and 19 cm, depending on the core that was sub-sampled. While we have not plotted the SRBC carbon data on the plot due to the confounding effects of coal, the model computations themselves are informative. We see that the highest concentrations of organic carbon, 3-5% are found in the upper portion of the reservoir and that there is a spatial decrease in sediment carbon along the length of Conowingo Pond, with the lowest concentrations, 0.5-2% in the lower Pond.

For TN, we also see a spatial gradient along the length of the Pond, with highest concentrations (0.4-0.6%) in the upper Pond and lowest concentrations (0.08-0.25%) in the lower Pond. The model is generally within the range of the surface 2000 data, but the model appears to be too high in the upper Pond and perhaps a little too low in the lower Pond. For TP, we also see a spatial gradient, which is consistent with that observed for carbon and nitrogen, i.e., higher concentrations in the upper Pond and lower concentrations in the lower Pond. In the case of phosphorus, the model computations of TP appear to be biased high by about 0.25-0.05%. Also, as noted, the model computes a spatial gradient that is not evident in the data. The reason for this discrepancy appears to be due, in part, to the dynamics of the sediment transport model, wherein, due to the higher settling velocity used in the sediment transport model for the silts (0.06 cm/sec = 51.8 m/day) most of the POM coming into Conowingo Pond during moderate and high flow events settle out in the upper portion of the Pond. This POM remains in the upper pond, until high flow events, which result in scour of the bed, remobilize the sediments and POM in the upper reservoir and either redistribute a portion of this POM in the middle and lower Pond or export the POM from the Pond to upper Chesapeake Bay.

As shown in Figure 50, the spatial gradient appears to grow over time, i.e., upstream concentrations of TOC, TN and TP increase, while downstream concentrations

decrease, which again is at odds with the observed data. However, there is also a subtle change in that the concentrations in the upper middle and middle Pond are also increasing. This may result from resuspension of upstream most sediments and re-deposition of these sediment nutrients, as well as new sediments delivered to the Conowingo Pond during the high spring flow events of 2005 and 2011, as well as Tropical Storm Lee in 2011. Compared to a Pond-wide average TN concentration of between 0.2 and 0.3% nitrogen, the model shows values of about 0.5, 0.3 and 0.1% in the upper, middle and lower Pond, respectively. For TP, the model shows values of about 0.25, 0.18 and 0.1% in the upper, middle and lower Pond, respectively. There are not enough 2015 data to estimate a Pond-wide average TP, but the 2000 SRBC data suggest perhaps an average of between 0.1 and 0.15%.

It appears that the nutrient component of the CPMBM may settle too much POM in the upper portion of Conowingo Pond at the expense of downstream settling of POM. However, it is mainly these upstream depositional areas that are resuspended during high flow events, which redistributes a portion of this POM further downstream as well as exporting POM from the reservoir. This will be discussed further in Section 4. Results

4 Results

Recent papers by Zhang et al. (2013, 2016) have suggested that the Lower Susquehanna River Reservoir System reached a dynamic equilibrium and that perhaps this equilibrium was reached in the early 2000's. This conclusion is based on observations and statistical analysis that suggests that Conowingo Pond is trapping less suspended sediments, total phosphorus and, to a lesser degree, total nitrogen. We evaluated the trapping efficiency of Conowingo Pond for total and particulate nutrients as determined by the CPMBM. This computation was based on annual average loading of total and particulate nutrients to the Pond as well as export from the Pond. The trapping efficiency was expressed as a percentage and was determined as:

$$TE = 100 \cdot \left(\frac{W_{in} - W_{ex}}{W_{in}}\right) \quad (5)$$

Where:

TE = trapping efficiency,

W_{in} = load into Conowingo Pond,

W_{out} = exported load from Conowingo Pond.

Figure 51 presents a time-series of the trapping efficiencies for the various forms of particulate phosphorus and TP. Generally, the trapping efficiency for the particulate forms of phosphorus varies between 30 and 45 percent, but is lower in years with some higher flow events, such as 1998 and 2004. The trapping efficiency for TP is slightly lower (on average about 12%) than for the particulate phosphorus because the dissolved components (dissolved organic and dissolved inorganic phosphorus) essentially pass through the Pond. During years with very high flow springs, (2005 and 2011), and

Tropical Storm Lee (2011) the model computes a "negative" trapping efficiency, meaning that more particulate phosphorus was exported from the Pond. This is due to scour and resuspension of particulate phosphorus from the sediment bed. As can also be noted on this figures during these scour and resuspension events G_3 and PIP form the largest components of the export. This is due to the fact that G_1 and G_2 phosphorus undergo diagenesis fairly rapidly and sorb to bed solids forming particulate inorganic phosphorus (PIP). G_3 undergoes diagenesis at a much slower rate and remains in the sediment bed for a longer period of time resulting in larger residuals of G_3 material as compared to G_1 and G_2.

Figure 52 shows the resuspension of quantities and composition of the resuspension fluxes for phosphorus as a function of flow as computed by the CPMBM water quality model. Resuspension is determined by the hydrodynamic/sediment transport model based on computed shear stresses and the parameter – critical shear stress for erosion. The figure indicates that resuspension does not occur under flows of about 2,000 m^3/sec (about 70,000 cfs) and that larger fluxes (> 100 kg organic P or > 1,000 kg inorganic P) do not occur until flows of about 5,000 m^3/sec (about 140,000 cfs) or greater are reached. The figure also shows that when resuspension occurs that the G_3 fraction of organic phosphorus is the largest of the organic pools to be resuspended and that it is almost a factor of four greater than G_2 organic phosphorus and more than a factor of ten greater than G_1 organic phosphorus. The figure also shows that the resuspended mass of particulate inorganic phosphorus is about a factor of ten greater than the resuspended organic phosphorus.

Figure 53 shows a plot of the various G-fractions for exported particulate carbon, nitrogen, and phosphorus as a function of flow. At low flows the composition of the exported particulate nutrient fractions is the same as the imported or inflow nutrient fractions. However, as the river flow increases to about 5,000 m^3/sec (140,000 cfs) the fractions begin to change, with an increase in the G_3 fraction and reductions in the G_1 and G_2 fractions.

Figure 54 presents a similar trapping efficiency analysis for particulate nitrogen and TN. Trapping efficiencies for particulate nitrogen forms is quite similar to that computed for phosphorus, between 30 and 45 percent. However, the overall trapping efficiency for total nitrogen is smaller than that computed for phosphorus and is only about 5 percent. This is due to the fact that the dissolved forms of nitrogen, and in particular, NO_x, constitutes a more significant fraction of the TN than do the dissolved forms of phosphorus in contributing to the TP. As was observed for phosphorus, during the resuspension and scour years of 2005 and 2011, more nitrogen is exported from the Pond than is imported to the Pond. As can be seen in Figure 55, the behavior of particulate carbon is very similar to that of the particulate nitrogen.

5 Management Scenarios

The CPMBM was used to simulate management scenarios to explore a range of alternative sediment and nutrient inputs and corresponding export from Conowingo

Pond. The selection of the scenario runs were made by the USEPA CBP and the results of these simulations were provided to the USEPA CBP to be used to help inform the USEPA watershed model.

5.1 Management Scenario Set-Up

Two sets of simulations were performed. The first set of simulations consisted of three modifications to the nutrient loadings (C, N, and P) delivered to the Pond from Holtwood and from the tributaries that discharge directly to the Pond. These loadings were reduced by 50%, 15% and increased by 20% and are called S1, S2, and S3, respectively. These simulations or scenario runs were run using the calibration or baseline (named C1) hydrodynamic/ sediment transport model output (1997-2014 – long-term simulation). Each of the scenario run simulations were cycled twice. This involves running the model with the appropriate management scenario reduction or increase in nutrient loading for the 1997-2014 period and then taking the ending state of the nutrients in the sediment bed and rerunning the model a second time using the same hydrologic/loading cycle (1997-2014). This helps to ensure that the active layer of the sediment bed has time to approach a new dynamic equilibrium with respect to particulate organic nutrients.

The second set of scenario runs were performed in a similar fashion; the nutrient loads were reduced or increased consistent with the first set of scenario runs. The difference was that the hydrodynamic/sediment transport model was also rerun for these management scenarios. Four new hydrodynamic/sediment transport simulations were performed. In the first run (named C2), the ending condition (2014) of the sediment bed bathymetry and bed composition (particle size classes) was used as an initial condition and the calibration hydrologic and suspended sediment loadings (1997-2014) were repeated. For the other three new hydrodynamic/sediment transport scenario runs, the ending sediment bed bathymetry/bed composition was used as the initial conditions for the new runs and the sediment loadings were also modified in a fashion consistent with scenario runs S1-S3. For scenario run S4, the suspended sediment loads were reduced by 35%, for scenario run S5, suspended sediment loads were reduced by 10.5% and for scenario run S6, they were increased by 14%. The outputs from these new hydrodynamic/sediment transport model simulations were then used for the water quality model simulations. These water quality simulations were also cycled twice to allow the nutrients in the sediment bed to approach a quasi-equilibrium with the changes in nutrient loads. Table 4 presents a summary of the bathymetries and sediment and nutrient scale factors that were used in the calibration or baseline and management scenarios runs.

5.2 Management Scenario Results

While we have only run two sets of three nutrient management scenarios, the USEPA CBP and its agency partners will have to consider many more combinations of carbon, nitrogen and phosphorus management alternatives. It is, therefore, important for them to have a means to estimate how nutrient management alternatives will affect Conowingo Pond sediments and their scour and resuspension from the sediment bed and transport

into Chesapeake Bay under high flow conditions. Previous water quality modeling efforts have generally shown water column and sediment bed nutrients to respond in a linear fashion to decreases or increases to nutrient loading. One of the first checks we performed was to determine if this would still be the case when a sediment transport model was added to the modeling framework for Conowingo Pond. As shown in Figure 56, each of the three nutrient constituents is linear in response to changes in nutrient inputs. So, averaged over the 18-year simulation period, a 50% reduction in carbon inputs to the Pond, relative to the baseline loading, results in a 50% reduction in carbon exported from the Pond. This is true for both the baseline 1997-2014 bathymetry and the 2014+ bathymetry.

Next, we evaluated how trapping efficiency (the ratio of Conowingo nutrient export or output to the nutrient import or input to the Pond) varied as a function of nutrient loading. These results are presented in Figure 56. Again, we see that, when averaged across the 18-year simulation period, the model is very linear in response. The 18-year average ratio of output to input for total carbon (TC) is about 0.7 for all eight simulations, implying a 30% trapping efficiency. As can be seen, there is a range in these output to input ratios, which is due to the fact that in very high flow years there is scour and resuspension which results in a greater output or export of TC relative to the input or import of TC. Note, however, that the computed ranges are also about the same for all eight simulation runs. The ratio of output to input for TN is just a little less than 1. This is due to the fact that the dominant forms of nitrogen are in the dissolved pools (nitrate+nitrite, ammonium and dissolved organic nitrogen) as opposed to particulate nitrogen. The 18-year average ratio of output to input for TP is about 0.9, implying a trapping efficiency of about 10%. As one can see, however, maximum output to input ratios are about 2.5, implying that at least in one year (2011) the export of TP is two and a half times greater than the import. Also note that there are some small differences in the maximum values. This reflects that for phosphorus the time to equilibrium is greater than the two 18-year cycles that the model was run for.

6 Summary and Conclusions

A coupled three-dimensional hydrodynamic, sediment transport and nutrient fate and transport model was developed as part of an overall project designed to simulate sediment and nutrient transport in Conowingo Pond. This integrated model is known as the Conowingo Pond Mass Balance Model (CPMBM). Hydrodynamic and sediment transport simulations were developed and provided to the water quality portion of CPMBM. The water quality portion of the model considers the fate and transport of dissolved and particulate nutrients within Conowingo Pond and its sediment bed. A key component of the water quality model is a sediment nutrient diagenesis and flux model, SFM. SFM accounts for the deposition and resuspension of particulate organic nutrients, the diagenesis or decomposition of these particulate organic nutrients within the sediment bed, and the flux of resulting inorganic nutrients back to the overlying water column. The SFM was extended to include an archive stack, so as to keep track of the burial and resuspension of the various fractions of particulate organic nutrients and particulate inorganic phosphorus within the deeper layers of the sediment bed. The

settling, deposition, burial and resuspension of particulate nutrients in the SFM and its archive stack were driven by information provided by the sediment transport portion of the CPMBM. The transport of particulate and dissolved nutrients in the overlying water column was driven by the hydrodynamic portion of the CPMBM. The purpose of this model is to evaluate nutrient conditions within the Pond and its sediment bed and to determine the magnitude, composition and reactivity of nutrient loads discharged from the Pond to the upper Chesapeake Bay. A second purpose of the model and its load estimates is to help inform the Phase 6 HSPF watershed model that USEPA will use for the 2017 mid-point assessment.

The veracity of the CPMBM's nutrient loading estimates is influenced by a number of factors, including:

- Availability and quality of water column nutrient data in the surface water and sediment bed of Conowingo Pond,
- Estimates of nutrient inputs entering Conowingo Pond from its upstream boundary at Holtwood and from the immediate drainage basin of the Pond via Muddy Creek, Broad Creek and other smaller tributaries that drain to the Pond provided by the USEPA CBP watershed model,
- Estimates of the various G-pool fractions of the particulate-phase nutrients delivered to the Pond from the USEPA CBP watershed model,
- Estimates of diagenesis rates for the various G-pools of particulate nutrients, and
- Estimates of particulate settling rates, deposition, scour and resuspension provided by the CPMBM sediment transport model.

As has been described in the main body of this report each of these factors has been shown to have limitations, flaws and uncertainties that affect the water quality model. In the case of data there is virtually no water column water quality data for the surface waters of the Pond for our period of interest save for temperature and dissolved oxygen data collected by Exelon during 1998-2000. Sediment nutrient data are primarily limited to data collected by SRBC in 2000 and UMCES field efforts in 2015 and early 2016 performed under this study. Both of these studies indicate considerable spatial and vertical variation in nutrients within the Pond sediments. Even some of replicate samples from the same core show considerable variation.

As has been shown in the water quality calibration to the USGS gage, the USEPA WSM has some fundamental calibration flaws, as such, the loading estimates provided to CPMBM by the WSM contribute, in part, to the poor calibration of some of the water quality variables.

Estimates of the diagenesis rate for G_3 from the long-term diagenesis experiments have considerable uncertainty. The G_3 diagenesis rate estimate was really guided only by the nitrogen data, as the data from the carbon experiments seemed to be seriously flawed and information from the phosphorus experiments could not be used due to partitioning of the dissolved inorganic phosphorus that was produced by diagenesis of the organic

phosphorus onto solids. Estimates of the G-fractions were largely driven by the application of the stand-alone SFM. While these G-fraction estimates appear reasonable, it should be noted that changing these G-fractions within a 20-30% range did not yield significantly different calibration results.

Finally, as was shown in the calibration of the sediment bed, it appears that using information concerning settling rates and resulting deposition from the sediment transport model computations may result in the settling of excess nutrients in the upper Pond at the expense of settling of nutrients in the lower portion of the Pond. However, it should be noted when a sufficiently high flow occurs that results in scour and resuspension, these same deposited sediments and nutrients are resuspended and redistributed within the Pond as well exported from the Pond.

Despite these limitations, it is believed that the CPMBM is sufficiently calibrated to support the following conclusions:

- Conowingo Pond appears to be in a state of dynamic equilibrium. By this we mean that the Pond still acts as an effective BMP during most years by reducing the quantity of nutrients that pass through the reservoir from the Susquehanna River watershed. However, during high flow years and events, scoured and resuspended sediment nutrients delivered to Chesapeake Bay may exceed the delivery of nutrients from the watershed alone to the Bay.
- Model computations show that the major component of the excess particulate form of these nutrients is in the G_3 pool, which is the least reactive fraction of the nutrients. Further, these high flow-scour and resuspension events only occur a very small portion of the time.
- Output from the CPMBM with respect to when scour and resuspension occurs and the magnitude and composition of the resuspended nutrients and their export to Chesapeake Bay appears reasonable and can be used by the USEPA Chesapeake Bay Program to support the refinement of the Bay watershed model.
- CPMBM computations demonstrate a linear behavior in response to decreases or increases in nutrients delivered to Chesapeake Bay from the watershed and Conowingo Pond. This linear behavior will help the USEPA facilitate the generation of nutrient loadings from the Susquehanna River watershed and Conowingo Pond in response to the myriad number of nutrient management scenarios that will be needed to develop the next TMDL allocations for the Bay

7 References

Boicourt, W.C., 1992. Influences of circulation processes on dissolved oxygen in the Chesapeake Bay. In *Oxygen dynamics in the Chesapeake Bay, a synthesis of recent research*, ed. D.E. Smith, M.

Leffler, and G. Mackiernan, 7–59. College Park, MD. Maryland Sea Grant.

Boynton, W.R., L. Lubbers, K.V. Wood, and C.W. Keefe, 1984. Seston Dynamics in the Lower Susquehanna River. Submitted to Martin Marietta Corp., Columbia, MD by the University of Maryland, Center of Environmental and Estuarine Studies, Chesapeake Biological Studies. Solomon, MD. 55pp.

Brady, D.C., J.M. Testa, D.M. Di Toro, W.R. Boynton, W.M. Kemp, 2013. Sediment flux modeling: calibration and application for coastal systems. Estuar. Coast. Shelf Sci. 117:107–124.

Burdige, D.J., 1991. The kinetics of organic matter mineralization in anoxic marine sediments. J. Mar. Res. 49:727-761.

Cerco, C.F., S-C. Kim and M.R. Noel, 2010. The Chesapeake Bay Eutrophication Model. A report to the US Environmental Protection Agency Chesapeake Bay Program and to the US Army Engineer Baltimore District. US Army Engineer Research and Development Center, Vicksburg, MS. 228 pp.

Cerco, C.F. and M.R. Noel, 2016. Impact of reservoir sediment scour on water quality in a downstream estuary. J. Environ. Qual. 45:894-905.

Cerco, C.F. and M.R. Noel, 2014. Appendix C: Application of the CBEMP to examine the impacts of sediment scour in Conowingo Reservoir on water quality in the Chesapeake Bay. Application of the Chesapeake Bay Environmental Model Package to examine the impacts of sediment scour in Conowingo Reservoir on water quality in Chesapeake Bay. A Report to the U.S. Army Corps of Engineers, Baltimore District. Draft Report. US Army Engineer Research and Development Center, Vicksburg MS.

Cornwell, J.C., L. Sanford, C. Palinkas, W.M. Kemp, M. Li and J. Testa, 2014. UMCES comprehensive proposal to address the impacts of Conowingo particulates on the Chesapeake Bay. Submitted to Maryland Department of Natural Resources, Annapolis, MD by University of Maryland Center for Environmental Sciences, Cambridge MD and the Chesapeake Biological Laboratory, Solomons, MD.

Di Toro, D.M., 2001. Sediment Flux Modeling. Wiley-Interscience, New York (624 pp.).

DiToro, D.M., and J.J. Fitzpatrick, 1993. Chesapeake Bay sediment flux model. Final report to the US Corps of Engineers, Waterways Experiment Station. HydroQual, Inc., Mahwah, NJ 07430.

Edwards, R.E., 2006. Comprehensive analysis of the sediments retained behind hydroelectric dams

of the Lower Susquehanna River. Watershed Assessment and Protection Program. Susquehanna River Basin Commission. Harrisburg, PA. Publication 239. 154 pp.

Hagy J.D., W.R. Boynton, C.W. Wood, K.V. Wood, 2004. Hypoxia in Chesapeake Bay, 1950–2001: long-term changes in relation to nutrient loading and river flow. Estuaries 27:634–658.

Hirsch, R.M., 2012. Flux of nitrogen, phosphorus, and suspended sediment from the Susquehanna River basin to the Chesapeake Bay during tropical storm Lee, September 2011, as an indicator of the effects of reservoir sedimentation on water quality. U.S. Geological Survey, Reston, VA.

Isleib, R.R., and A.J. Thuman, 2011. The role of estuarine eutrophication models in nutrient criteria development. Proc. Water Environ. Fed. 2011 (2):273–298.

Kemp, W.M., W.R. Boynton, J.E. Adolf, D.F. Boesch, W.C. Boicourt, G. Brush, G., et al., 2005. Eutrophication of Chesapeake Bay: historical trends and ecological interactions. Mar. Ecol. Prog. Ser. 303:1–29.

Langland, M. 1998. Changes in the sediment and nutrient storage in three reservoirs in the lower Susquehanna River basin and implications for the Chesapeake Bay. USGS Fact Sheet 003-98. USGS, Lemoyne, PA.

Langland, M., 2014. Sediment transport and capacity change in three reservoirs, lower Susquehanna River basin, Pennsylvania and Maryland, 1900–2012. Open-File Rep. 2014-1235. USGS, Reston, VA.

Linker, L.C., R.A. Batiuk, C.F. Cerco, G.W. Shenk, R. Tian, P. Wang, and G. Yactayo, 2016. Influence of reservoir infill on coastal deep water hypoxia. J. Environ. Qual. 45:887-893.

Linker, L.C., R.A. Batiuk, G.W. Shenk, and C.F. Cerco, 2013. Development of the Chesapeake TMDL Allocation. J. Am. Water Resour. Assoc. 49:986–1006.

McLean, R.I., J.K. Summers, C.R. Olsen, S.L. Domotor, I.L. Larsen and H. Wilson, 1991. Sediment accumulation rates in Conowingo Reservoir as determined by man-made and natural radionuclides. Estuaries. 14(2): 148-156.

Murphy, R.R., W.M. Kemp, W.P. Ball, 2011. Long-term trends in Chesapeake Bay seasonal hypoxia, stratification, and nutrient loading. Estuar. Coasts 34:1293–1309.

Pritchard DW, and J.R. Schubel, 2001. Human influences on the physical characteristics of the Chesapeake Bay. In: *Discovering the Chesapeake: the history of an ecosystem*. Curtin P.D., G.S. Brush and G.W. Fisher, editors. The Johns Hopkins University Press, Baltimore, MD. pg. 60–82.

Sanders, J.G., K.R. Kaumeyer and W.R. Boynton, 1982a. Plankton metabolism and benthic respiration in the Conowingo Reservoir. Prepared for Radiation Management Corp by the Academy of Natural Sciences, Benedict Estuarine Research Laboratory, Benedict, MD and the University of Maryland, Chesapeake Biological Laboratory, Solomons, MD.

Sanders, J.G., K.R. Kaumeyer and W.R. Boynton, 1982b. Plankton metabolism, benthic respiration and oxygen diffusion in the Conowingo Reservoir. Prepared for Radiation Management Corp by the Academy of Natural Sciences, Benedict Estuarine Research Laboratory, Benedict, MD and the University of Maryland, Chesapeake Biological Laboratory, Solomons, MD.

Schubel J.R., Pritchard D.W., 1986. Responses of upper Chesapeake Bay to variations in discharge of the Susquehanna River. Estuaries 9:236–249

Testa, J.M., D.C. Brady, D.M. Di Toro, W.R. Boynton, J.C. Cornwell, W.M. Kemp, 2013. Sediment flux modeling: nitrogen, phosphorus and silica cycles. Estuar. Coast. Shelf Sci. 131:245–263.

Testa, J. M., Y. Li, Y.-J. Lee, M. Li, D. C. Brady, D. M. Di Toro, W. M. Kemp, and J. J. Fitzpatrick, 2014. Quantifying the effects of nutrient loading on dissolved O2 cycling and hypoxia in Chesapeake Bay using a coupled hydrodynamic-biogeochemical model, J. Mar. Syst., 139:139–152.

USACE. 2015. Lower Susquehanna River watershed assessment, Maryland and Pennsylvania – Final Report. US Army Corps of Engineers, Baltimore, MD.

USEPA, 2010. Chesapeake Bay total maximum daily load for nitrogen, phosphorus, and sediment. US Environmental Protection Agency Chesapeake Bay Program Office, Annapolis MD.

Westrich, J.T., and R.A. Berner, 1984. The role of sedimentary organic matter in bacterial sulfate reduction: the G Model tested. Limnol. Oceanogr. 29(2):236–249.

Zhang, Q., Brady, D.C., Ball, W.P., 2013. Long-term seasonal trends of nitrogen, phosphorus, and suspended sediment load from the non-tidal Susquehanna River basin to Chesapeake Bay. Sci. Total Environ. 452-453:208–221.

Zhang, Q., Hirsch, R.M., Ball, W.P., 2016. Long-term changes in sediment and nutrient delivery from Conowingo dam to Chesapeake Bay: effects of reservoir sedimentation. Environ. Sci. Technol. 50:1877–1886.

Zhang, H., and S. Li, 2010. Effects of physical and biochemical processes on the dissolved oxygen budget for the Pearl River Estuary during summer. J. Mar. Syst. 79 (1–2):65–88.

Tables

Table 1. Sediment Oxygen Demand and Nutrient Fluxes Observed in Conowingo Pond and Lakes Clarke and Aldred							
Reservoir	**Date**	**Temperature (°C)**	**SOD (gm O_2/m^2-day)**	**J_{NH4} (mg N/m^2-day)**	**J_{NO3} (mg N/m^2-day)**	**J_{N2} (mg N/m^2-day)**	**SRP (mg P/m^2-day)**
Conowingo	5/19/2015	25	2.35 ±0.96	160.0 ± 88.5	-65.2 ± 27.9	69.0 ± 44.4	0.25 ± 0.37
Conowingo	7/22/2015	25	1.42 ± 0.22	37.4 ± 21.3	-21.6 ± 17.6	117.6 ± 37.2	-1.0 ± 6.2
Conowingo	9/22/2015	25.3	1.39 ± 0.22	3.62 ± 30.0	-43.3 ± 14.9	117.6 ± 37.2	0 ±0
Conowingo	12/3/2015	9.1	0.51 ± 0.11	-3.1 ± 26.6	-3.5 ± 9.6	69.1 ± 28.1	-4.3 ± 8.6
Conowingo	4/13/2016	9.6	0.69 ± 0.28	26.5 ± 22.5	-8.3 ± 23.9	56.0 ± 26.6	-0.73 ± 1.6
Lake Clark	4/27/2016	18	0.76 ± 0.18	43.9 ± 25.3	0.55 ± 22.1	22.3 ± 14.1	0 ± 0
Lake Aldred	4/27/2016	18	0.75 ± 0.28	5.3 ± 11.4	-52.9 ± 15.8	55.0 ± 15.3	0 ± 0

Table 2. G_3 Diagenesis Rates Estimated for Deep Core Diagenesis Experiments		
Core	**G_3 Nitrogen Diagenesis Rate (/day) Mean (Range)**	**G_3 Carbon Diagenesis Rate (/day) Mean and Range**
2	$5.1 \cdot 10^{-5}$ ($0.$-$1.5 \cdot 10^{-4}$)	$1.1 \cdot 10^{-4}$ ($0.$-$2.6 \cdot 10^{-4}$)
5	$1.7 \cdot 10^{-5}$ ($0.$-$6.0 \cdot 10^{-5}$)	$1.0 \cdot 10^{-3}$ ($0.$-$3.1 \cdot 10^{-3}$)
8	$8.8 \cdot 10^{-5}$ ($0.$-$1.6 \cdot 10^{-4}$)	$5.2 \cdot 10^{-5}$ ($0.$-$2.3 \cdot 10^{-4}$)
9	$1.1 \cdot 10^{-4}$ ($8.5 \cdot 10^{5}$-$1.5 \cdot 10^{-4}$)	$7.9 \cdot 10^{-5}$ ($0.$-$3.2 \cdot 10^{-4}$)
13	$6.2 \cdot 10^{-5}$ ($2.1 \cdot 10^{-5}$-$1.1 \cdot 10^{-4}$)	$9.3 \cdot 10^{-5}$ ($0.$-$2.8 \cdot 10^{-4}$)
Grand Average	$6.4 \cdot 10^{-5}$	$2.9 \cdot 10^{-4}$ ($7.0 \cdot 10^{-5}$)[1]
[1] average if one ignores two regression estimates for G_3 carbon that exceed the value for G_2 carbon ($1.8 \cdot 10^{-3}$ /day)		

Table 3. Fractions Metabolizable and Diagenesis Rates for Carbon and Nitrogen from the Short Core Diagenesis Experiments				
Carbon				
	Fraction metabolizable (%)		Diagenesis rate (/year)	
Core ID	Mean	Range	Mean	Range
02	1.0	1.0-1.0	10.3	9.9-10.8
4R	1.2	1.2-1.3	6.1	4.7-7.1
09	1.5	1.5-1.5	11.1	9.9-14.0
Nitrogen				
	Fraction metabolizable (%)		Diagenesis rate (/year)	
Core ID	Mean	Range	Mean	Range
01	3.9	3.9-3.9	3.49	3.48-3.50
02	6.4	6.4-6.5	2.72	2.69-2.76
03	9.2	9.1-9.2	3.14	3.12-3.20
04	5.7	5.6-5.8	1.59	1.53-1.64
05	23.3	22.2-24.3	1.88	1.76-2.04
5R	10.5	10.5-10.5	4.08	4.06-4.08
07	16.5	16.4-16.5	3.40	3.39-3.44
08	35.9	27.8-41.7	0.86	0.69-1.16
09	35.1	30.0-38.7	0.84	0.74-1.02
10	15.0	15.0-15.0	2.50	2.50-2.51
11	13.0	12.8-13.2	2.13	2.06-2.16
12	15.4	15.4-15.4	3.66	3.65-3.68

Table 4. Bathymetries and Nutrient and Sediment Scale Factors for the Scenario Runs			
Bathymetry	**Nutrient Scale Factor**	**Sediment Scale Factor**	**Water Quality Run**
1997-2014	1.0	1.0	C1
1997-2014	0.50	1.0	S1
1997-2014	0.85	1.0	S2
1997-2014	1.20	1.0	S3
2014+	1.0	1.0	C2
2014+	0.50	0.65	S4
2014+	0.85	0.895	S5
2014+	1.20	1.14	S6

Figures

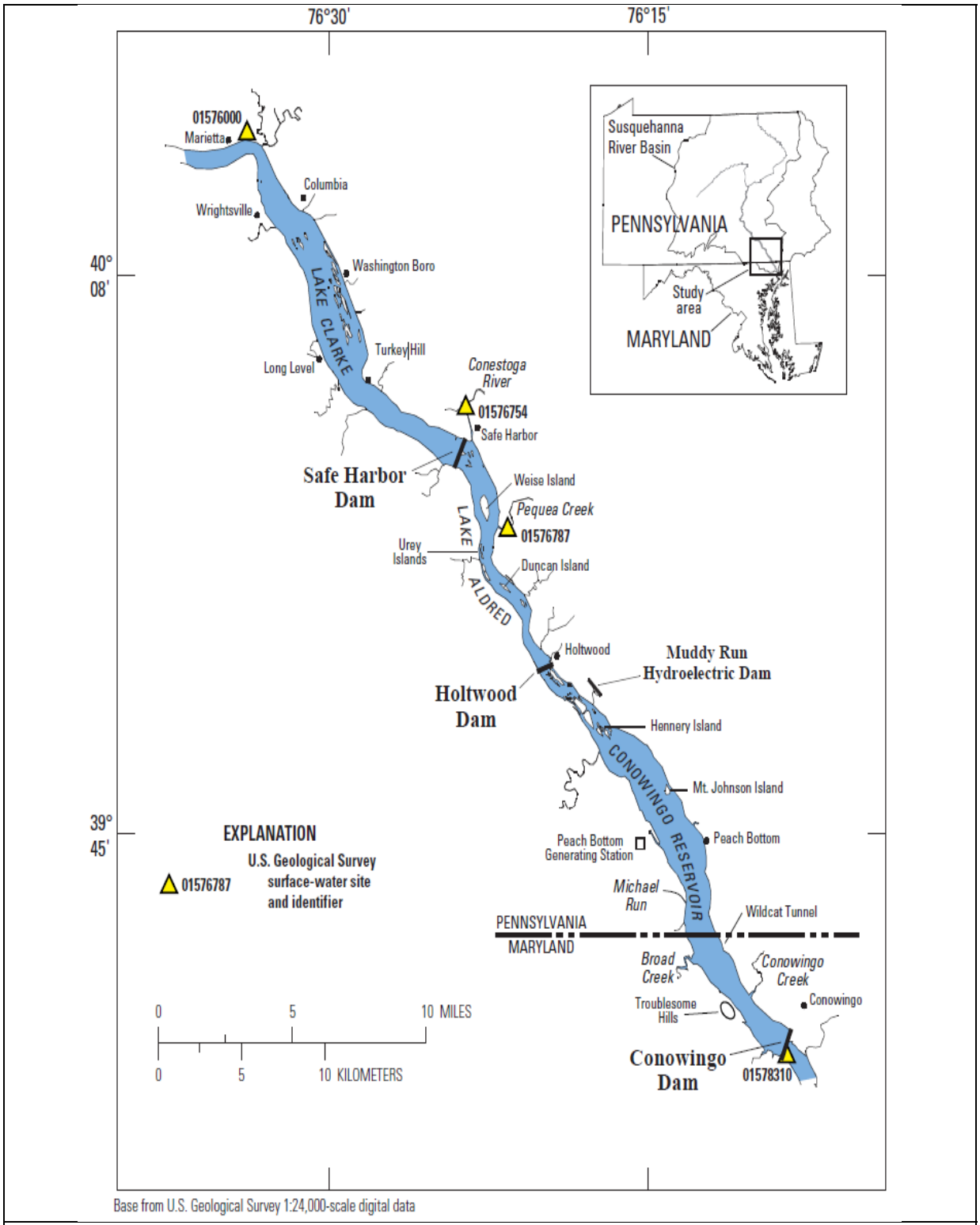

Figure 1. Location of the three reservoir system in the Lower Susquehanna River Basin, Pennsylvania and Maryland. (Langland, 2014)

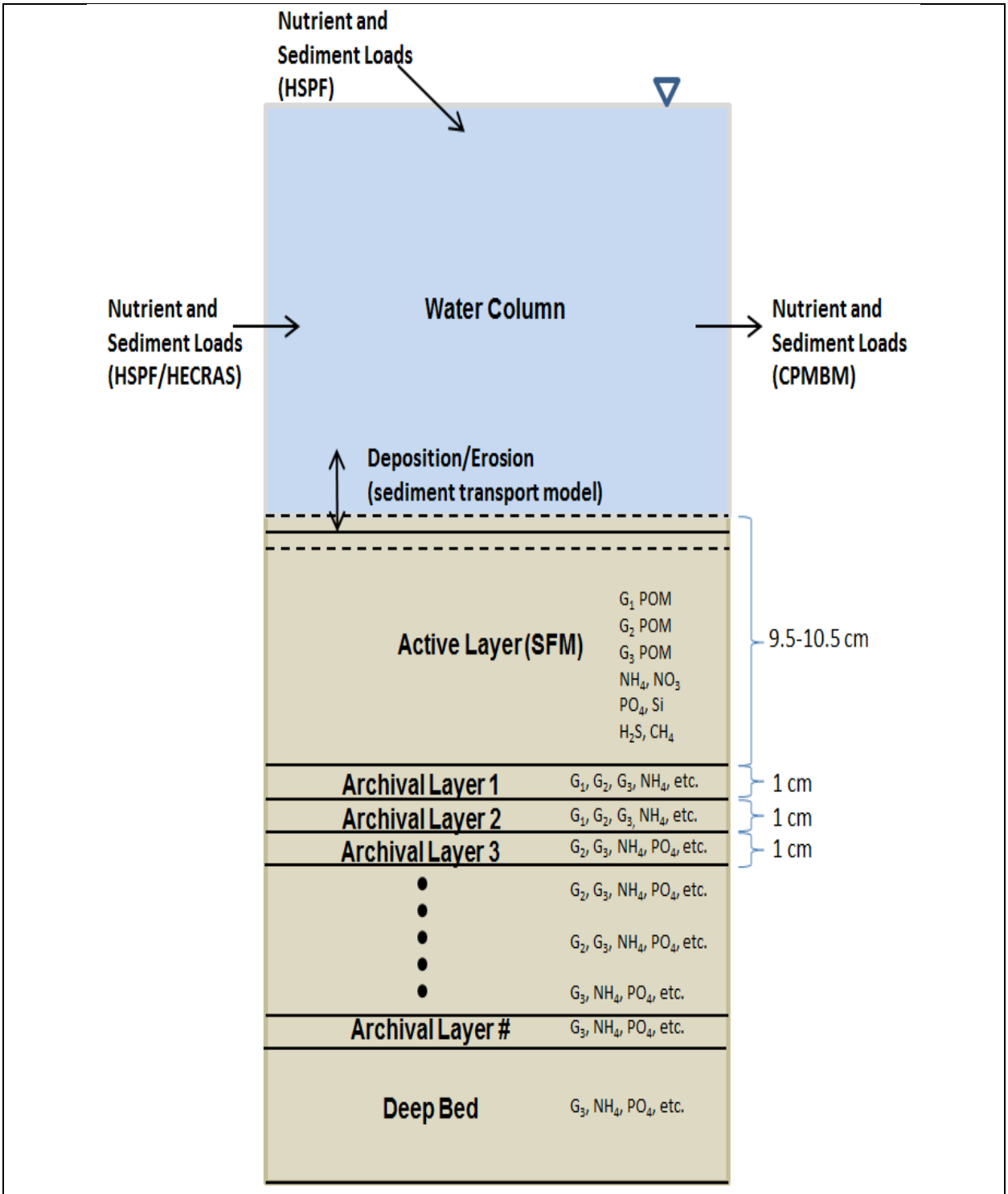

Figure 2. Conceptual framework of the Conowingo Pond Mass Balance Model (CPMBM).

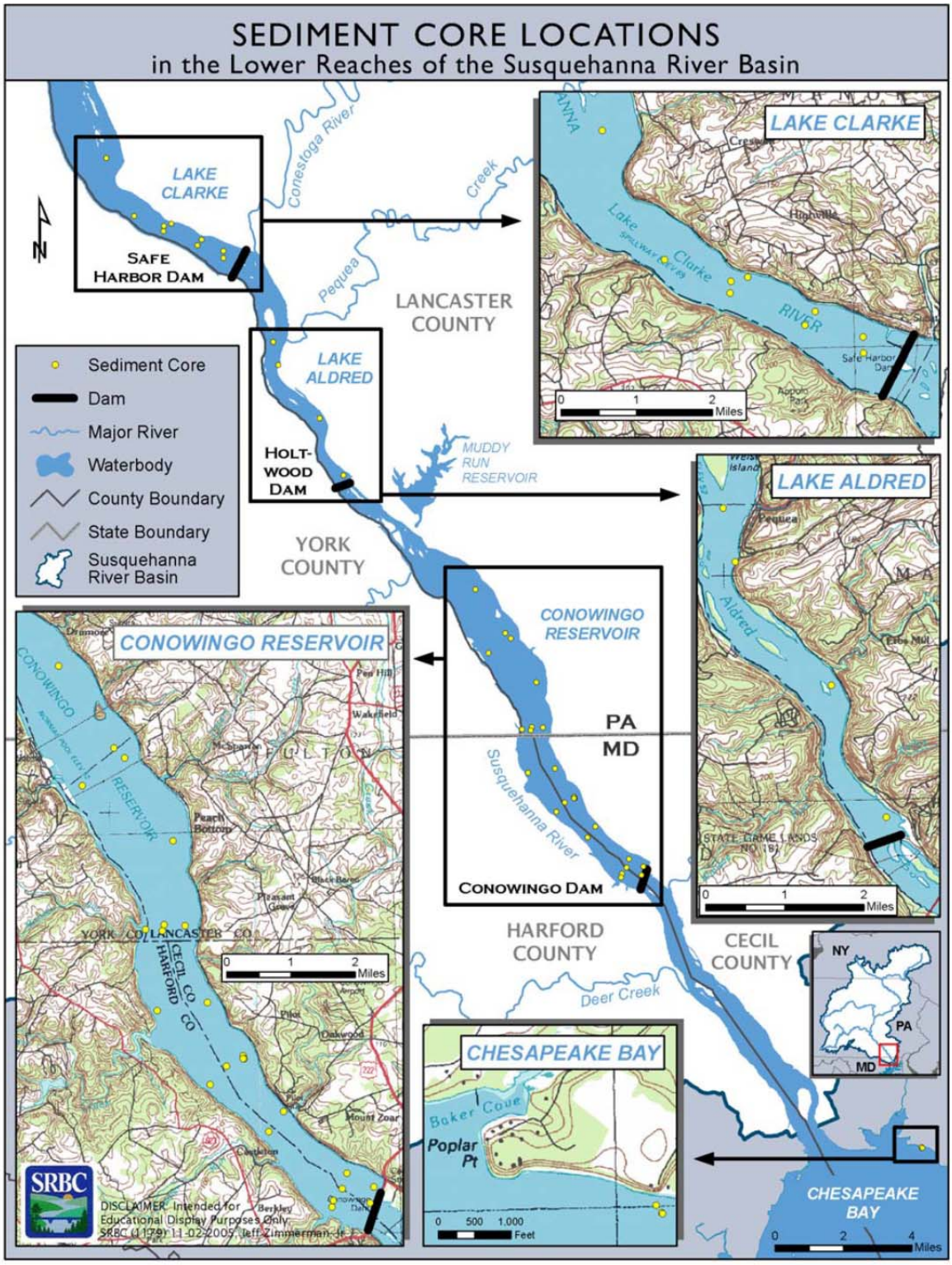

Figure 3. Sediment Core Sites Behind the Hydroelectric Dams on the Lower Susquehanna River and Upper Chesapeake Bay (Source SRBC, Edwards, 2006).

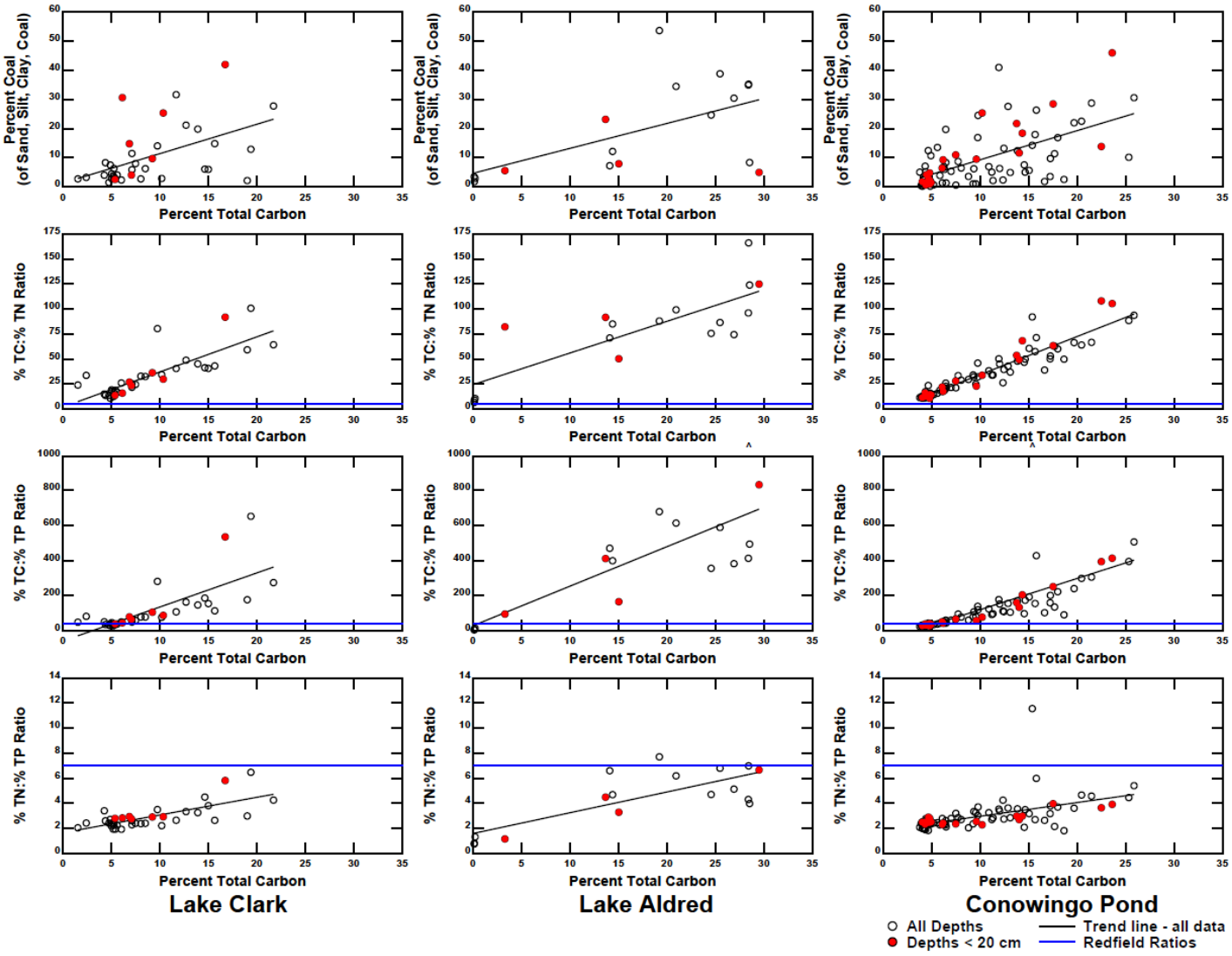

Figure 4. Sediment nutrient bed content as a function of sediment bed total carbon

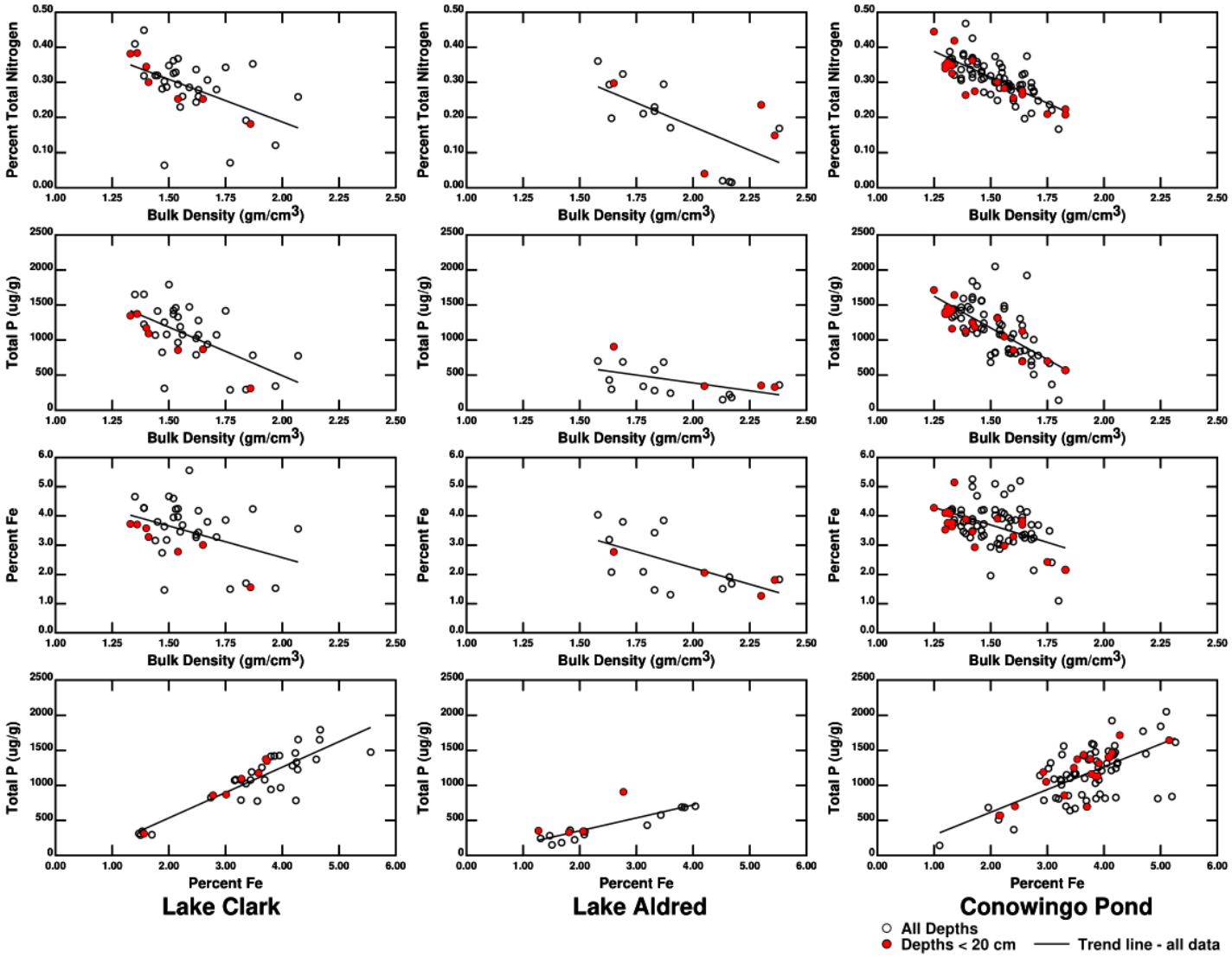

Figure 5. Sediment nutrient and iron content as a function of bulk density and sediment total phosphorus as a function of percent bed iron

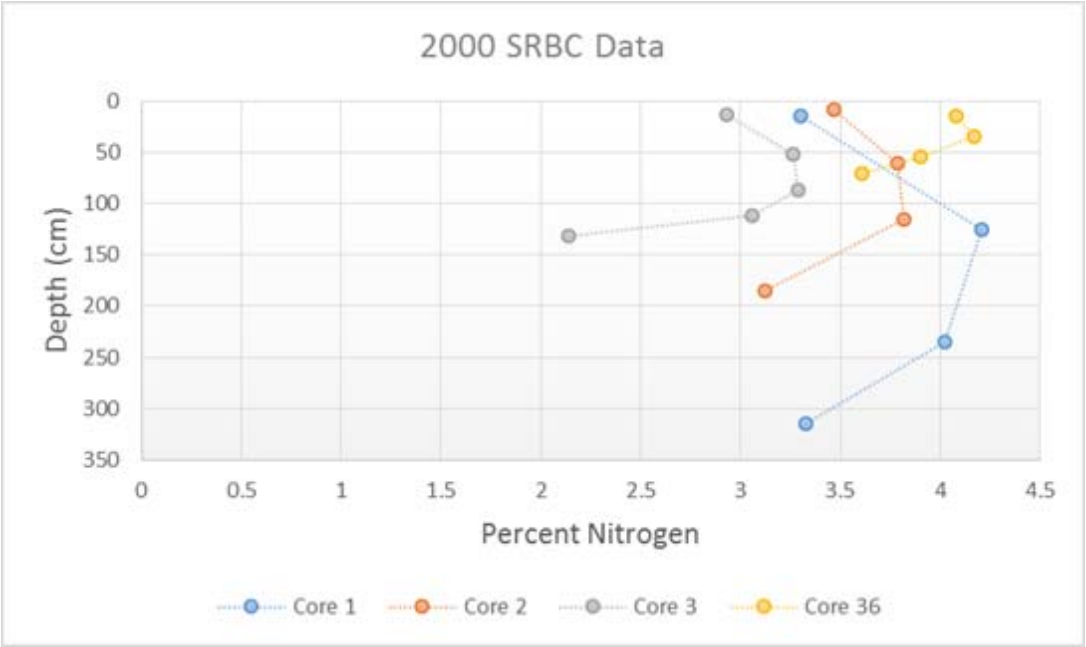

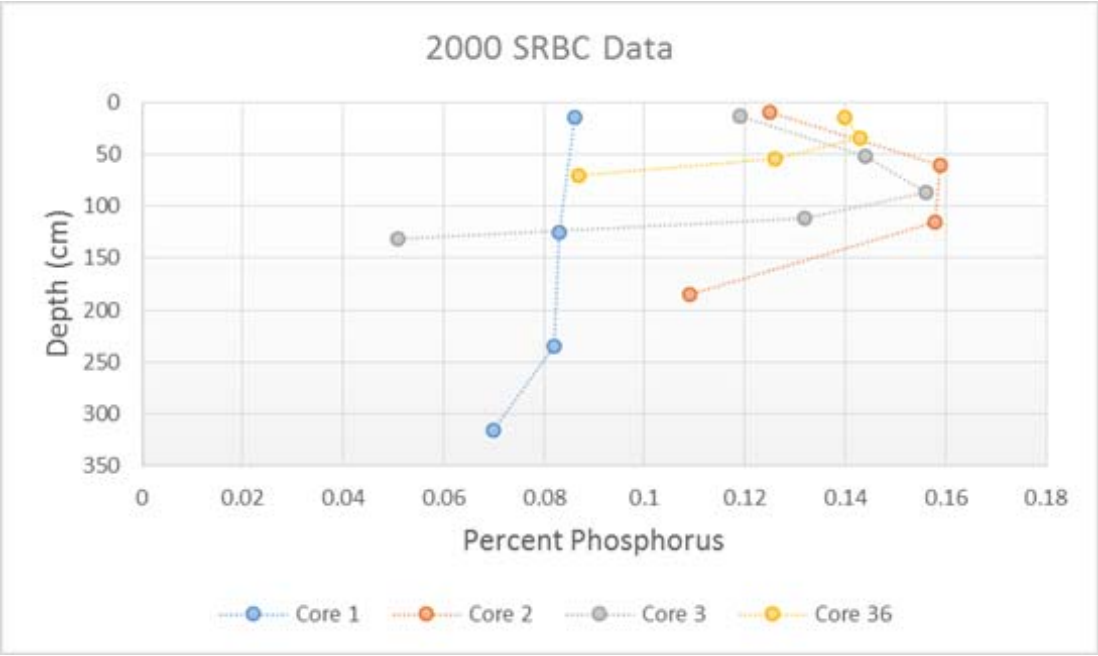

Figure 6. Vertical profiles of sediment total nitrogen and total phosphorus (SRBC, 2000).

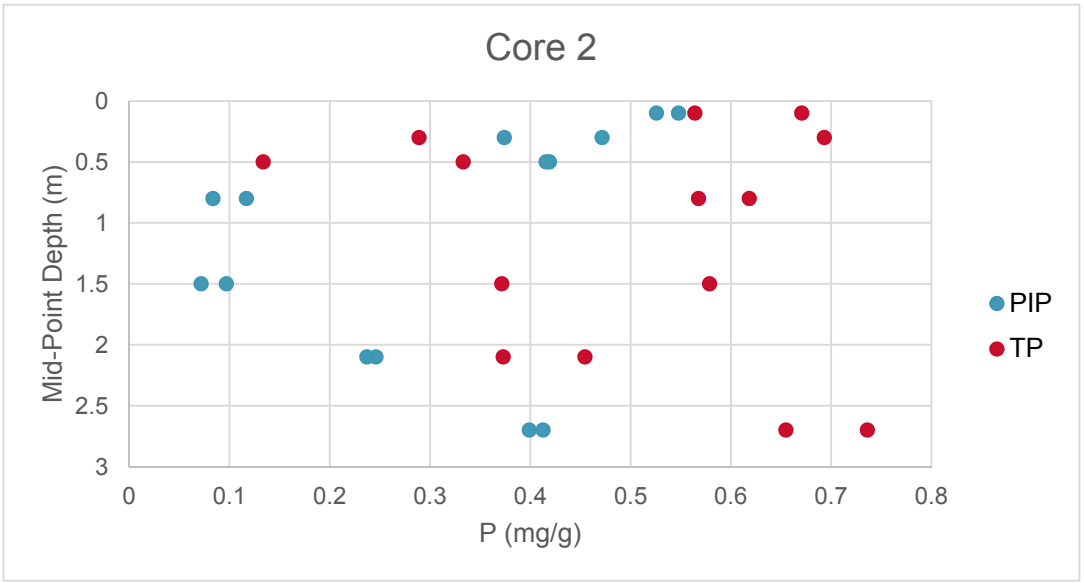

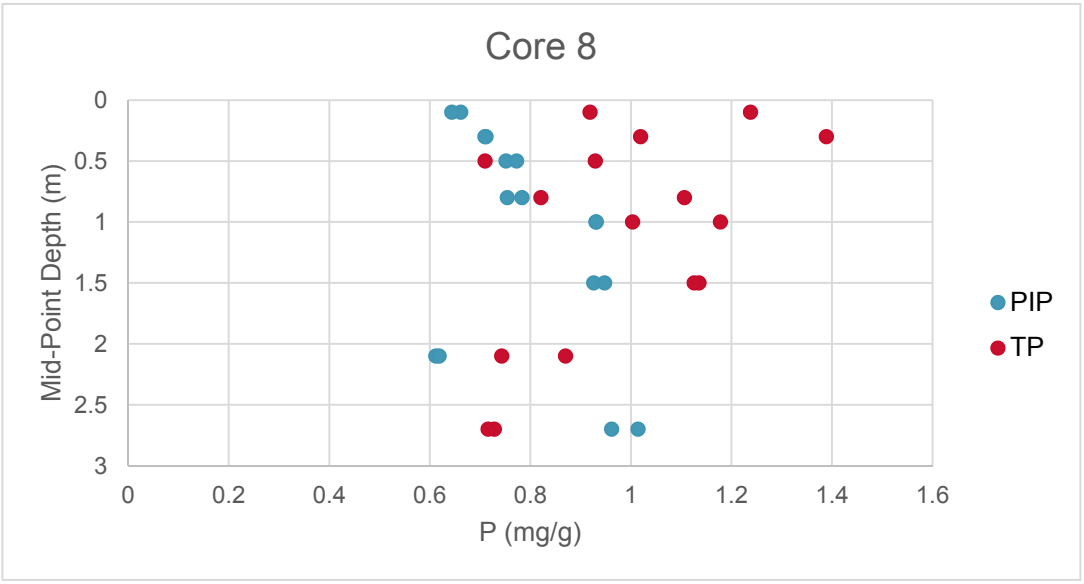

Figure 7. Vertical profiles of particulate inorganic phosphorus (PIP) and total phosphorus (TP) (UMCES, 2015)

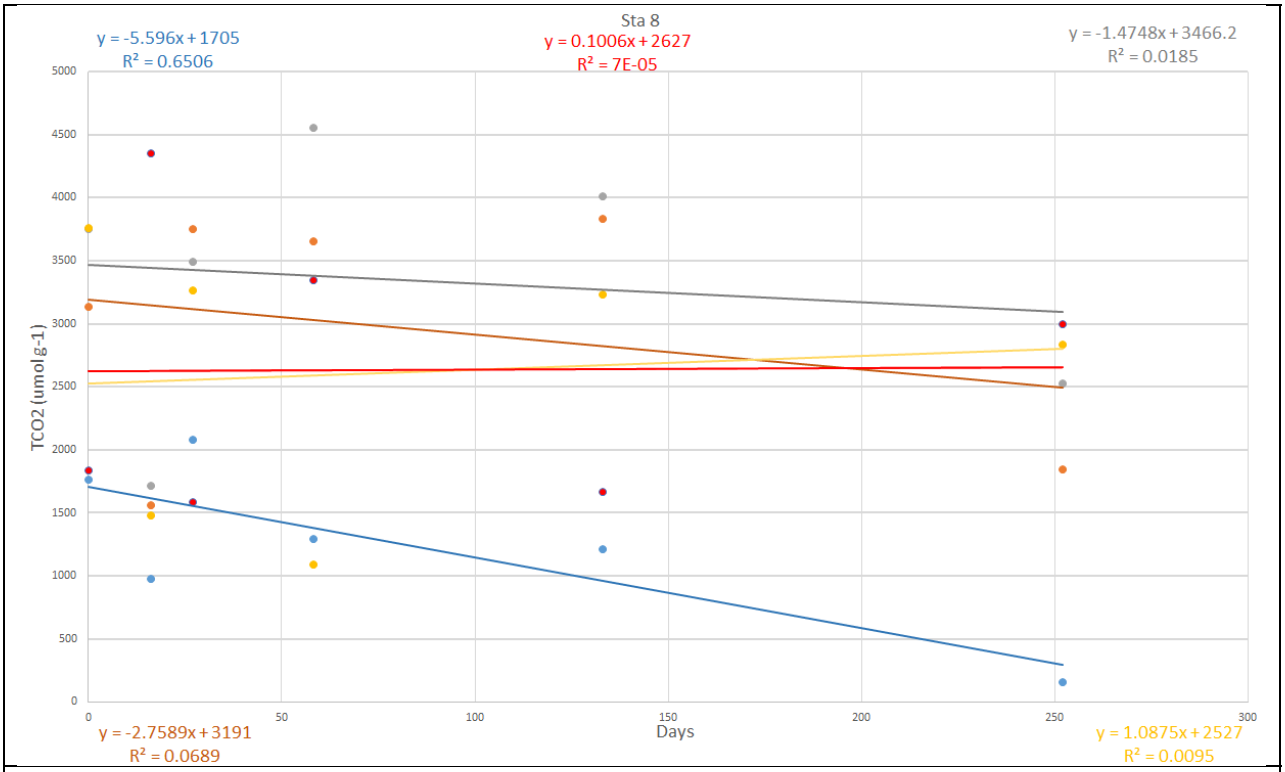

Figure 8. Deep core diagenesis analysis of station 8 for organic carbon-TCO_2

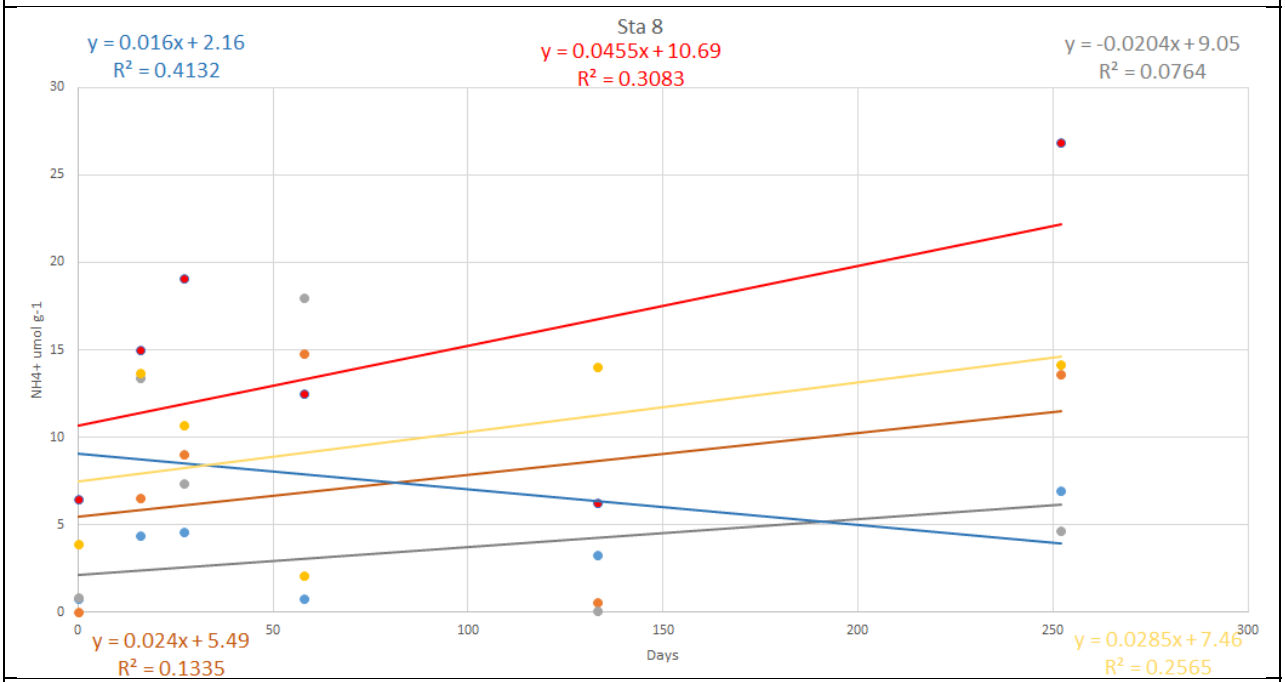

Figure 9. Deep core diagenesis analysis of station 8 for organic nitrogen-NH_4

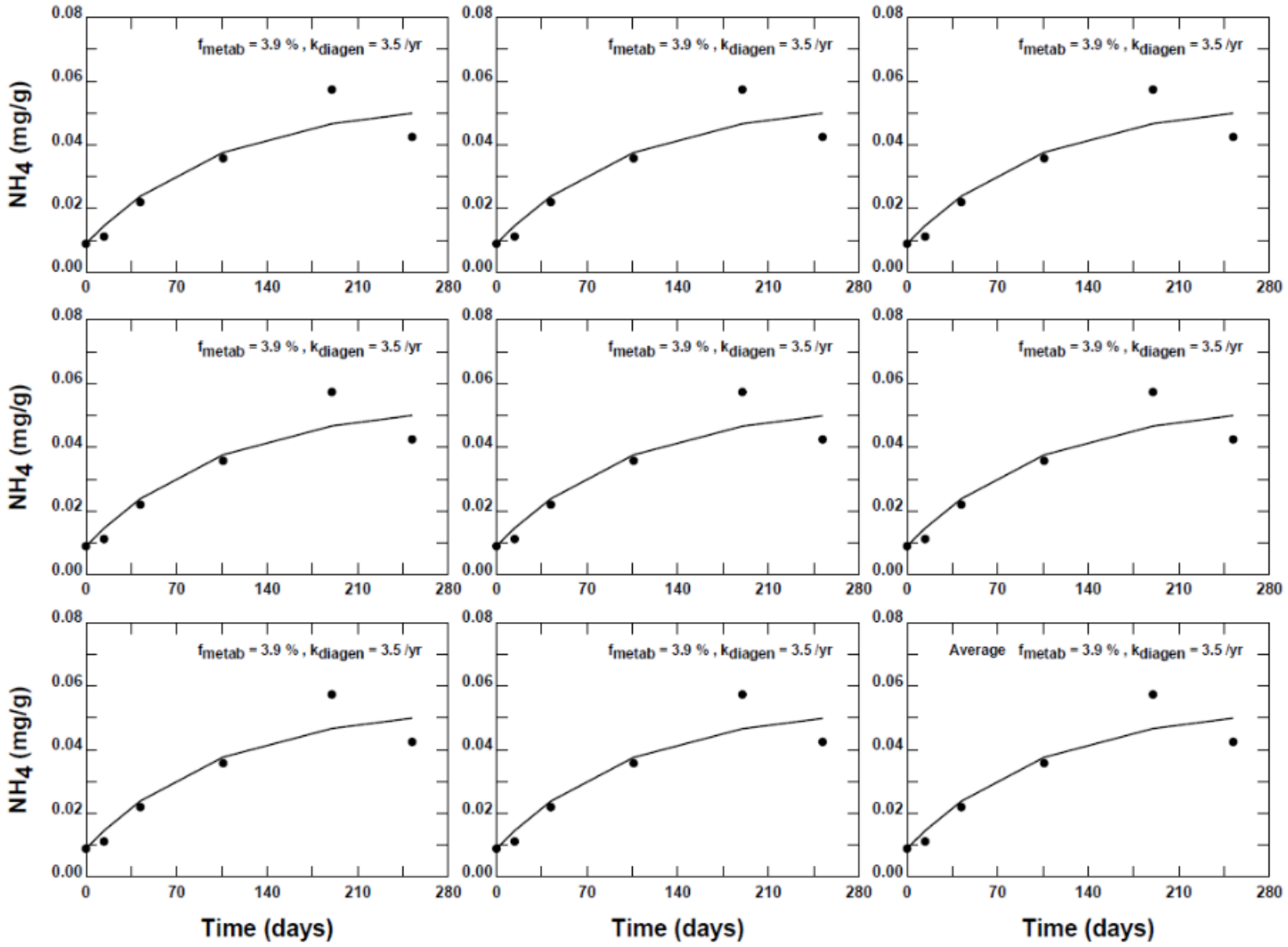

Figure 10. Diagenesis Results from Short Core 1

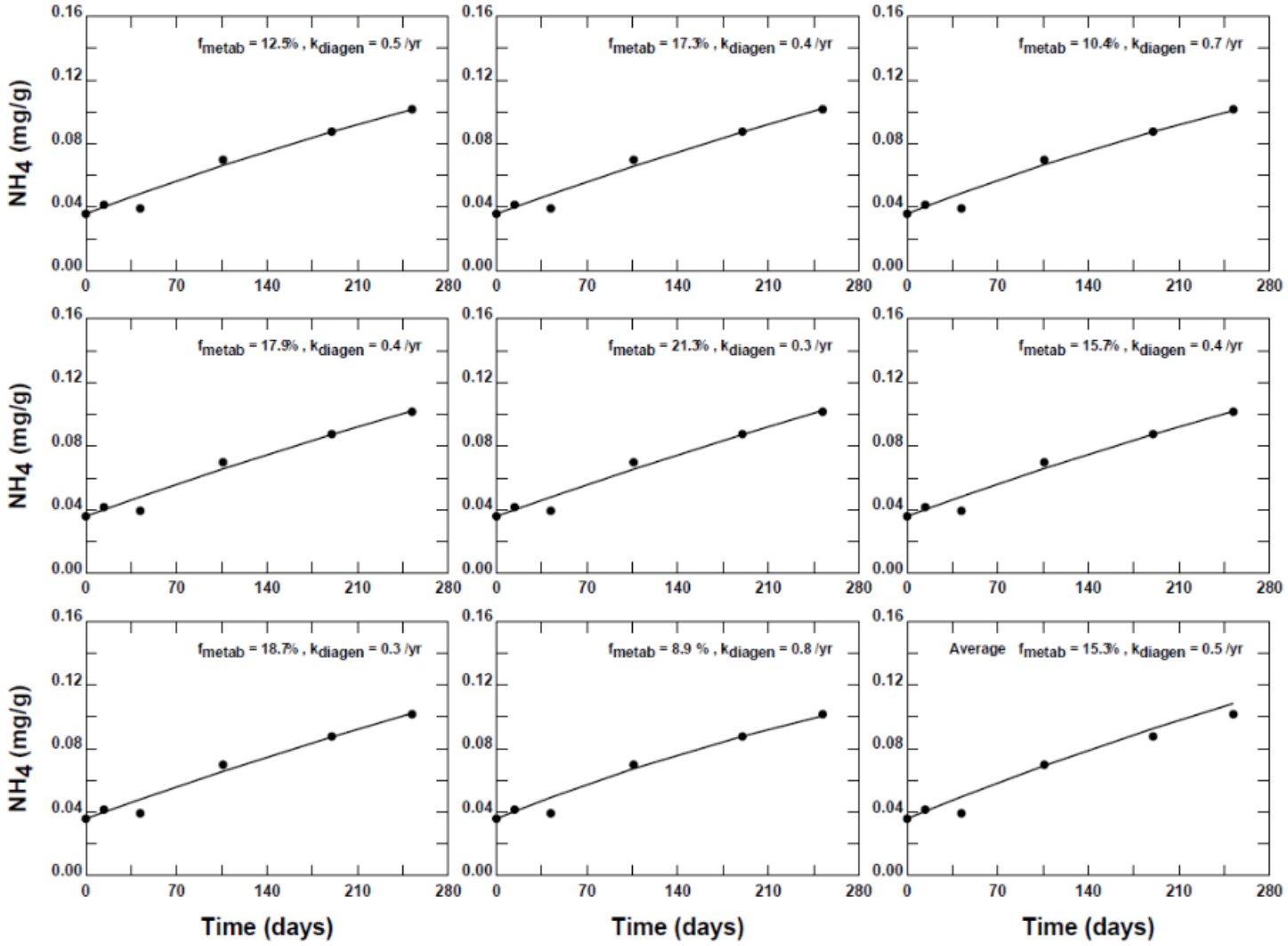

Figure 11. Diagenesis Results from Short Core 8rep

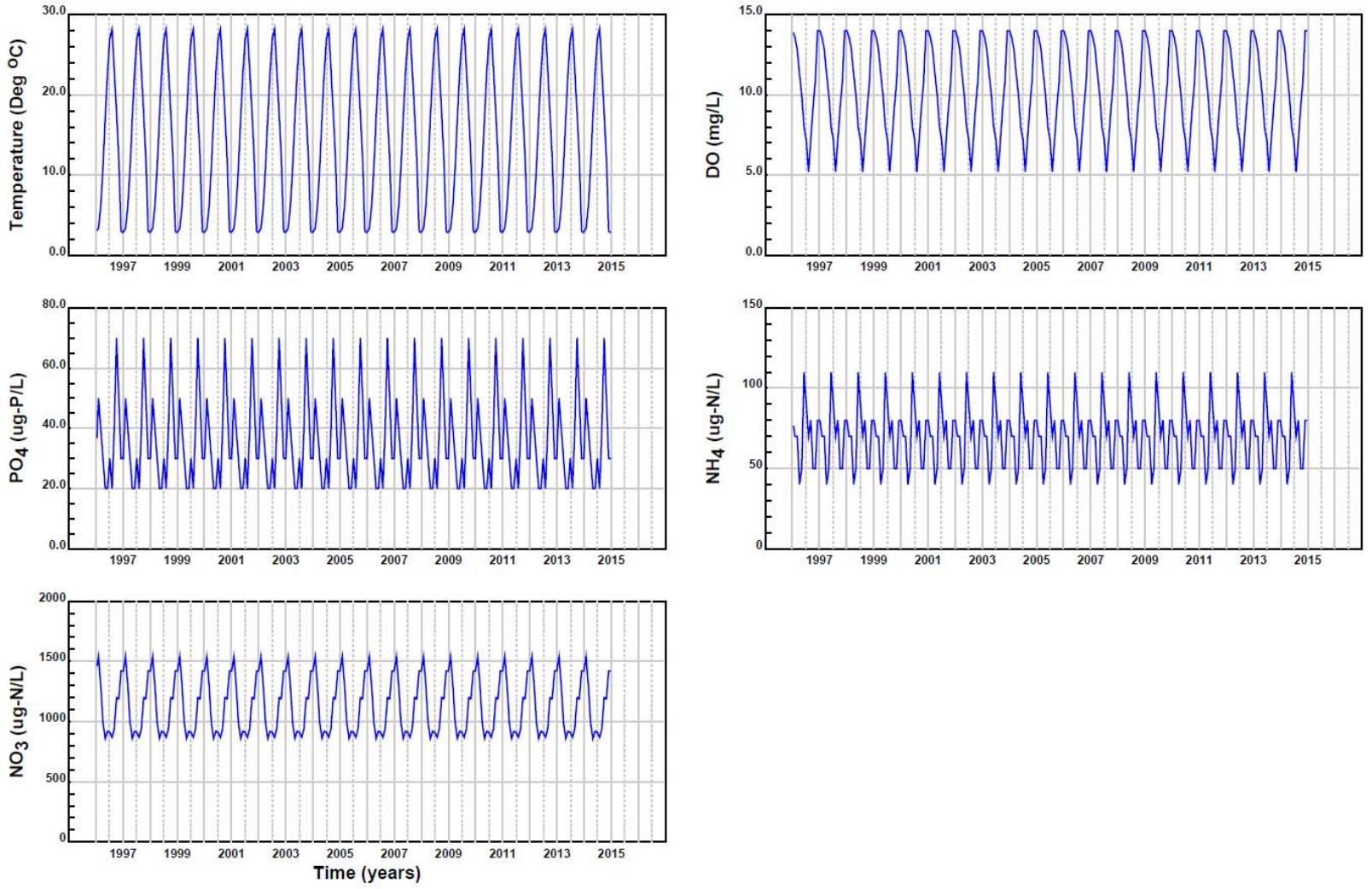

Figure 12. Overlying water column temperature, DO and nutrients for stand-alone SFM

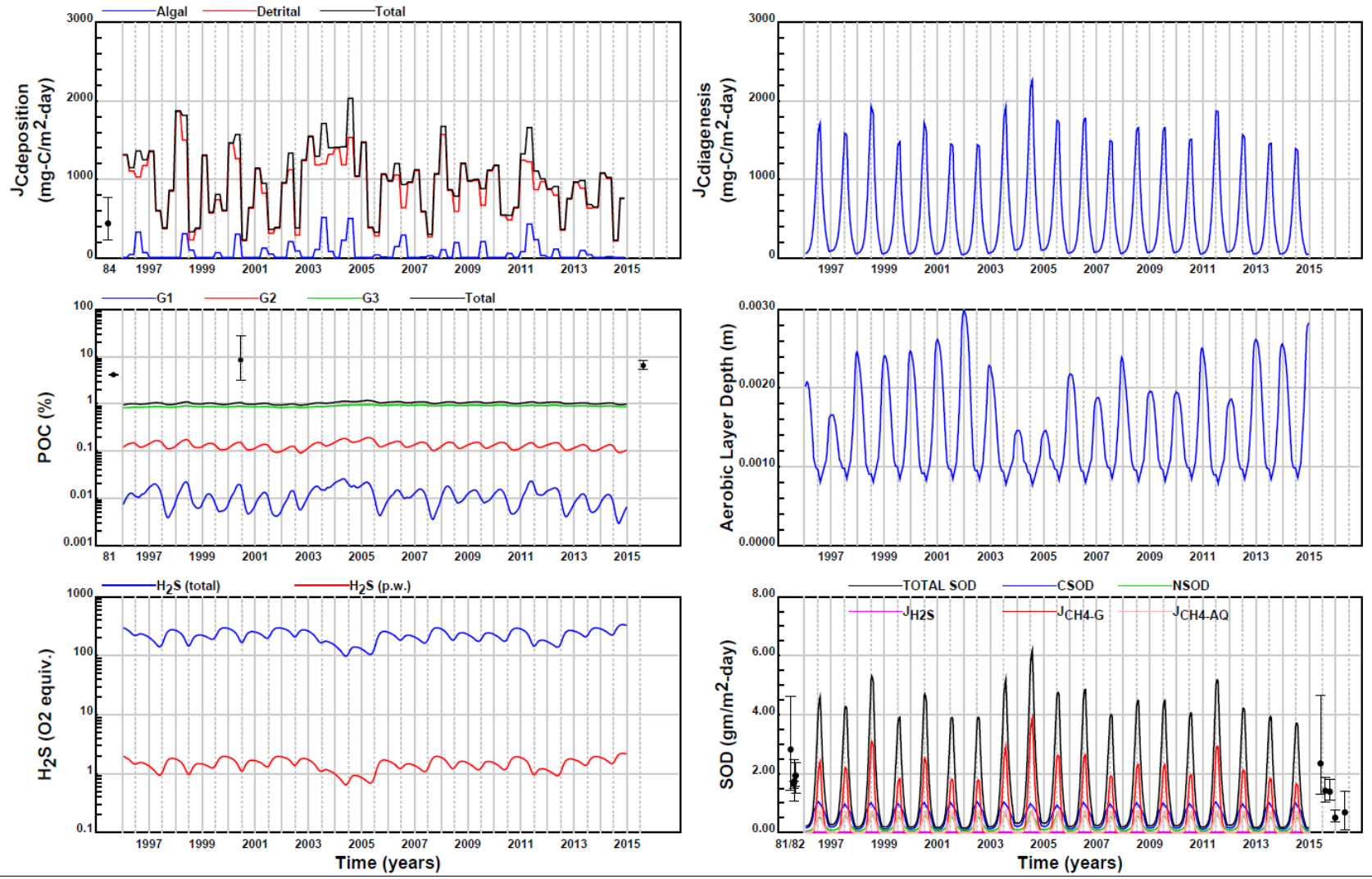

Figure 13. Carbon and SOD calibration results from Run 05

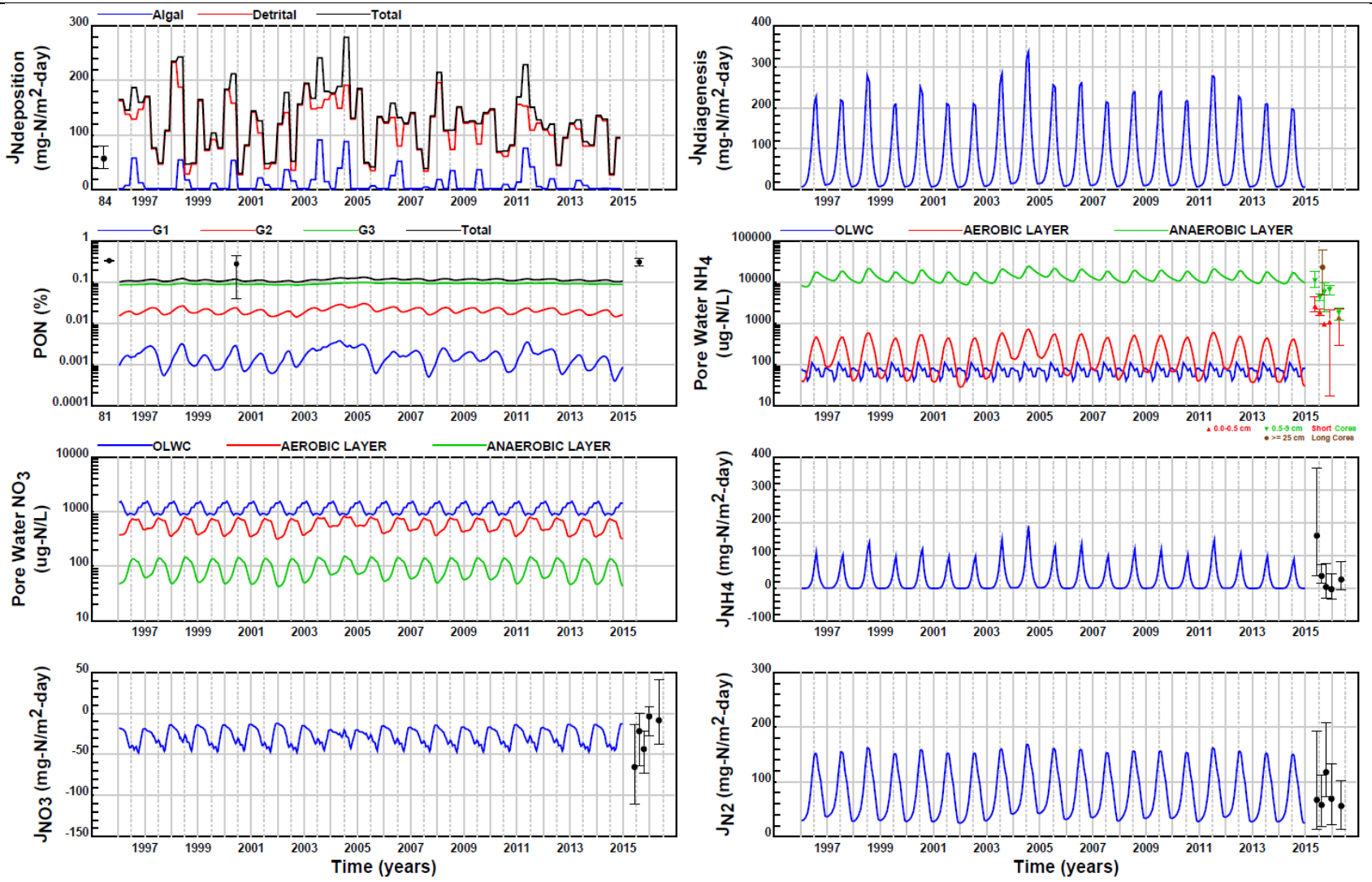

Figure 14. Nitrogen calibration results from Run 05

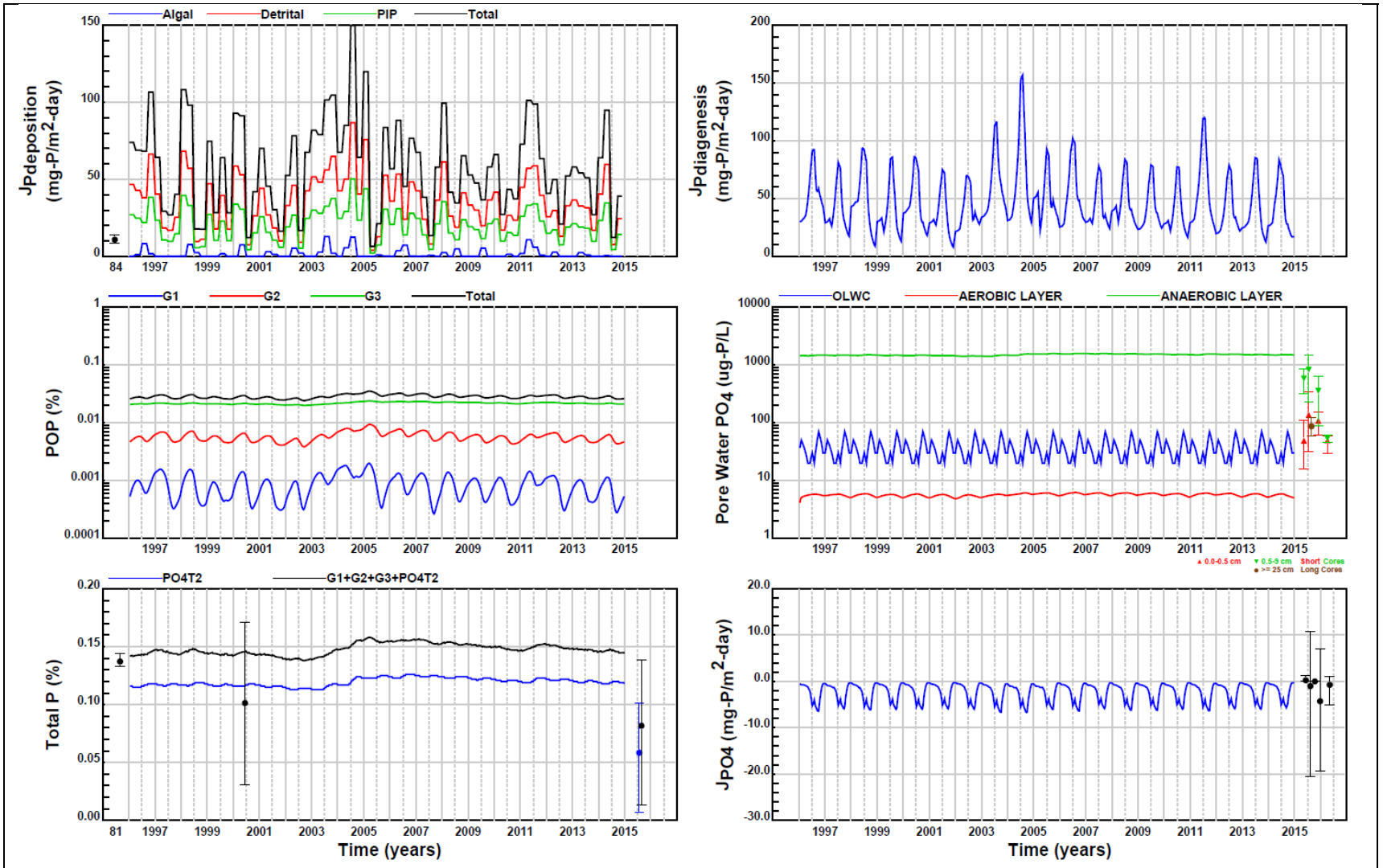

Figure 15. Phosphorus calibration results from Run 05

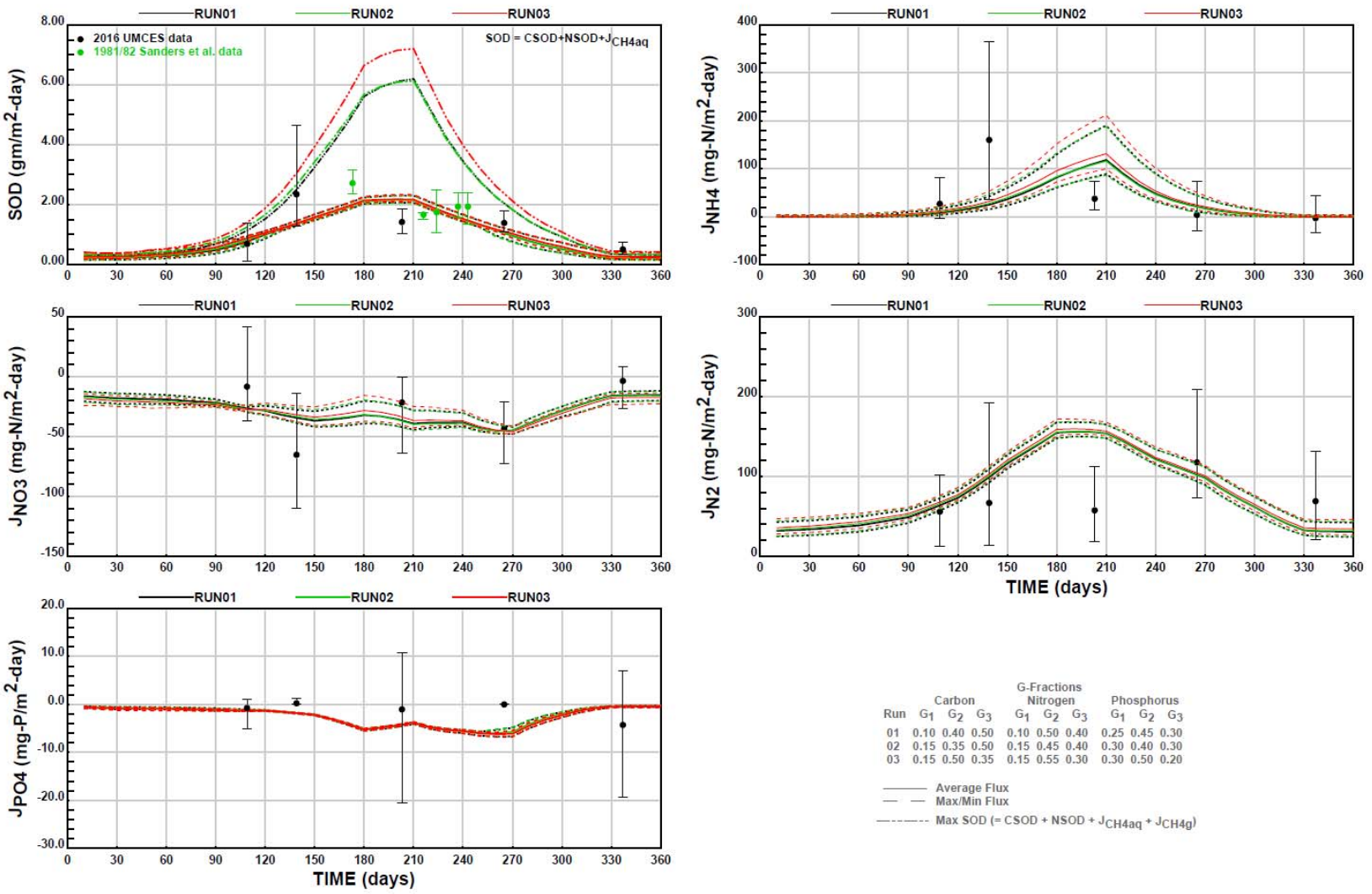

Figure 16. Comparison of flux calculations from Runs 01, 02 and 03

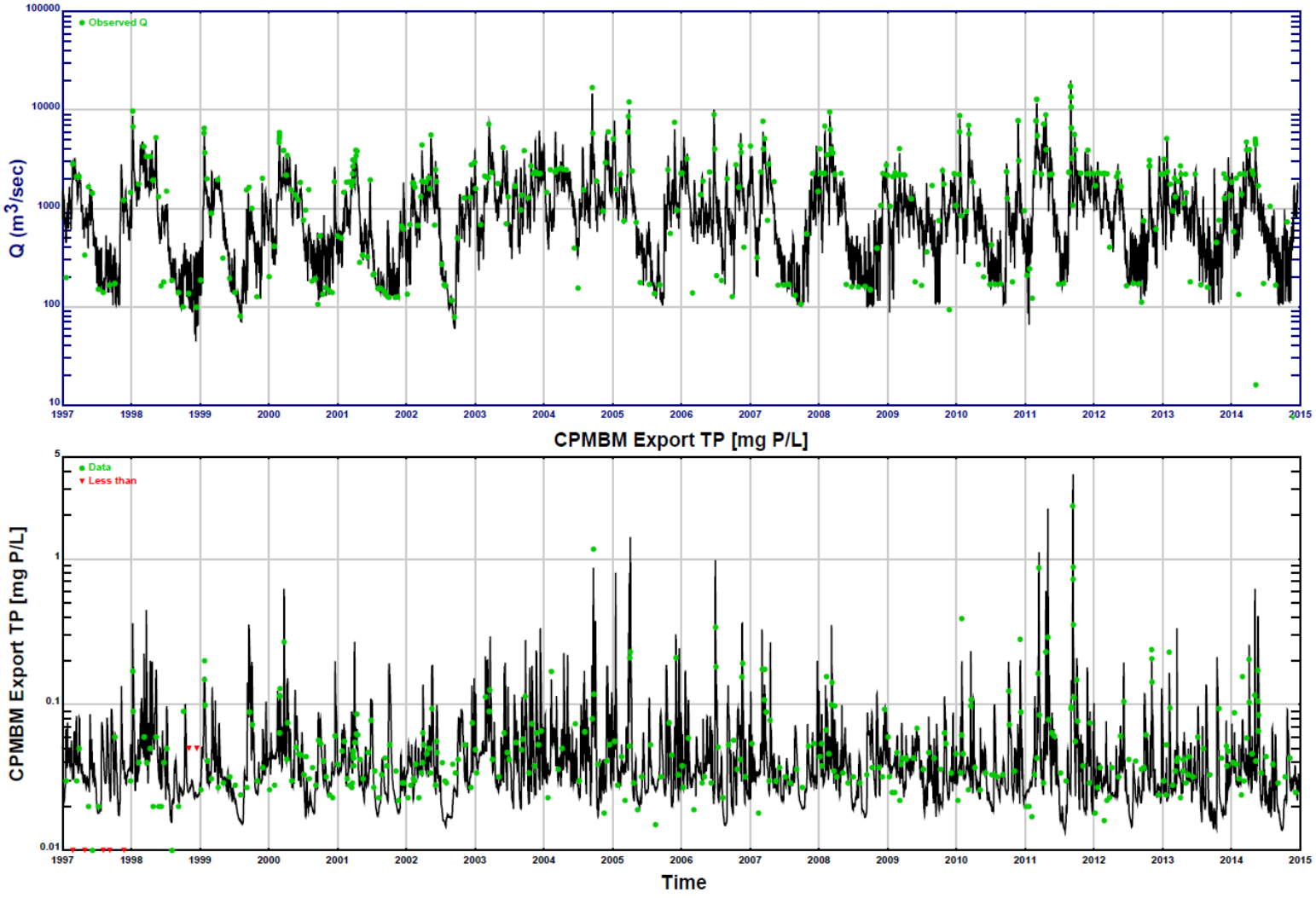

Figure 17. Calibration results for flow and total phosphorus.

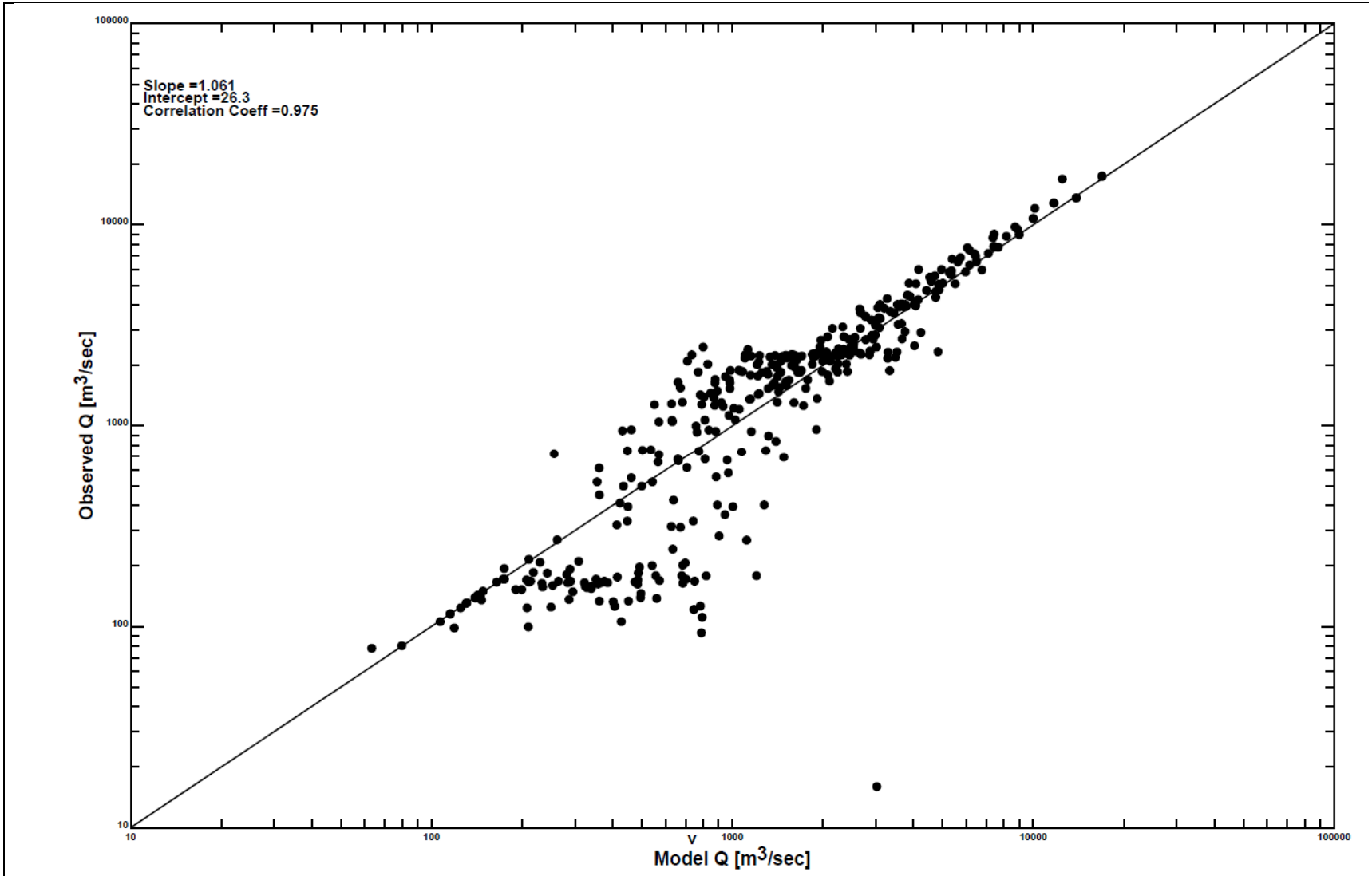

Figure 18. Cross-correlation of observed flow and CPMBM flow

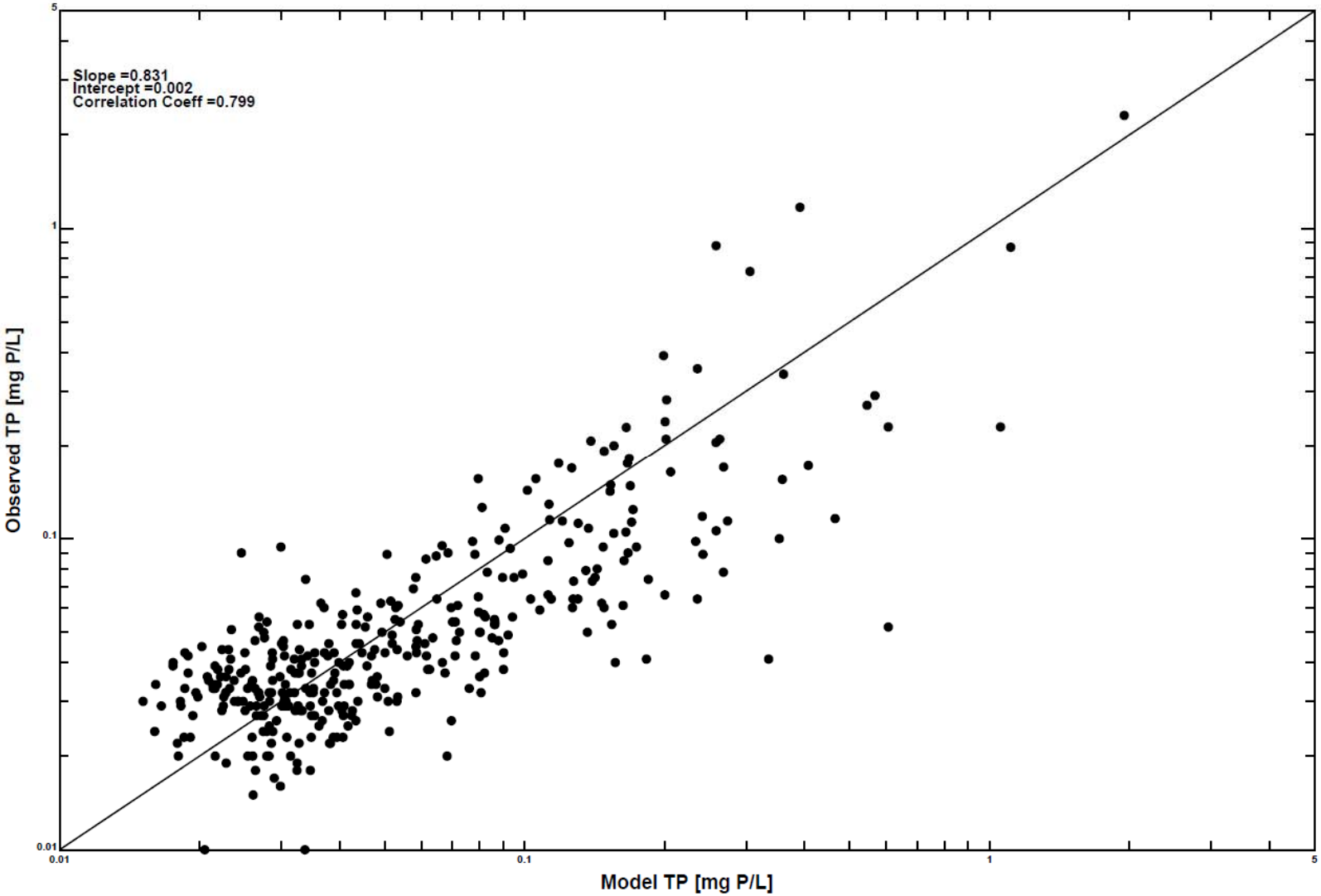

Figure 19. Cross-correlation of observed outflow TP and CPMBM TP.

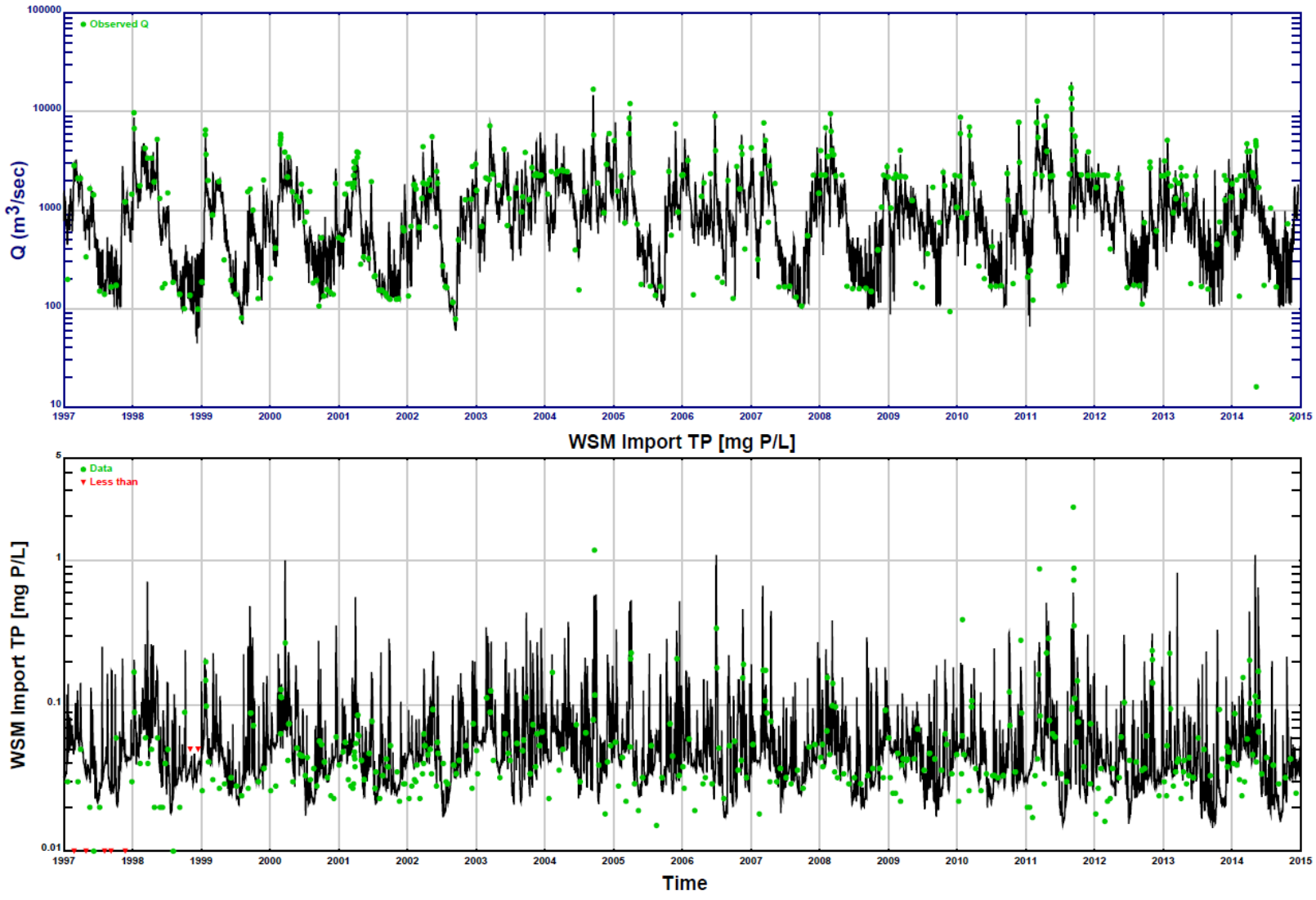

Figure 20. Observed outflow TP versus WSM TP.

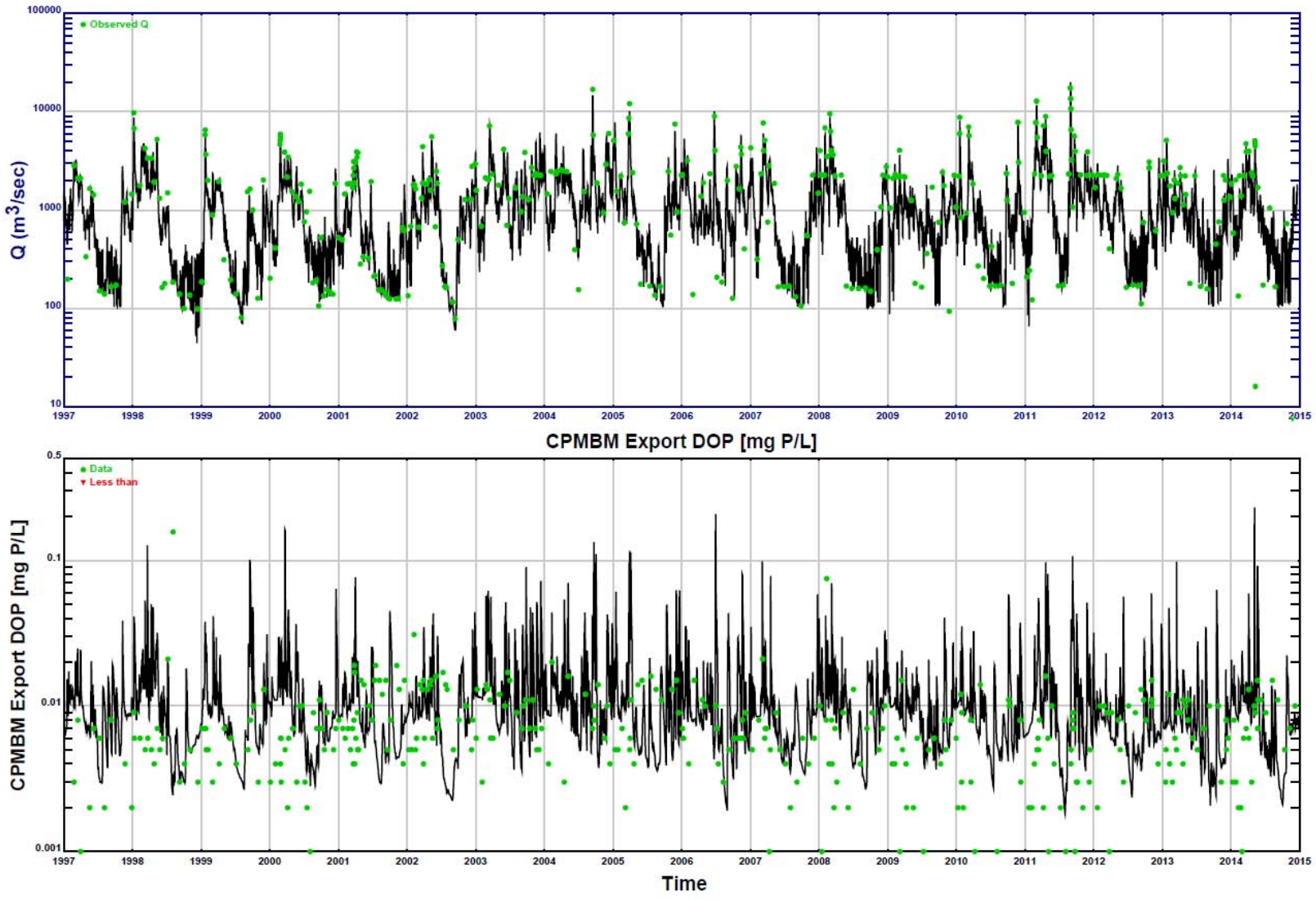

Figure 21. Calibration results for DOP

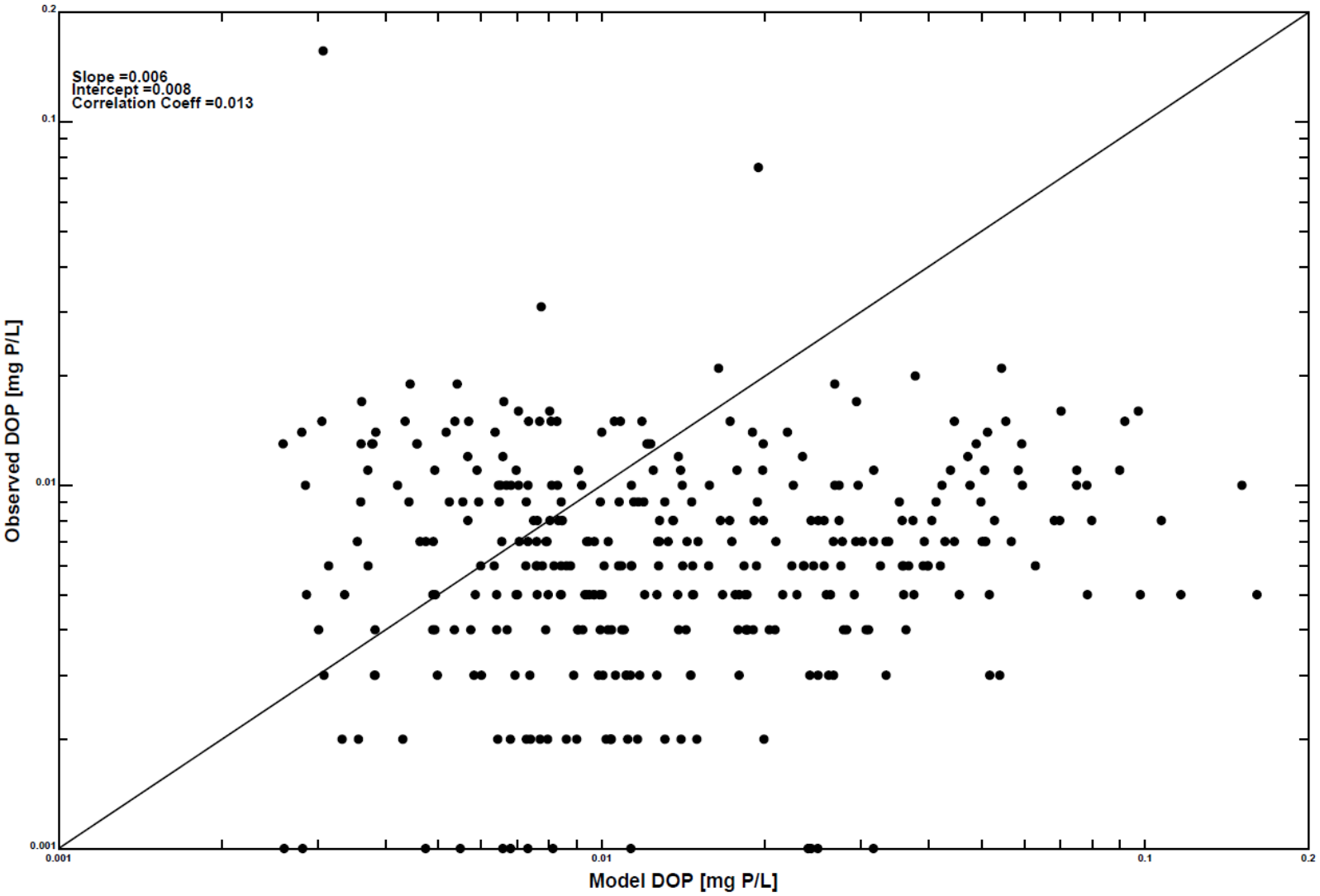

Figure 22. Cross-correlation of observed outflow DOP versus CPMBM DOP.

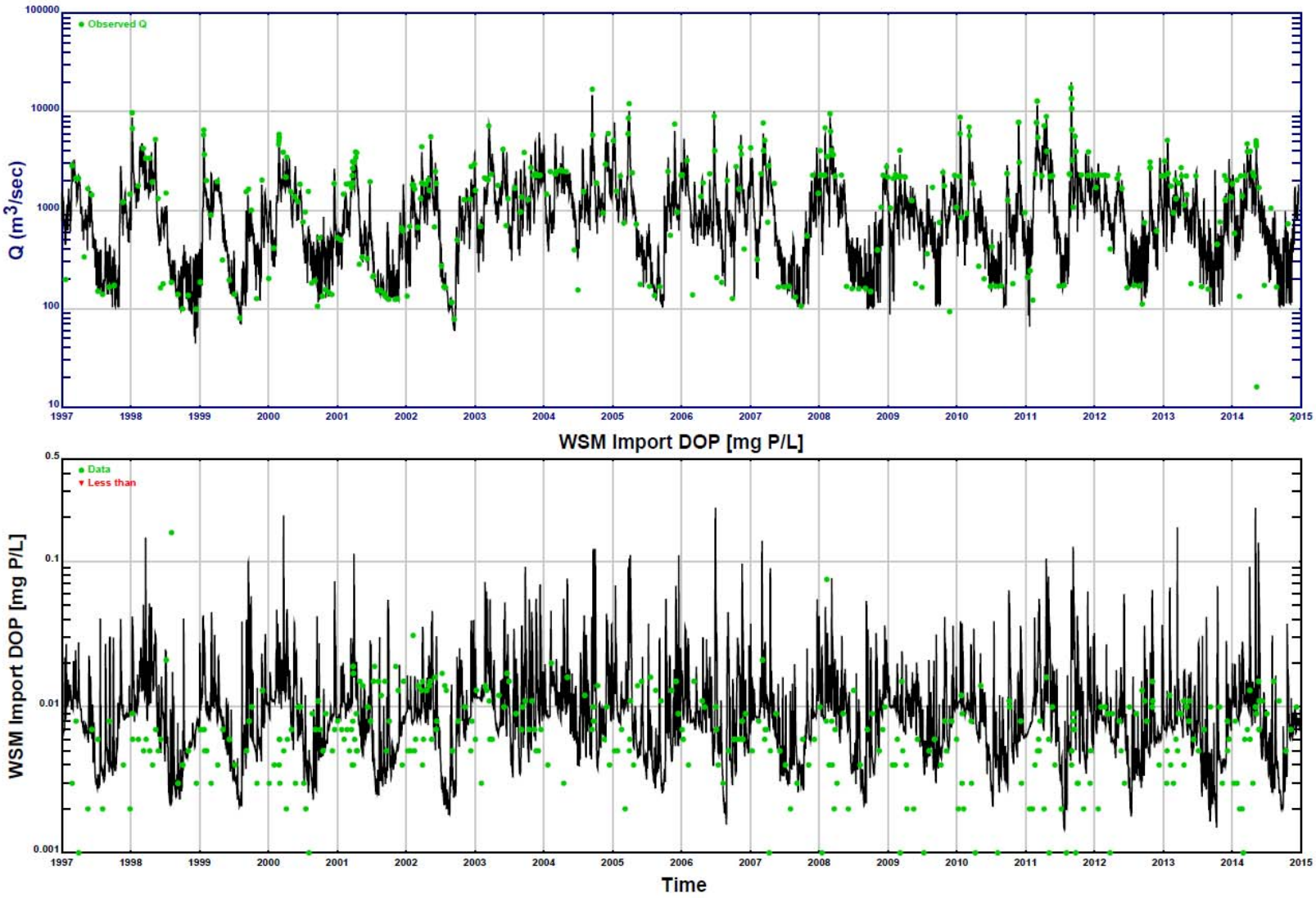

Figure 23. Observed outflow DOP versus WSM DOP.

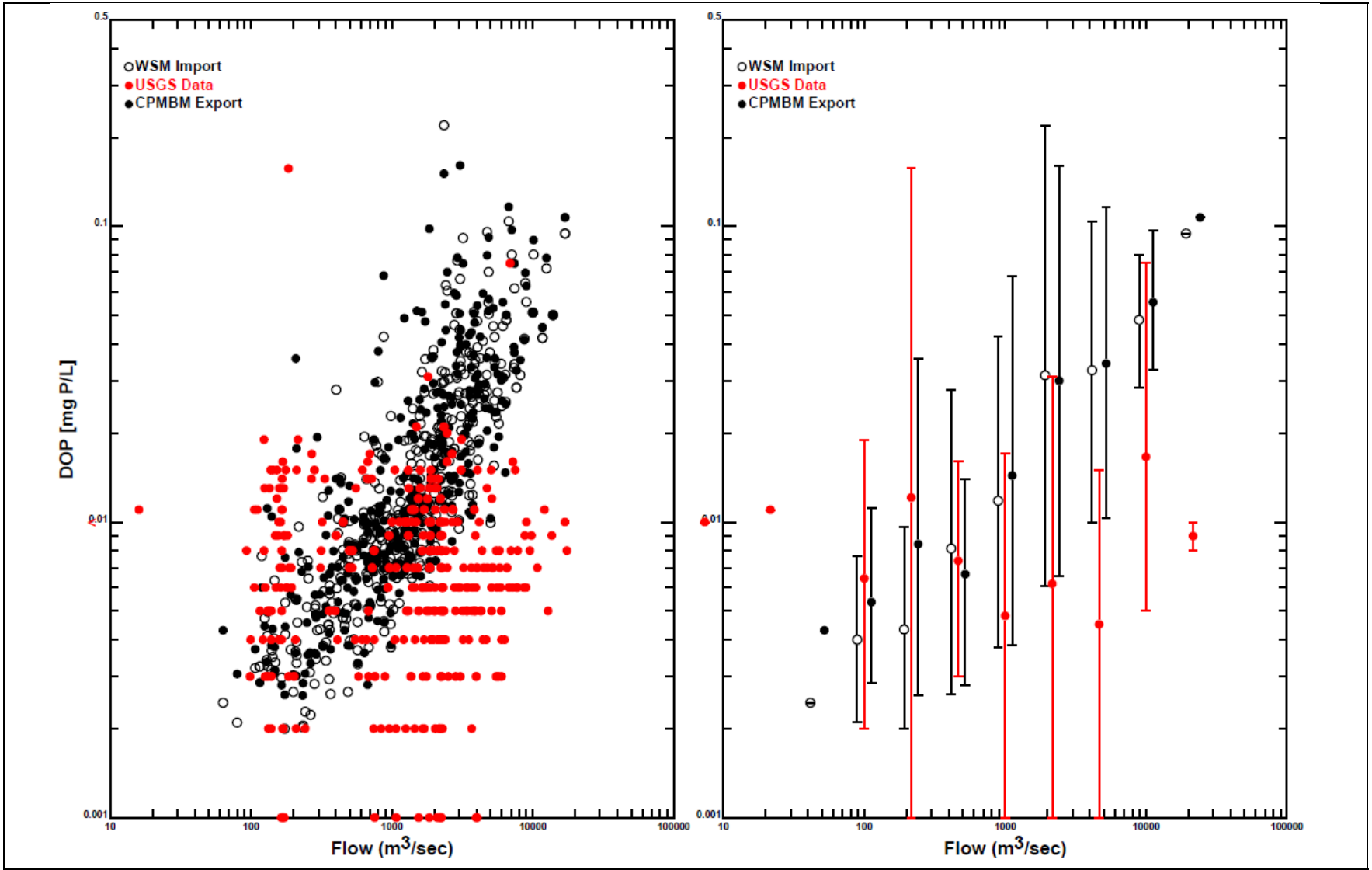

Figure 24. WSM DOP, observed DOP and CPMBM DOP versus flow.

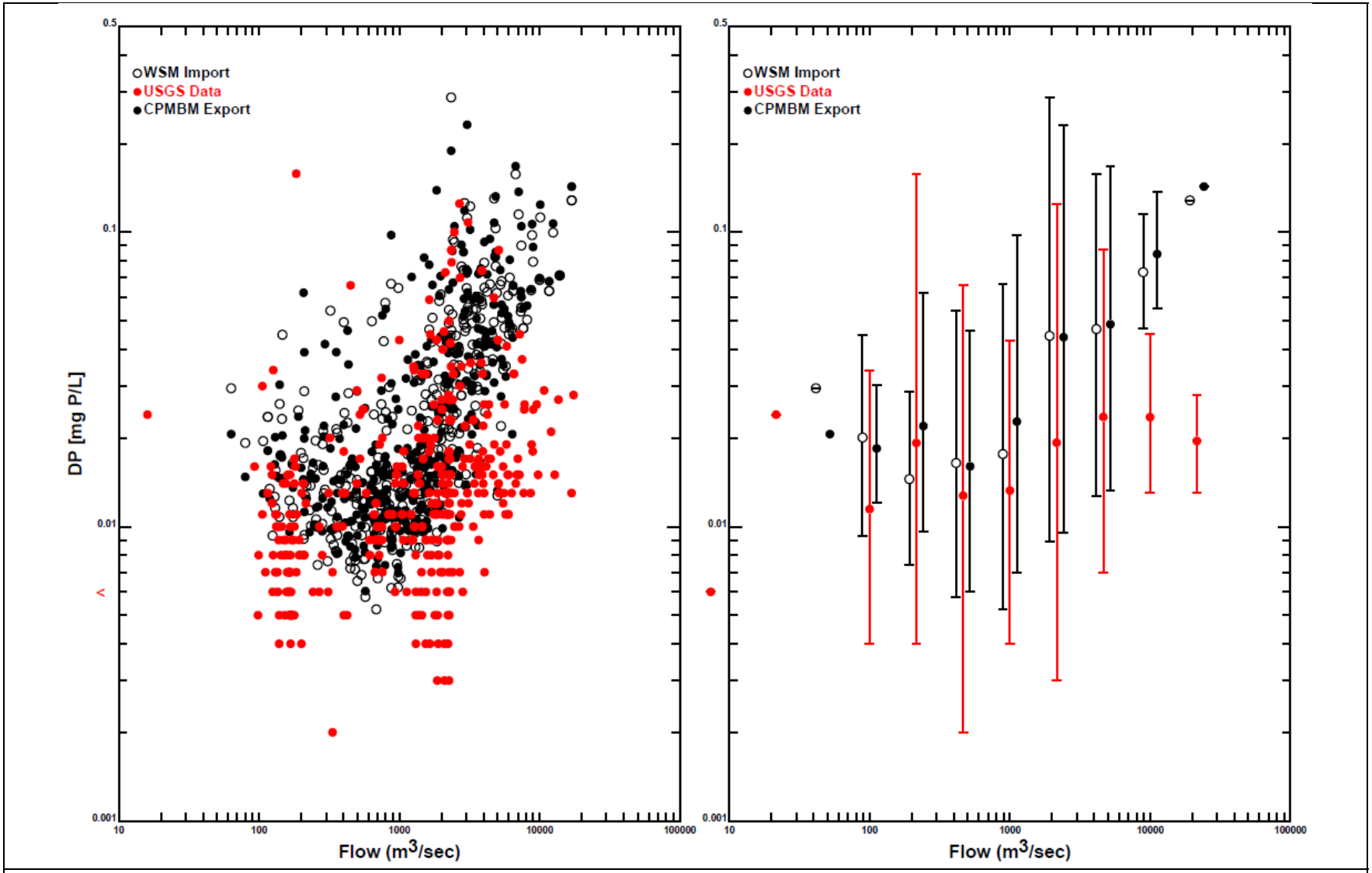

Figure 25. WSM DP, observed DP and CPMBM DP versus flow.

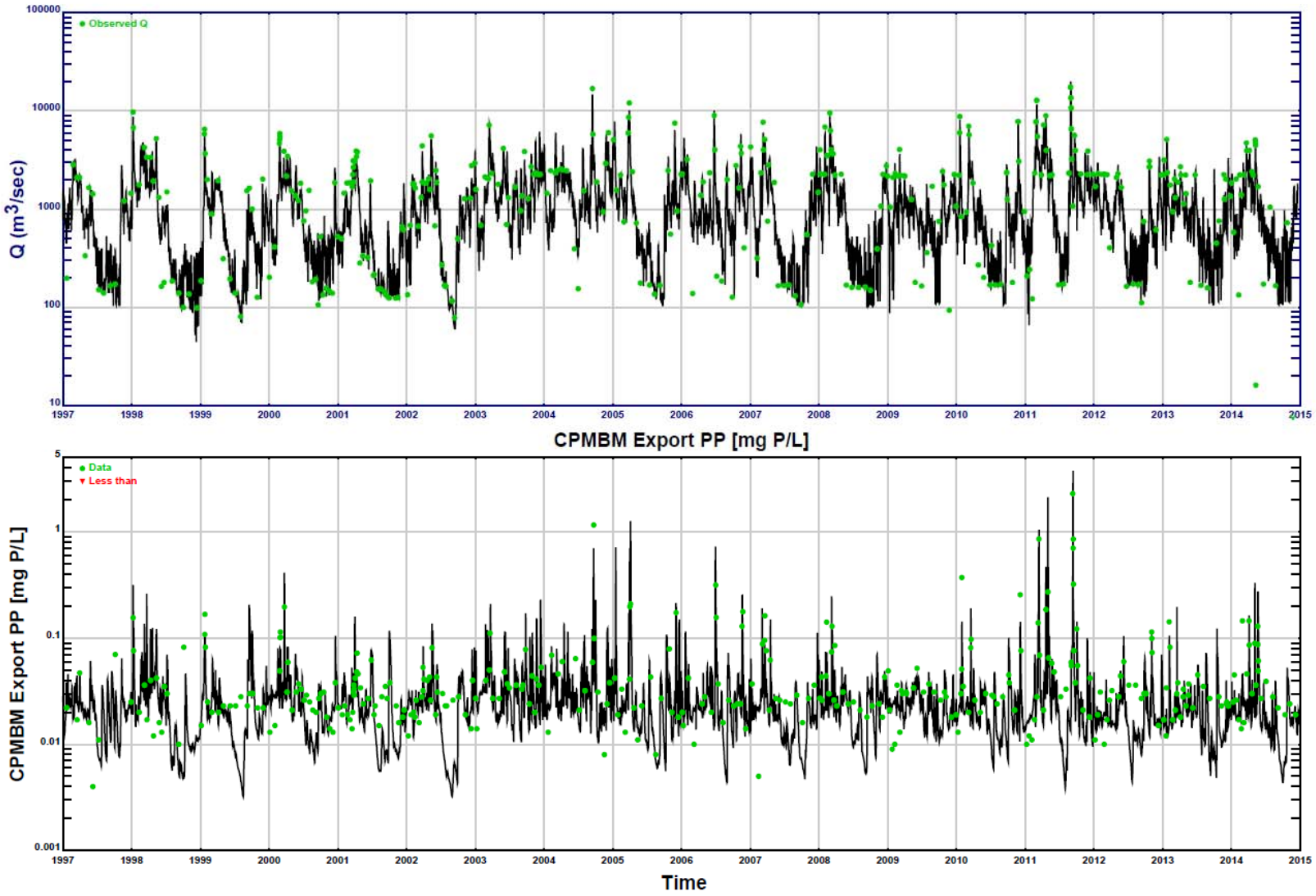

Figure 26. Calibration results for particulate phosphorus (PP).

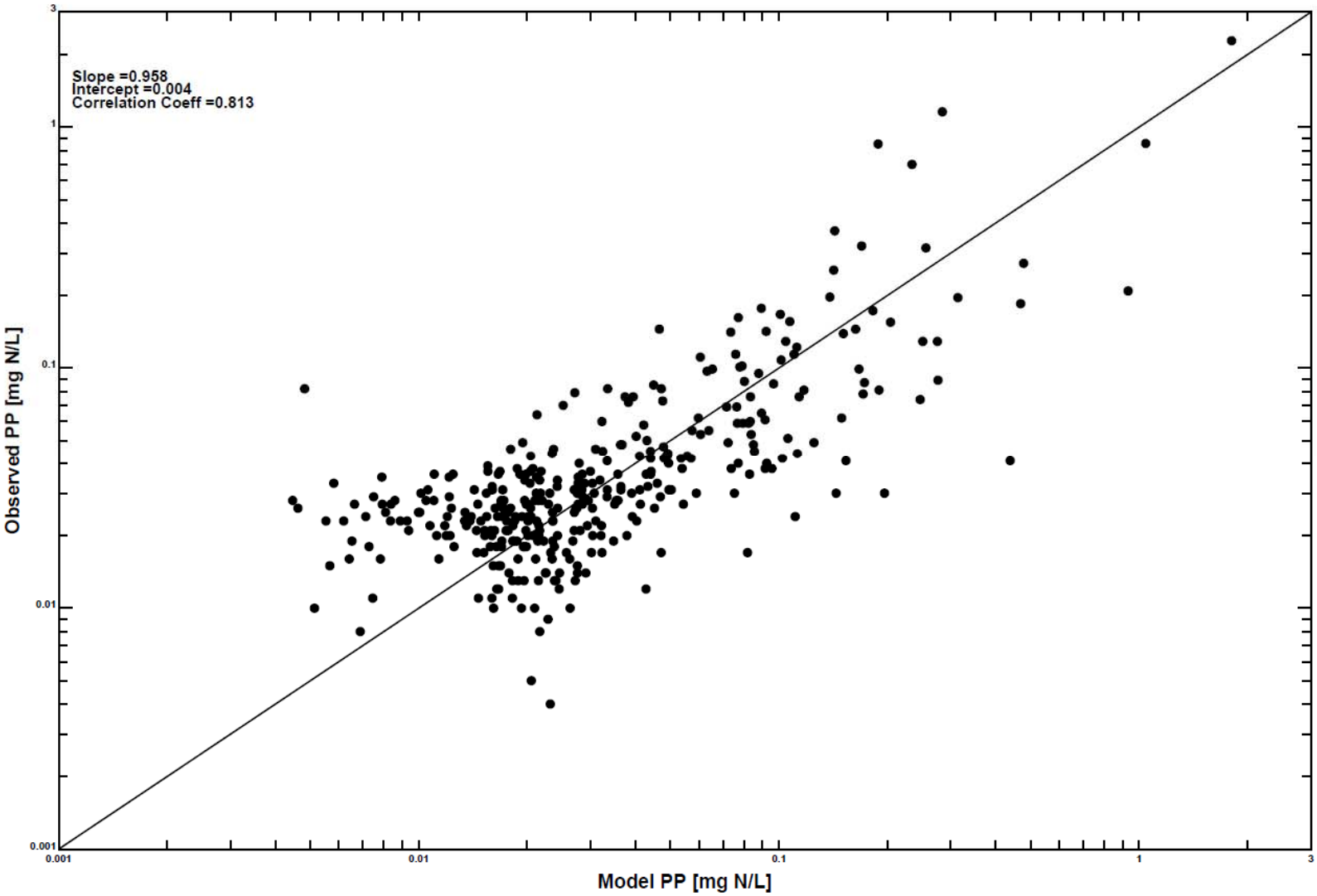

Figure 27. Cross-correlation of observed outflow PP versus CPMBM PP.

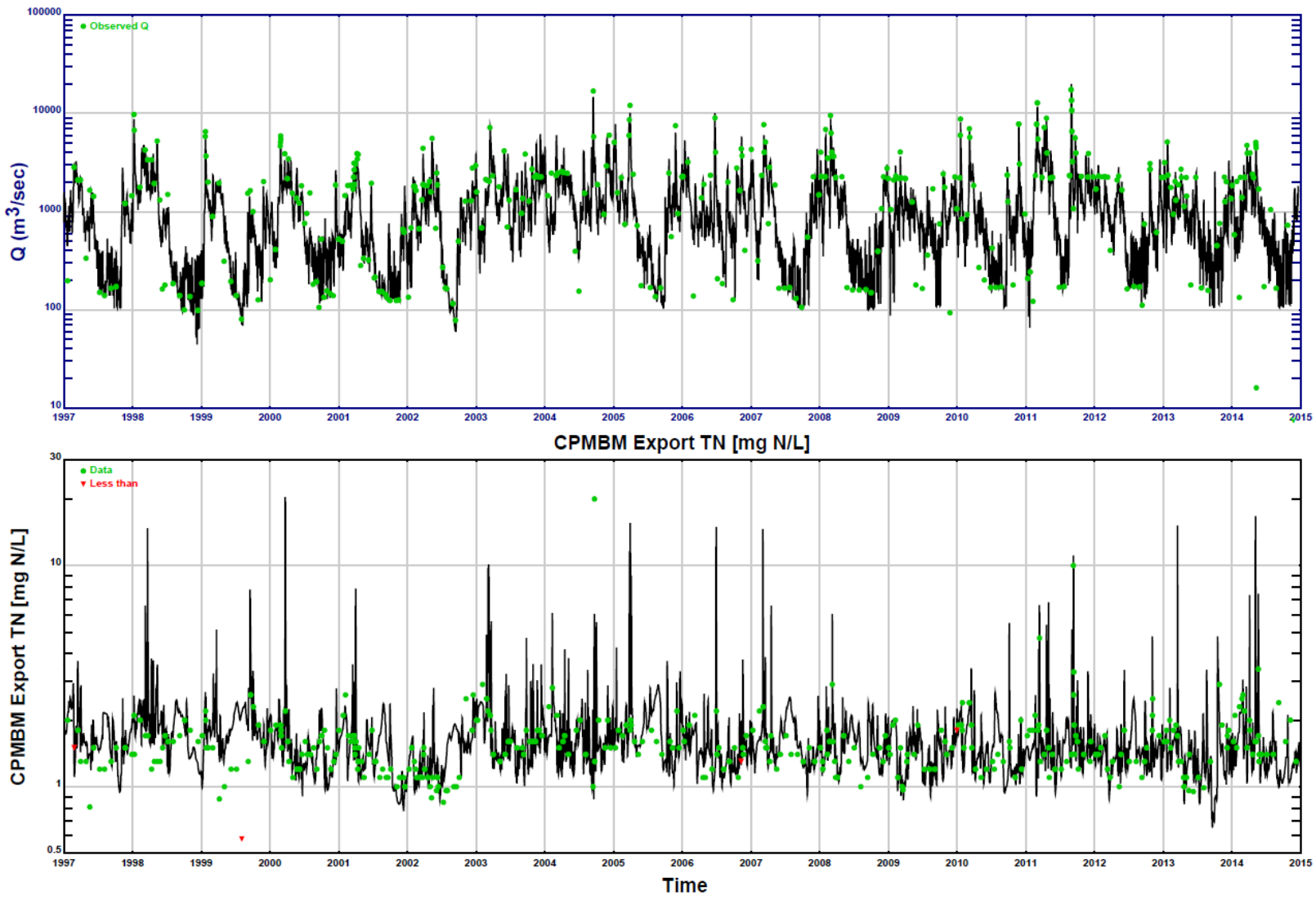

Figure 28. Calibration results for total nitrogen (TN).

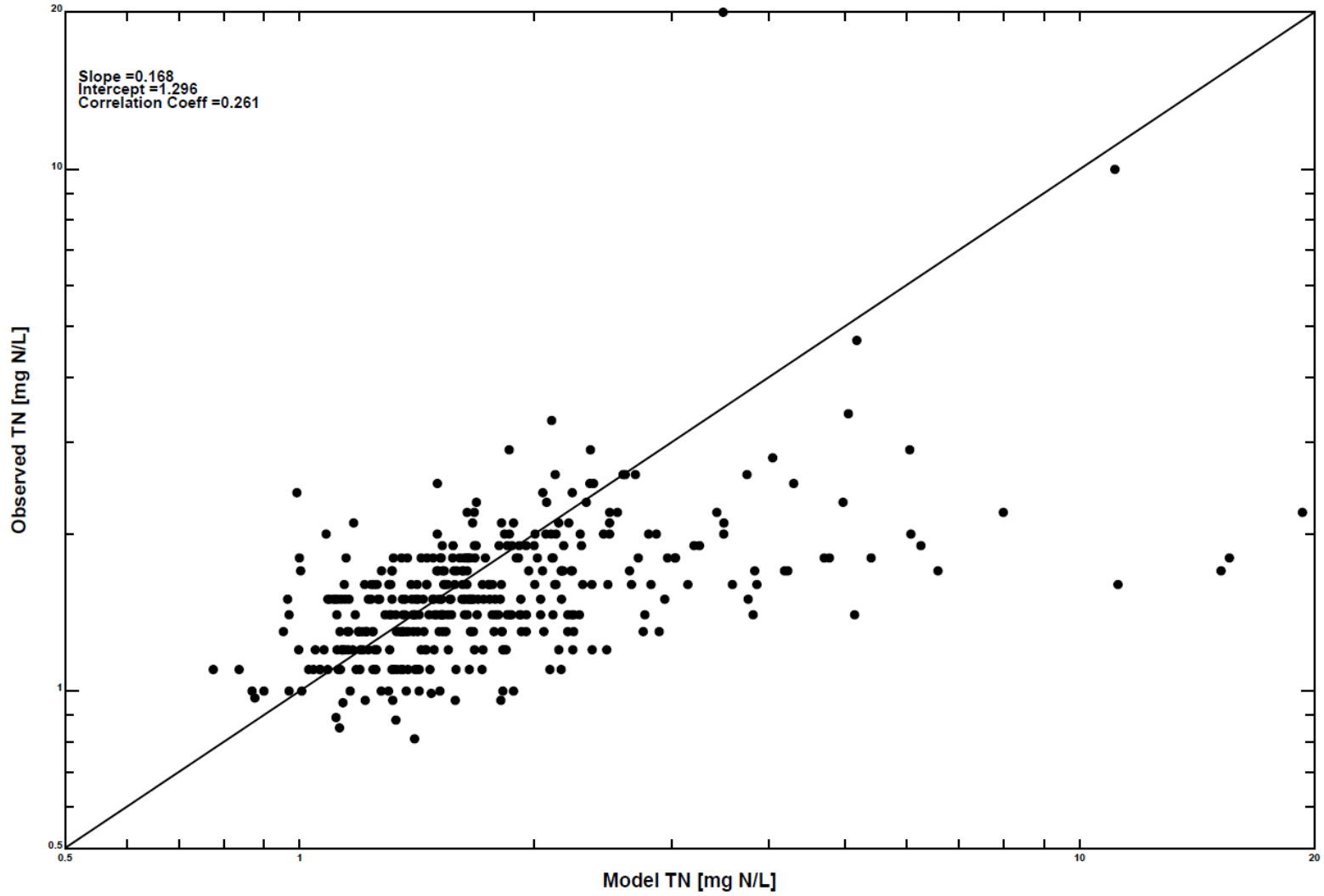

Figure 29. Cross-correlation of observed outflow TN versus CPMBM TN.

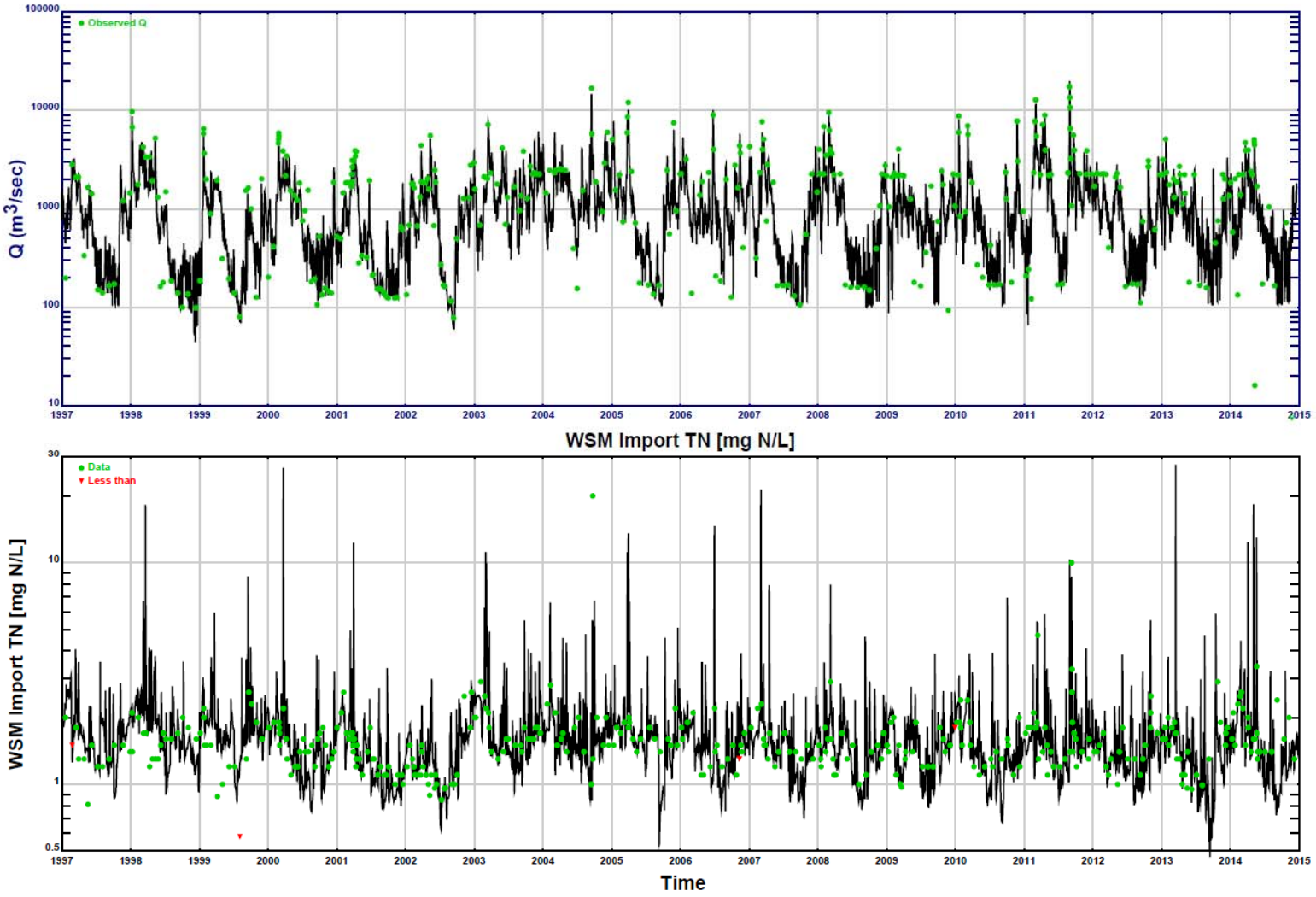

Figure 30. Observed outflow TN versus WSM TN.

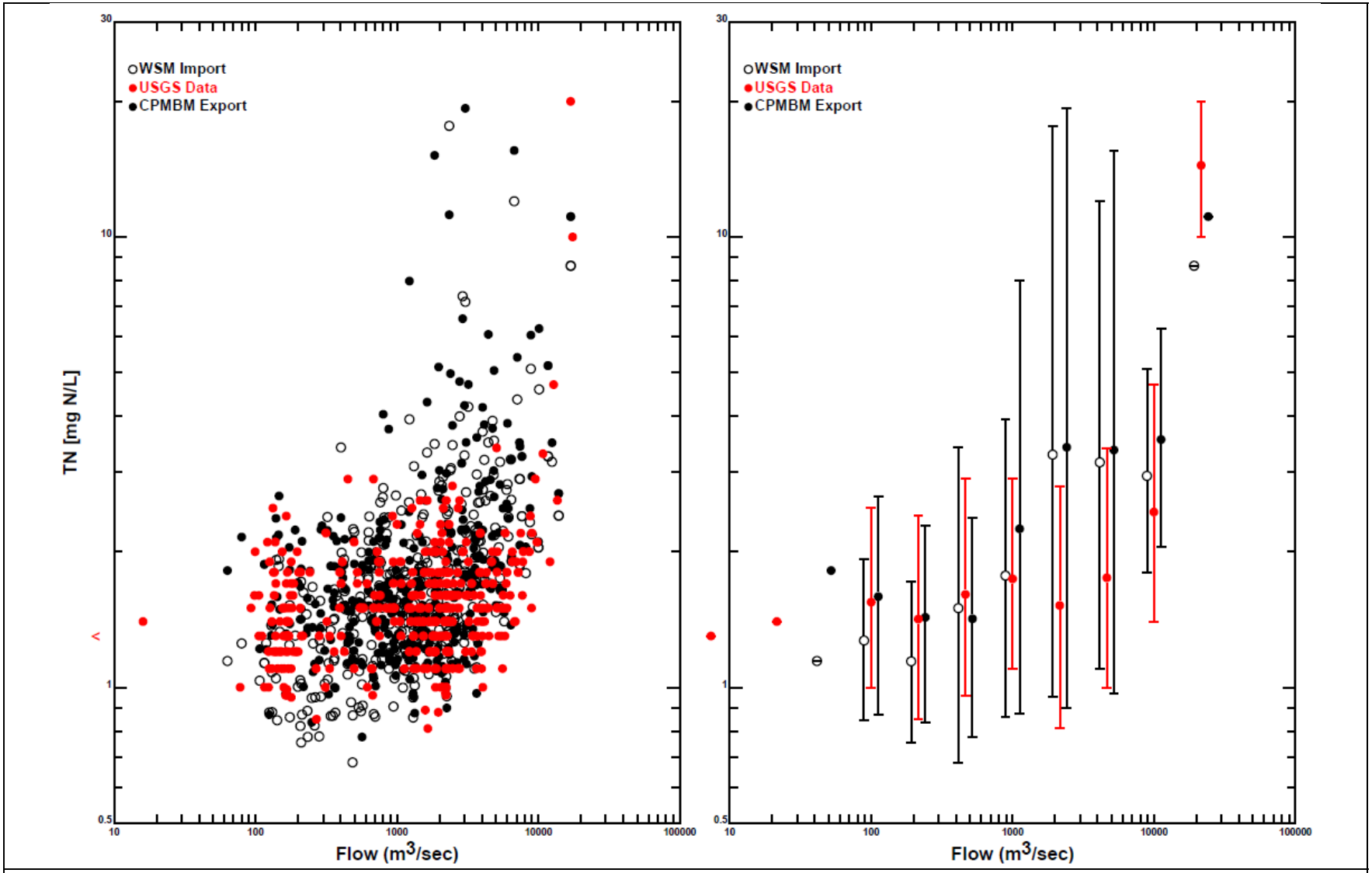

Figure 31. WSM TN observed TN and CPMBM TN versus flow.

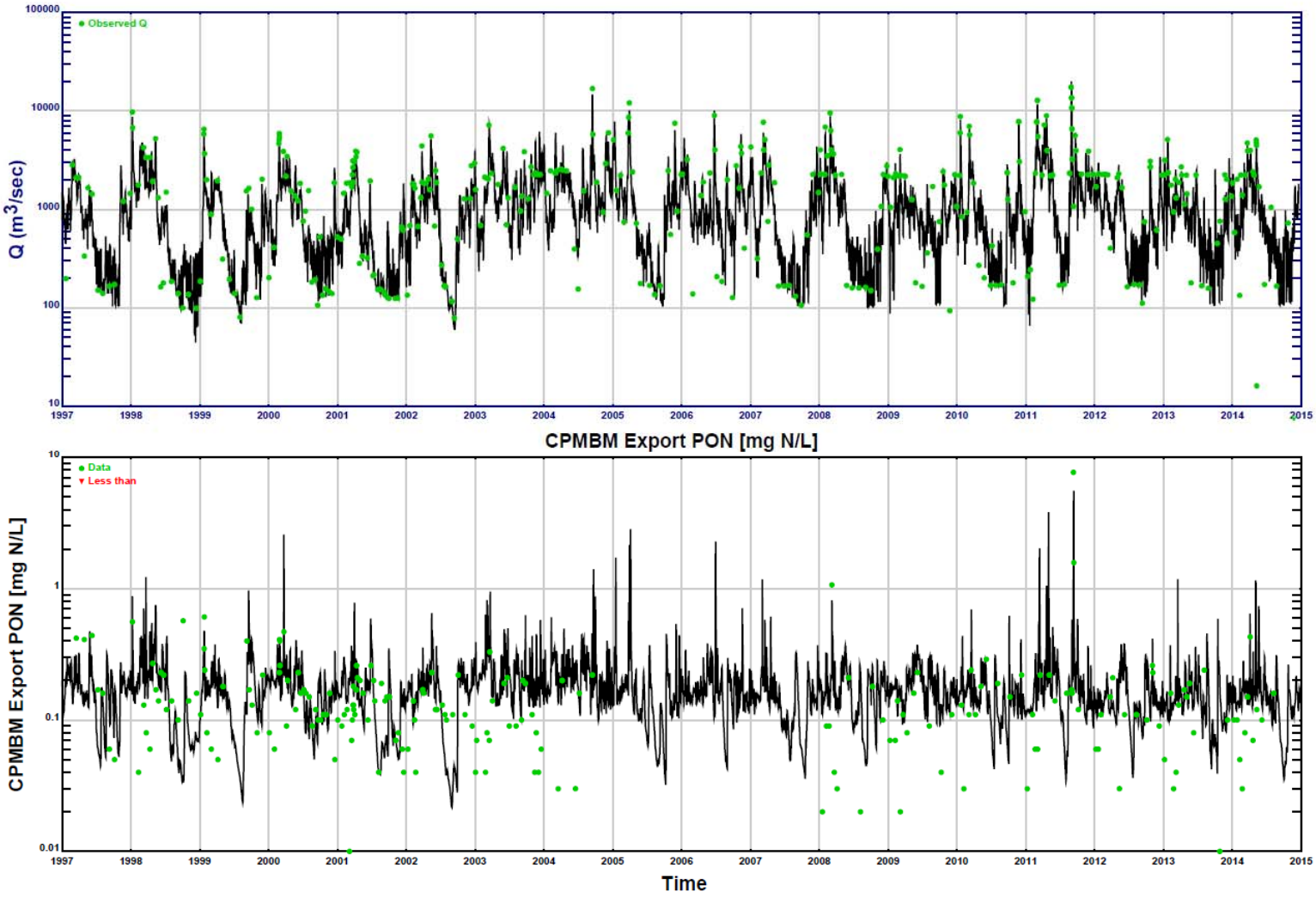

Figure 32. Calibration results for particulate organic nitrogen (PON).

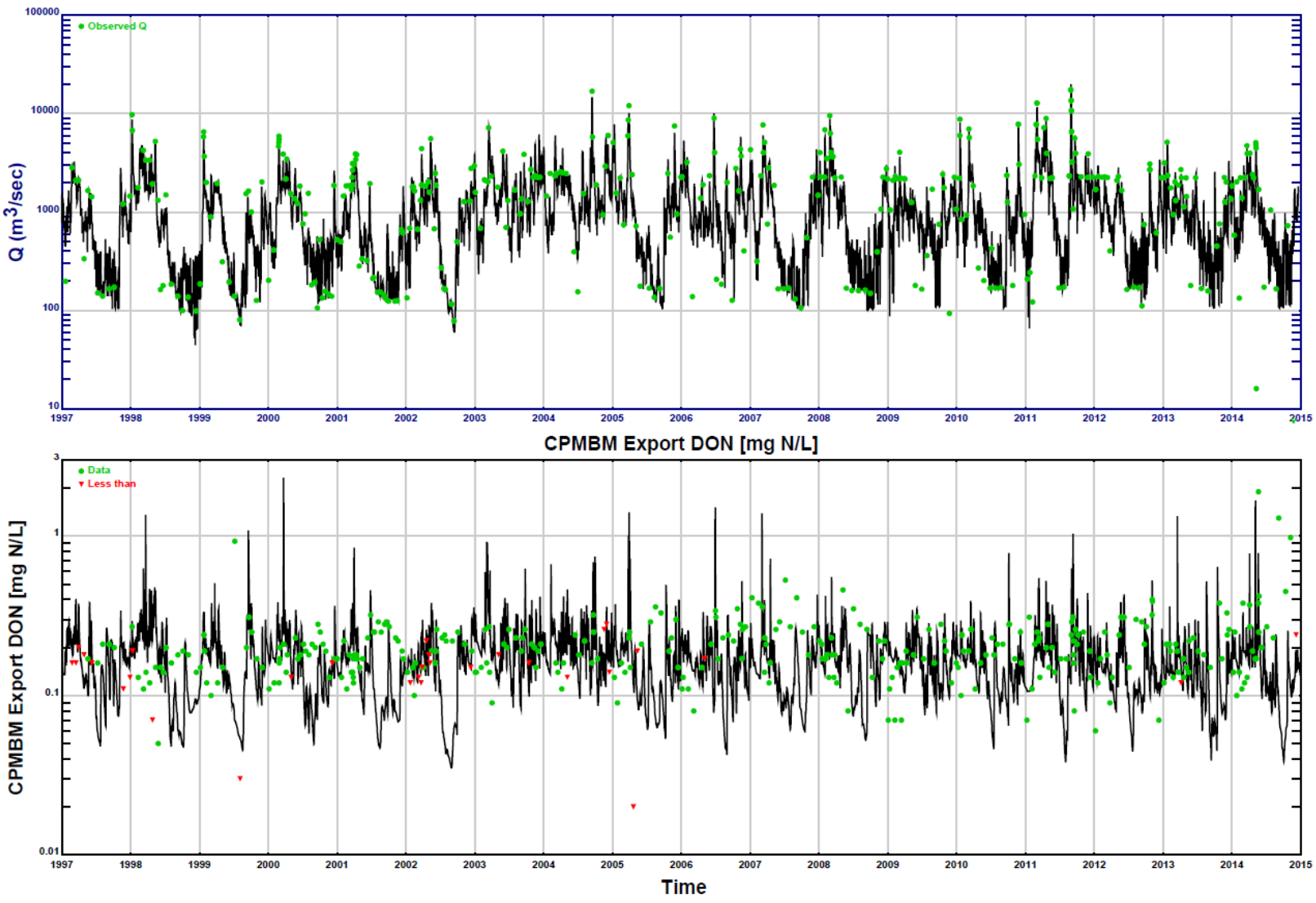

Figure 33. Calibration results for dissolved organic nitrogen (DON).

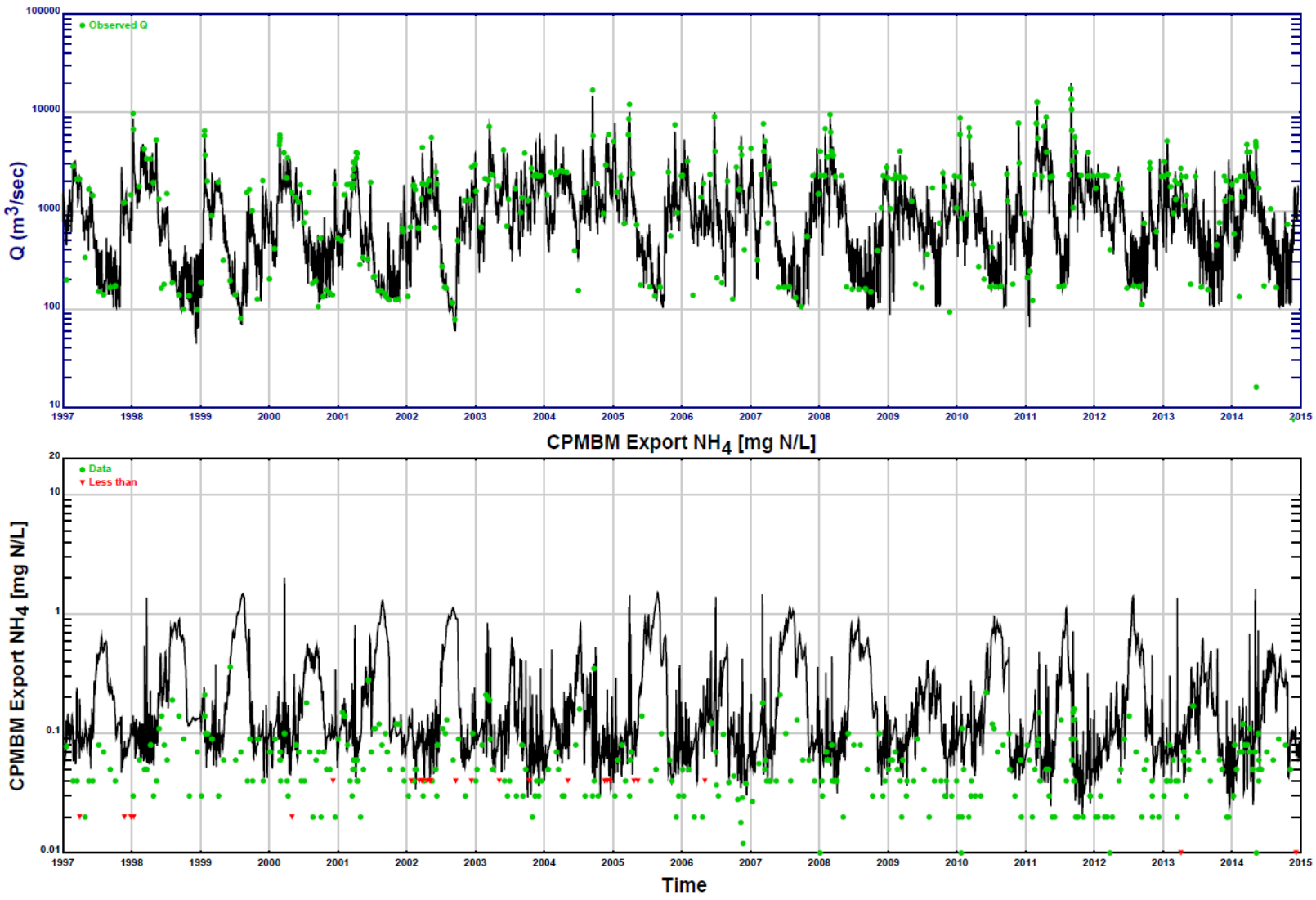

Figure 34. Calibration results for ammonium nitrogen (NH_4).

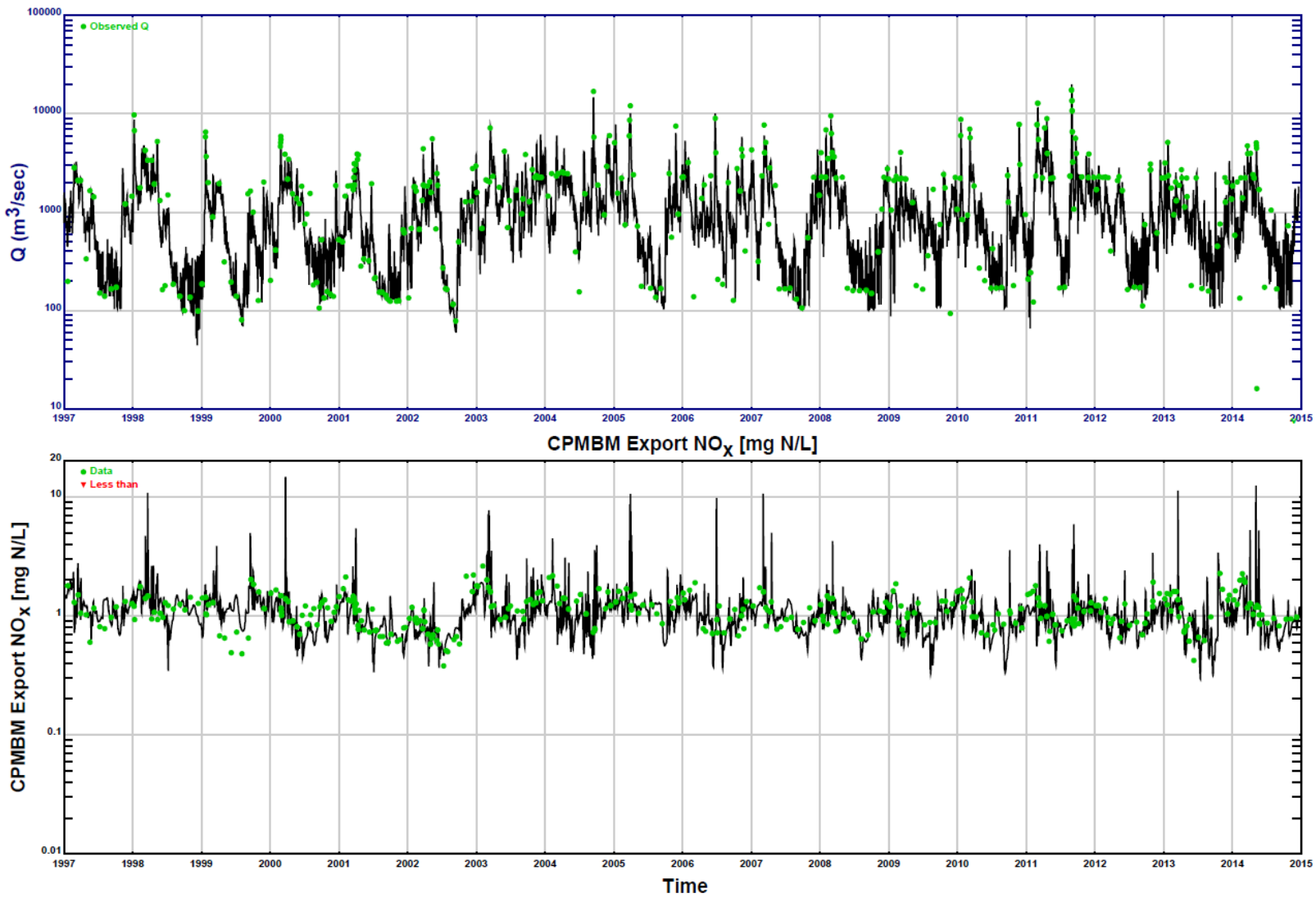

Figure 35. Calibration results for nitrate+nitrite (NO_x).

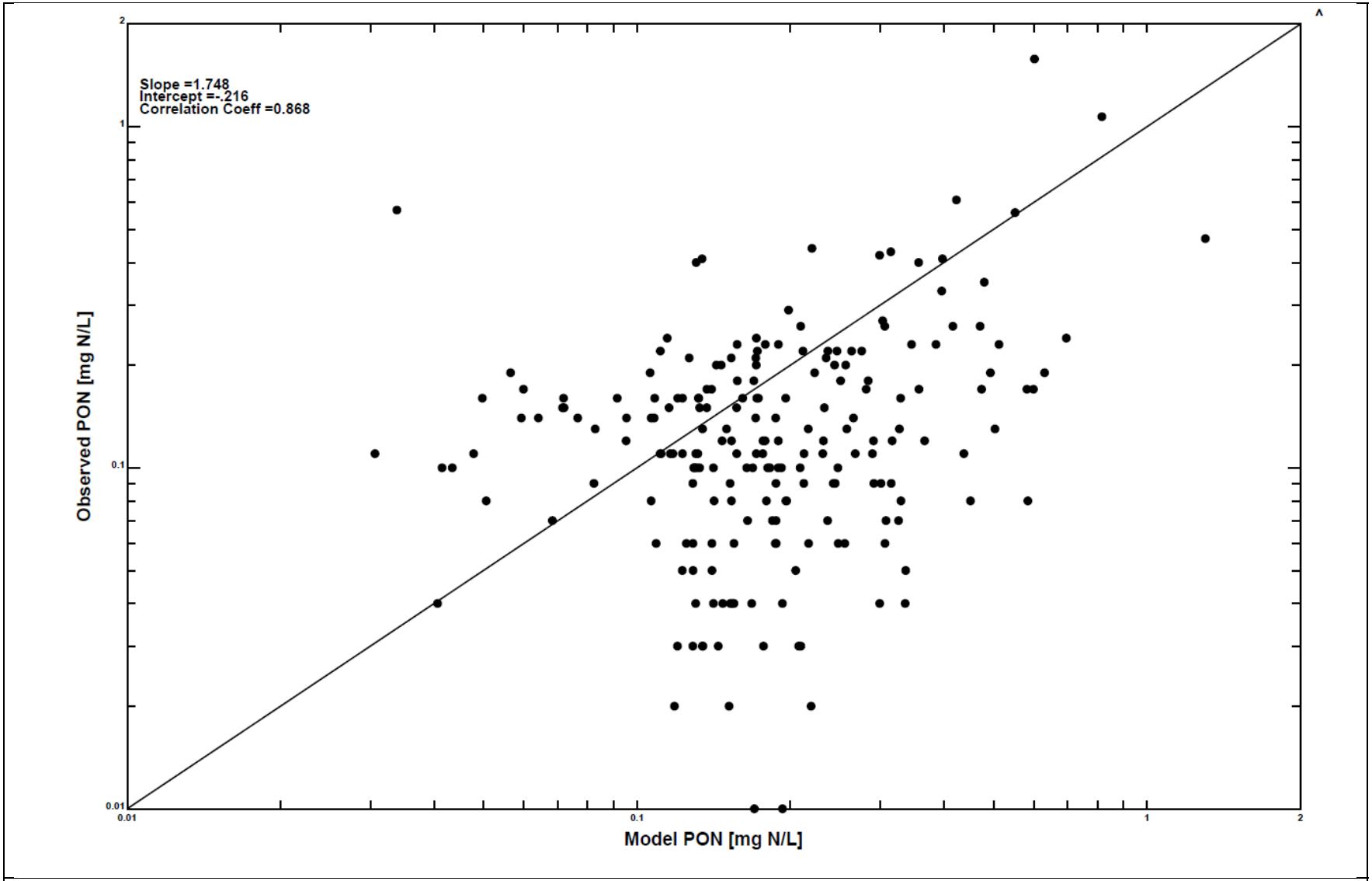

Figure 36. Cross-correlation of observed outflow PON versus CPMBM PON.

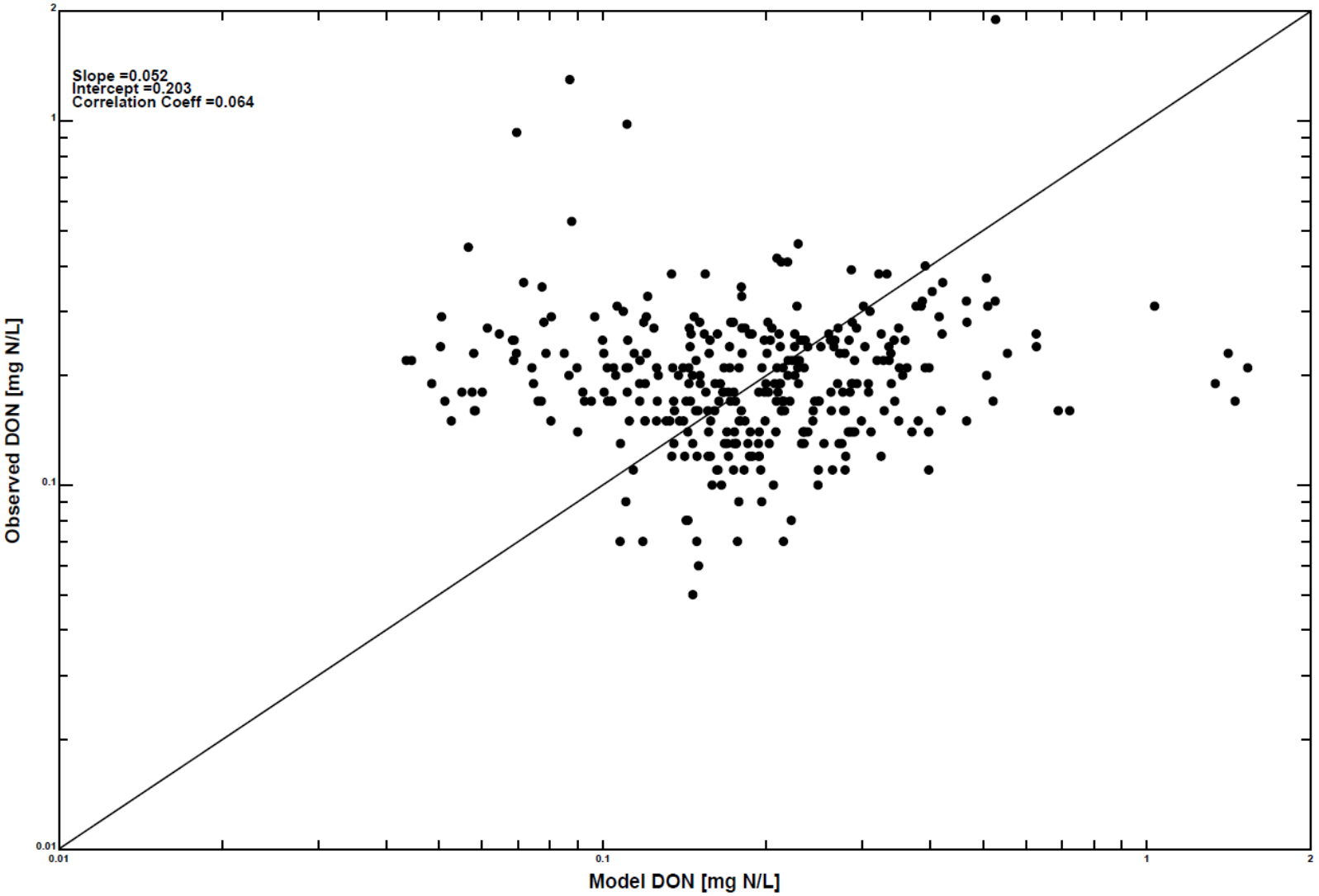

Figure 37. Cross-correlation of observed outflow DON versus CPMBM DON.

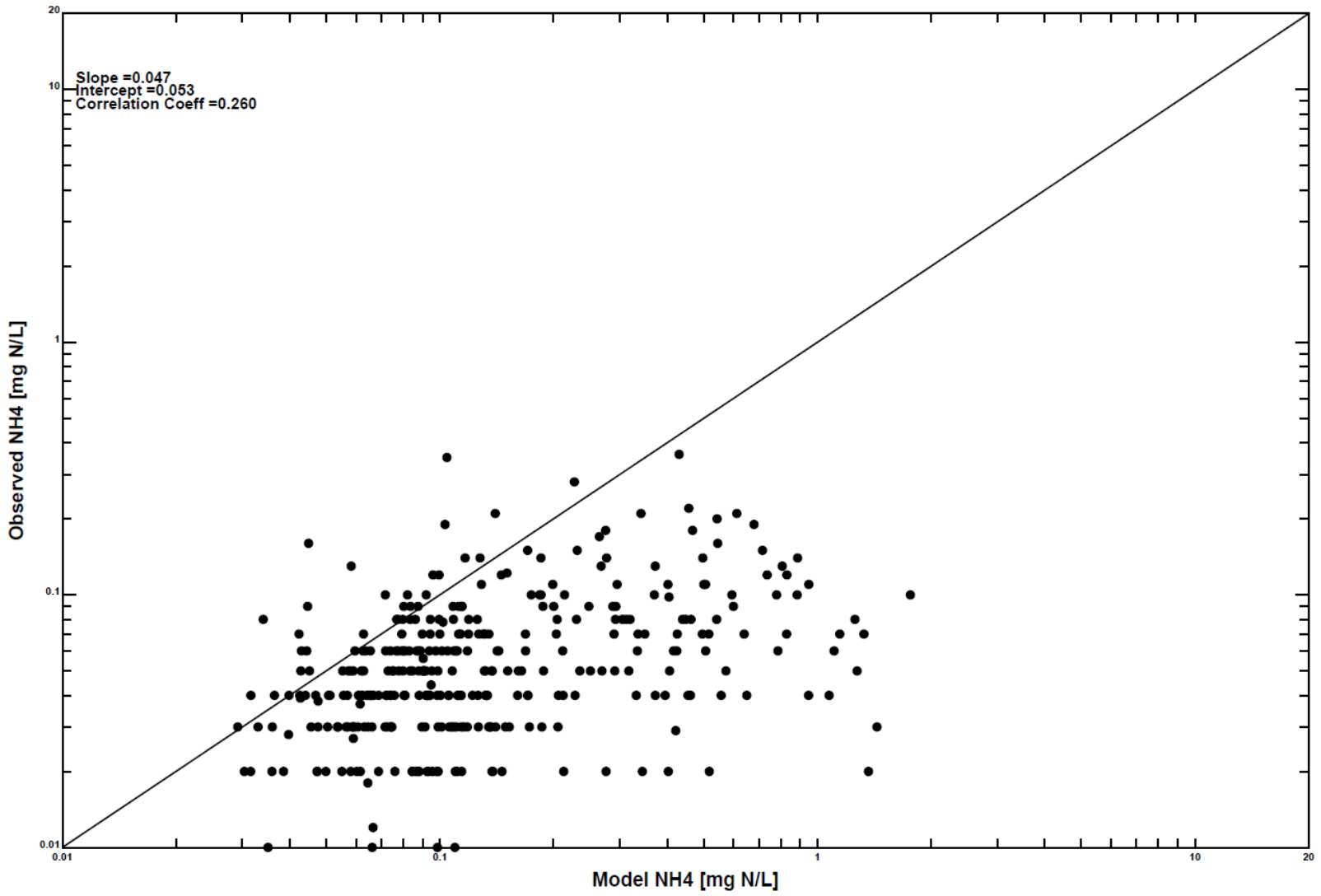

Figure 38. Cross-correlation of observed outflow NH_4 versus CPMBM NH_4.

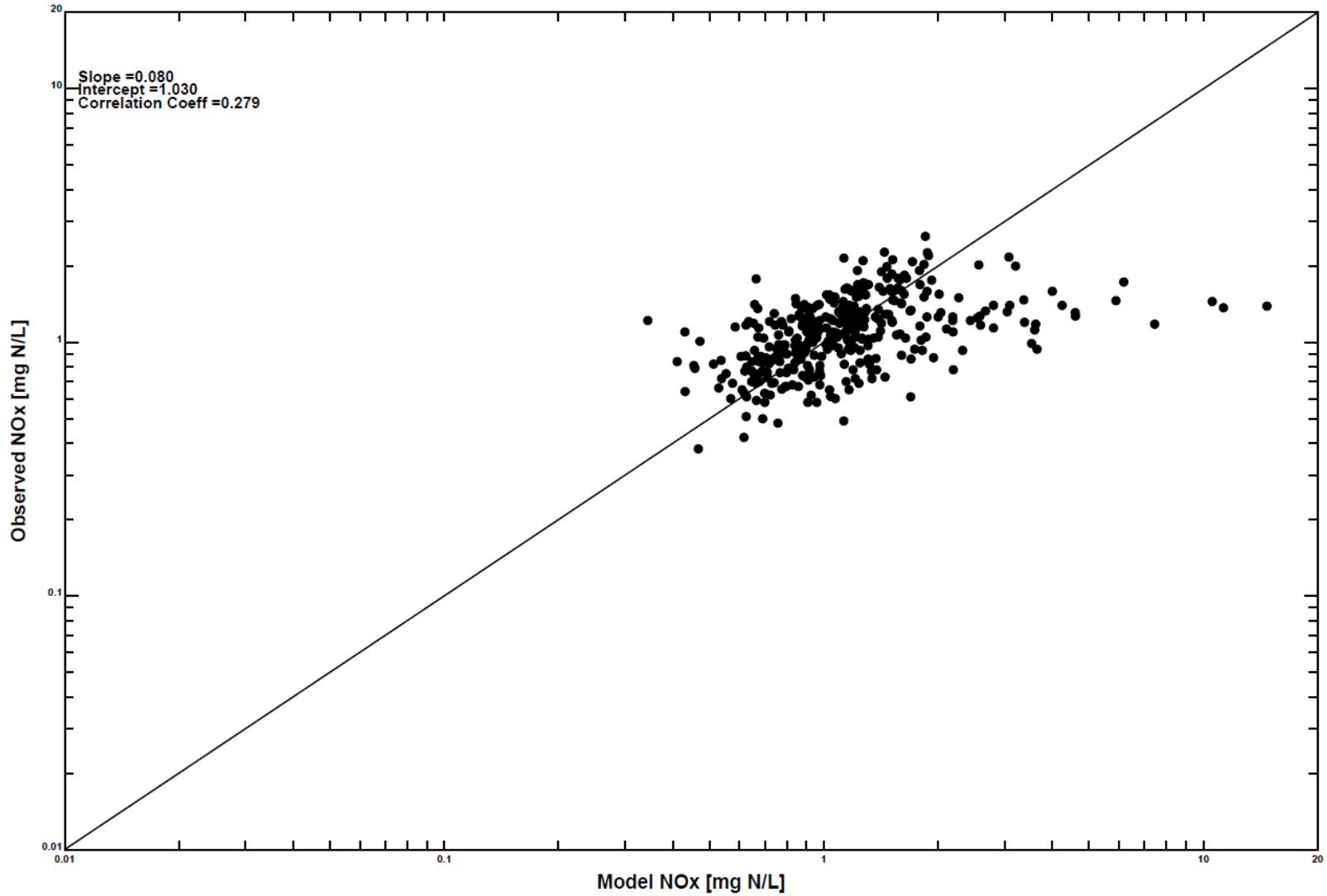

Figure 39. Cross-correlation of observed outflow NO_x versus CPMBM NO_x.

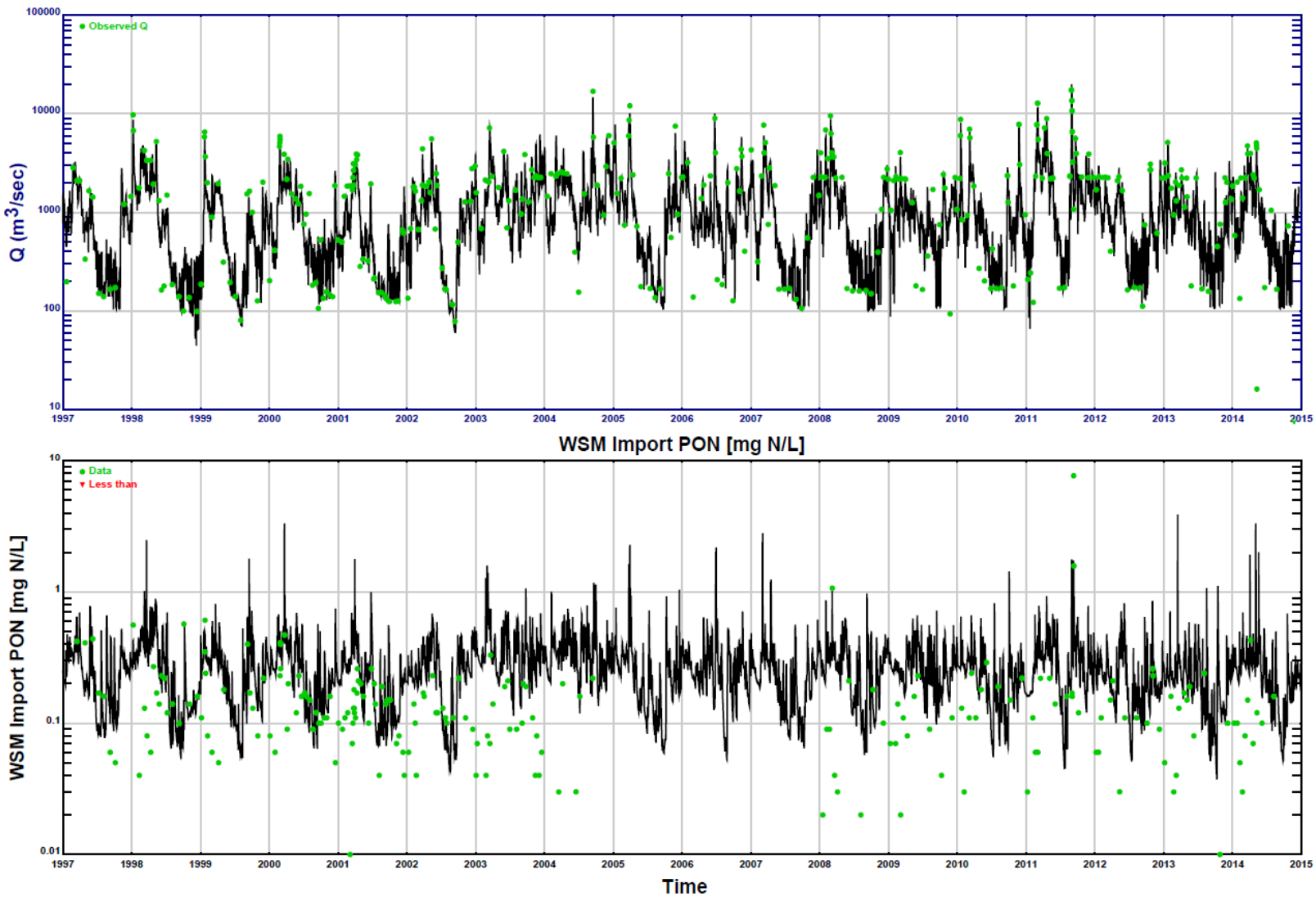

Figure 40. Observed outflow PON versus WSM PON.

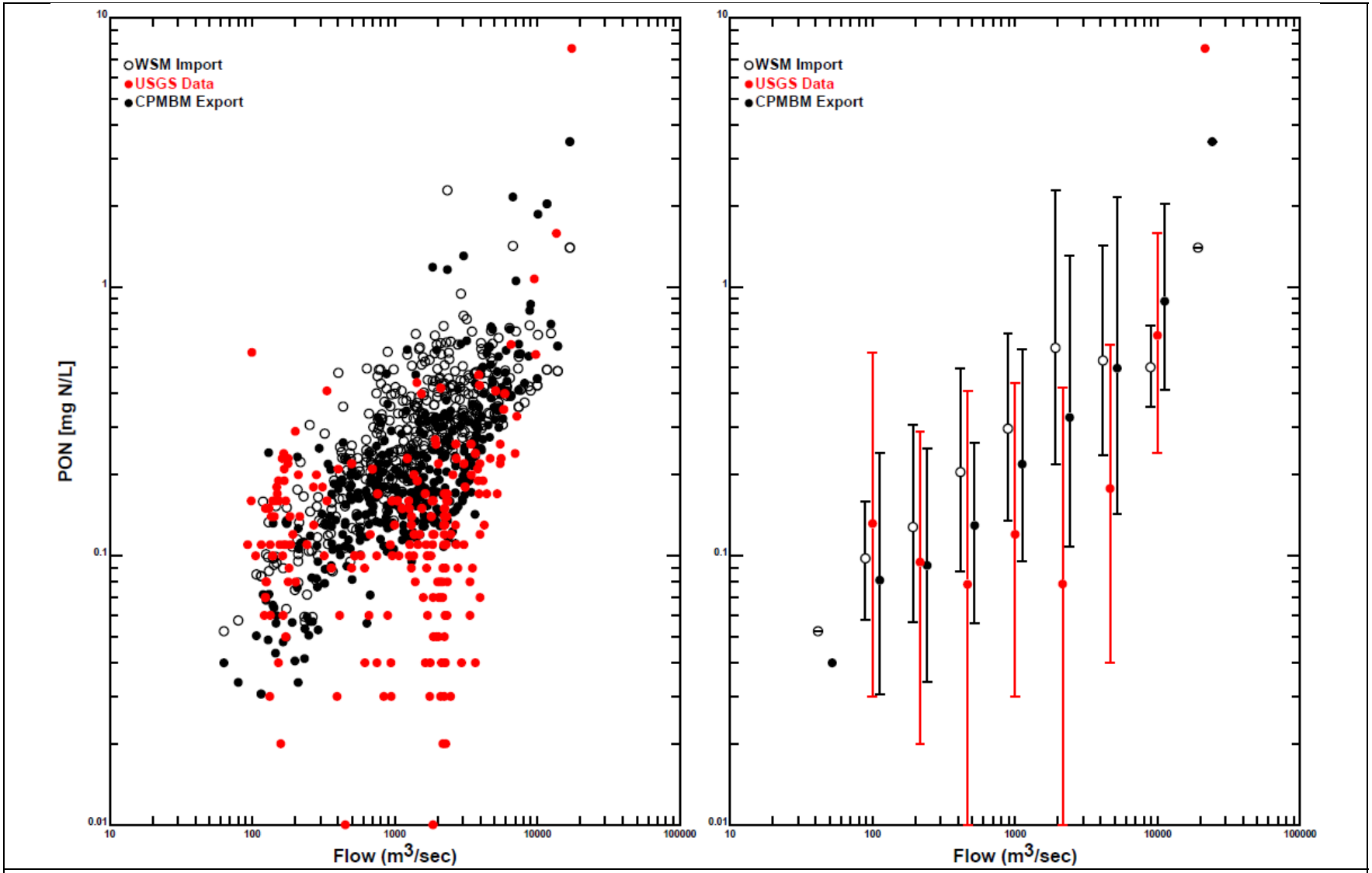

Figure 41. WSM PON, observed PON and CPMBM PON versus flow.

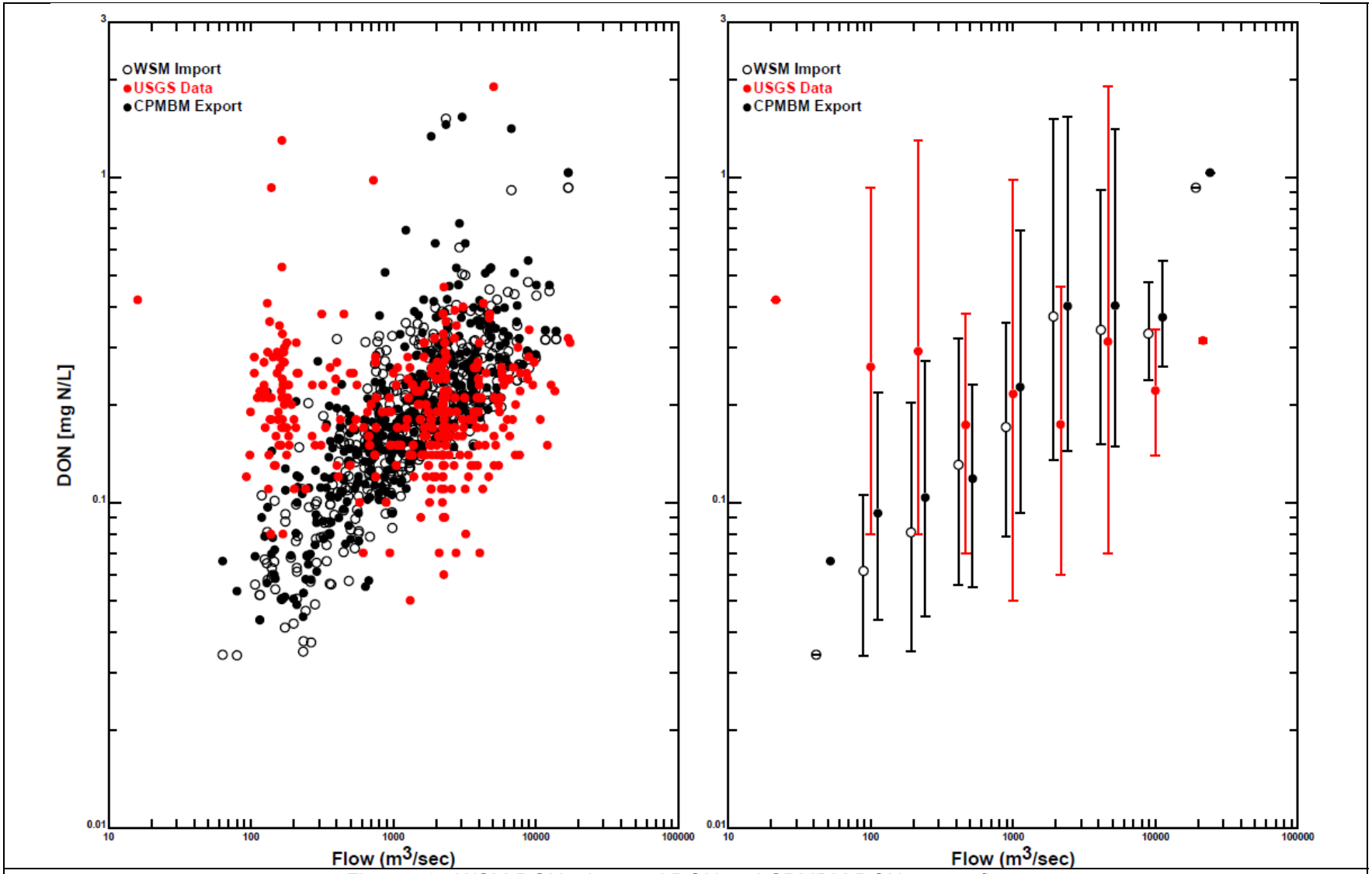

Figure 42. WSM DON, observed DON and CPMBM DON versus flow.

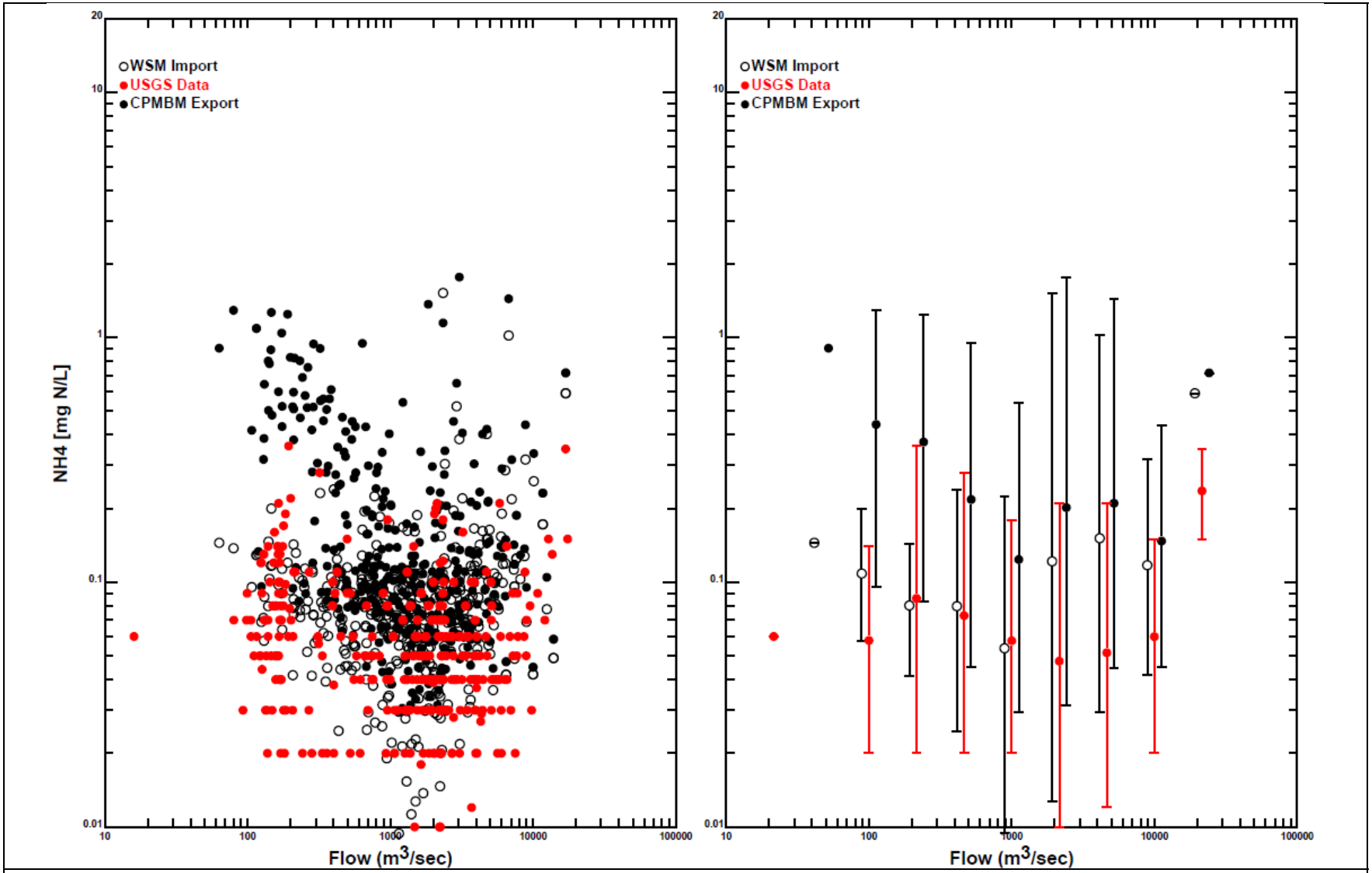

Figure 43. WSM NH_4, observed NH_4 and CPMBM NH_4 versus flow.

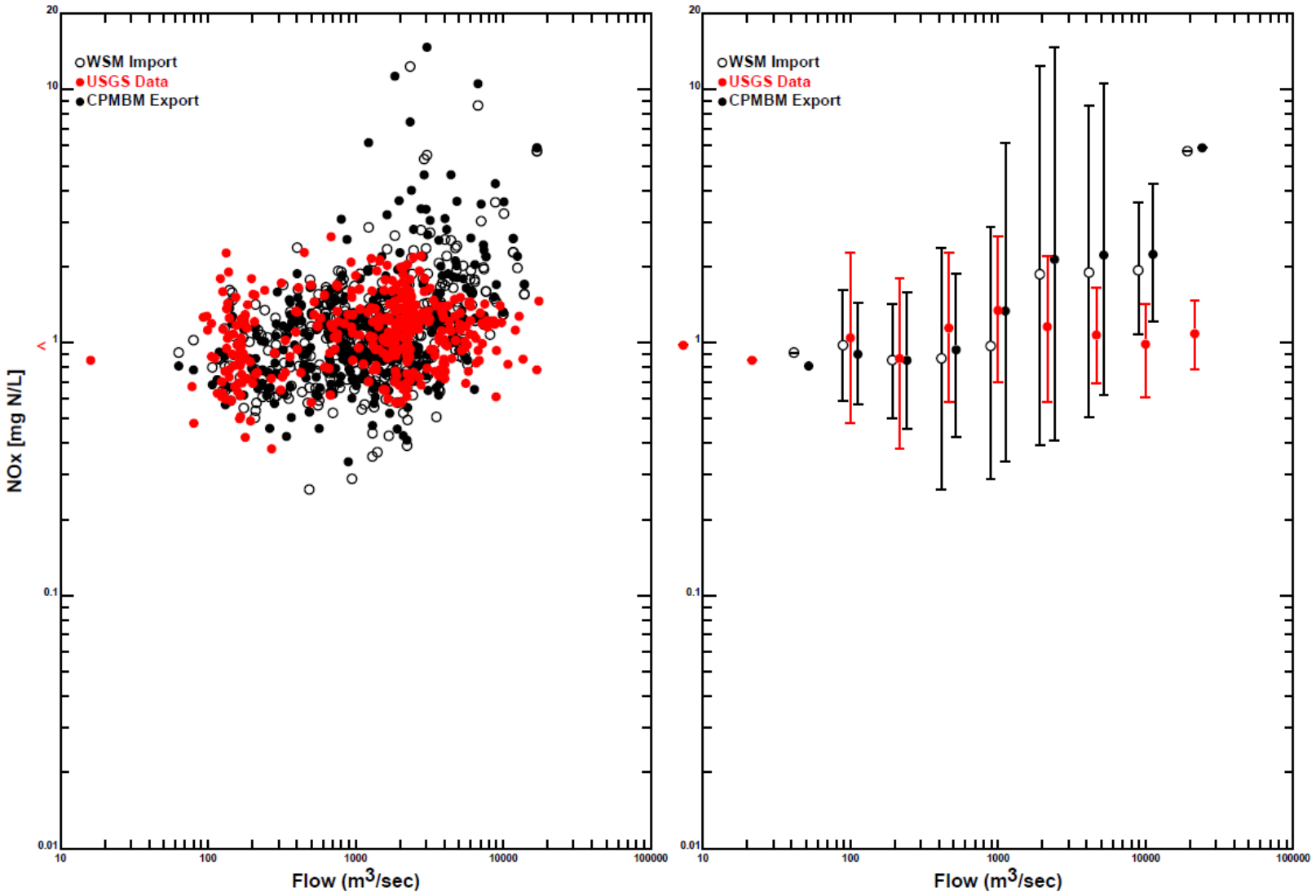

Figure 44. WSM NO_x, observed NO_x and CPMBM NOx versus flow.

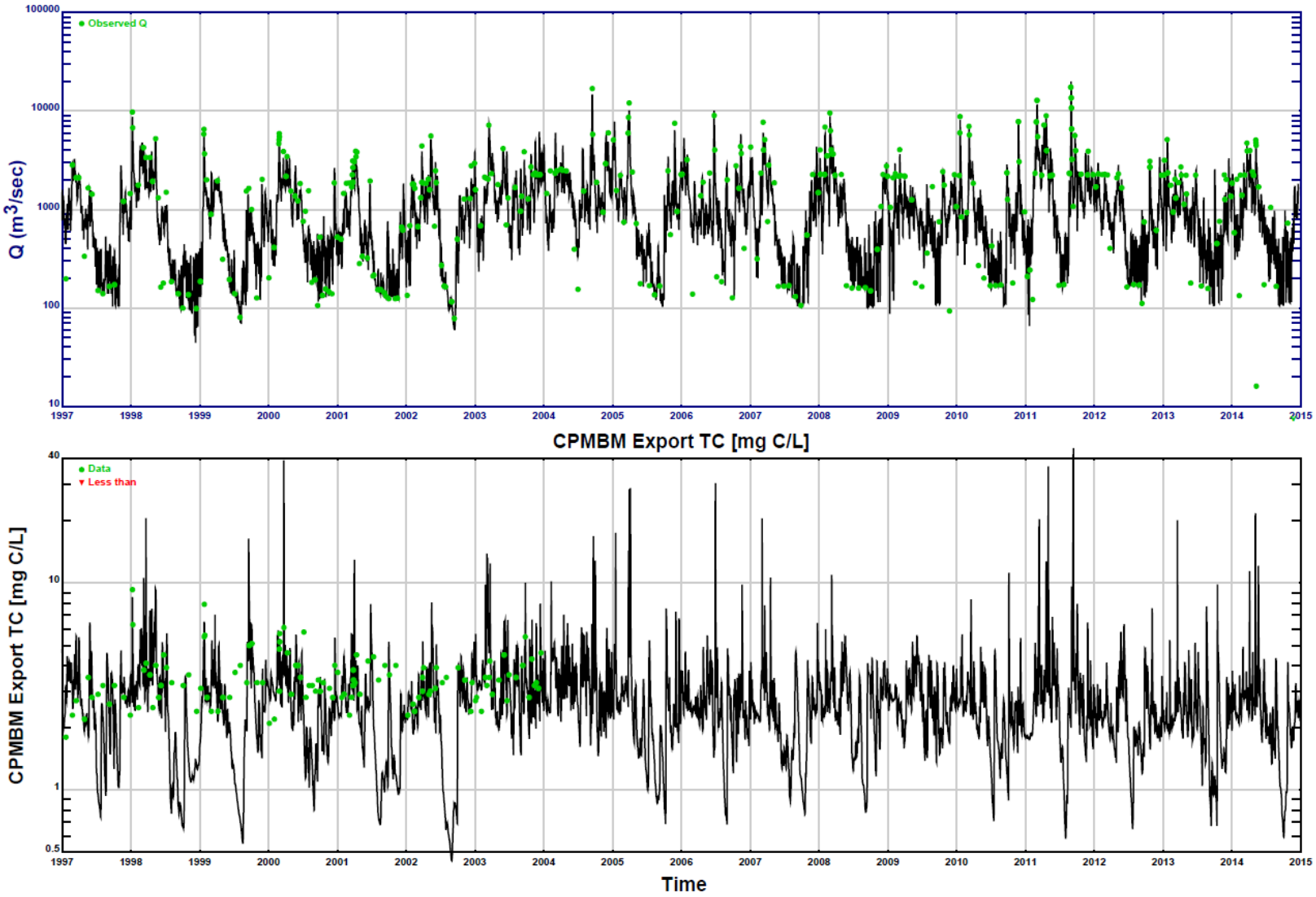

Figure 45. Calibration results for total carbon (TC).

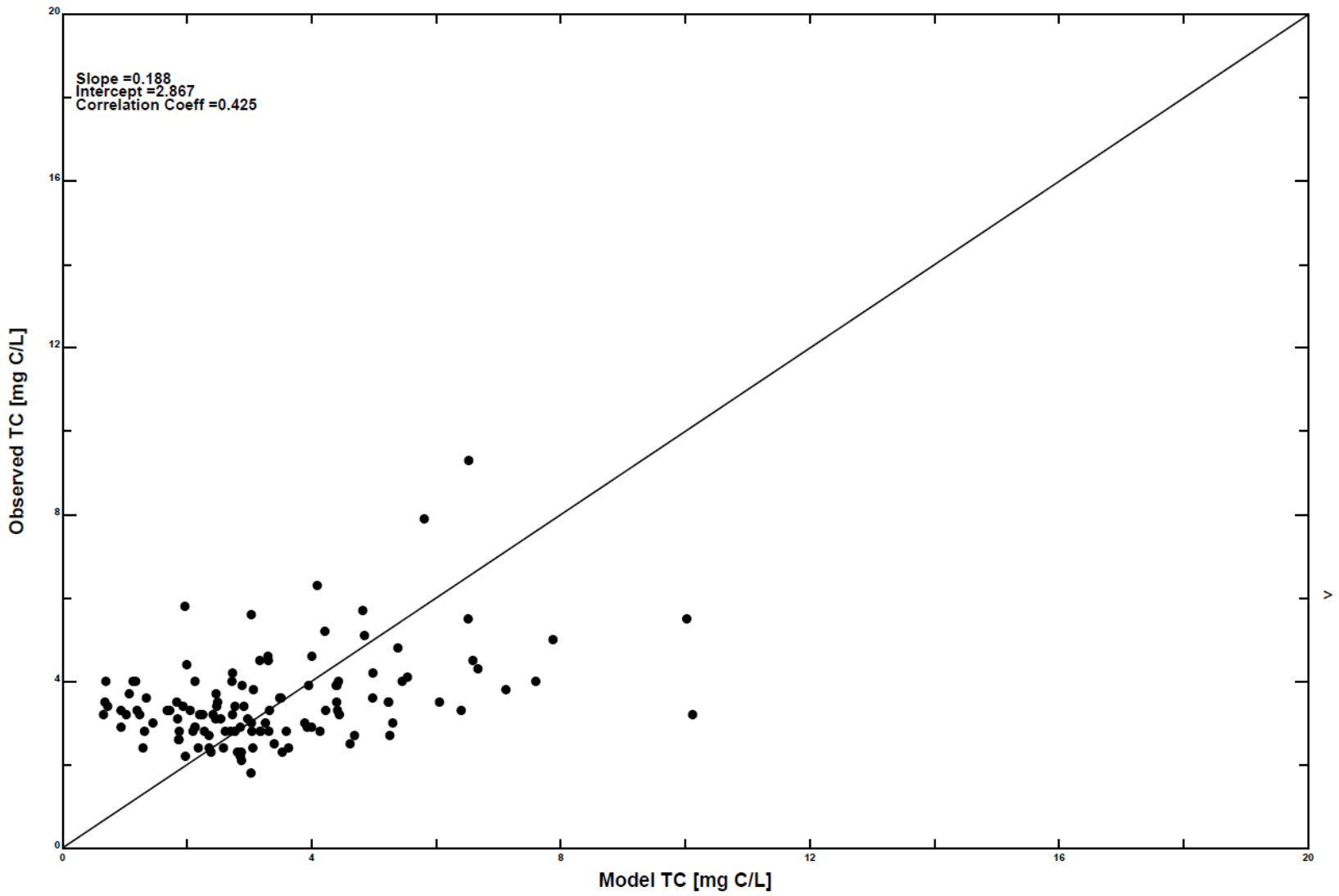

Figure 46. Cross-correlation of observed outflow TC versus CPMBM TC.

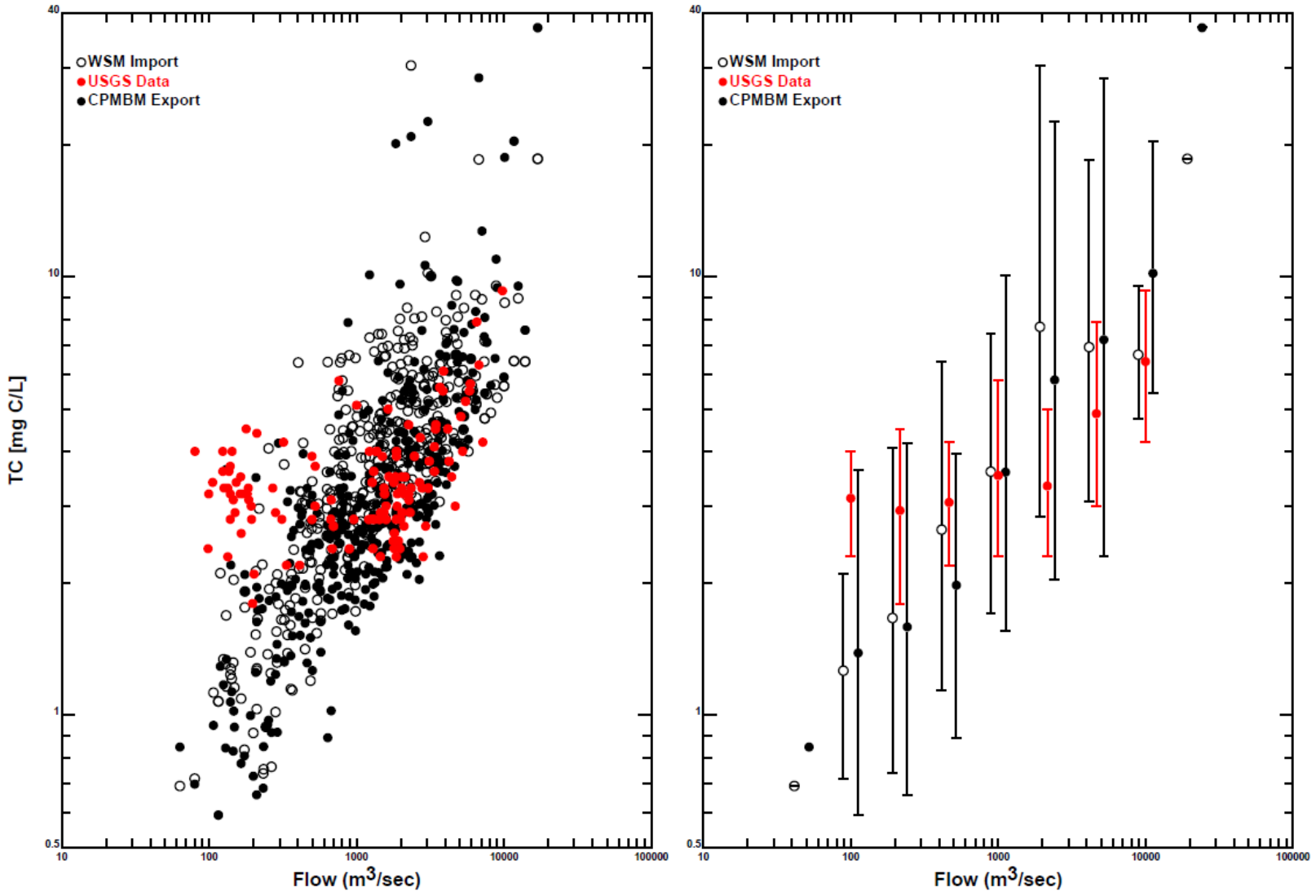

Figure 47. WSM TC, observed TC and CPMBM TC versus flow.

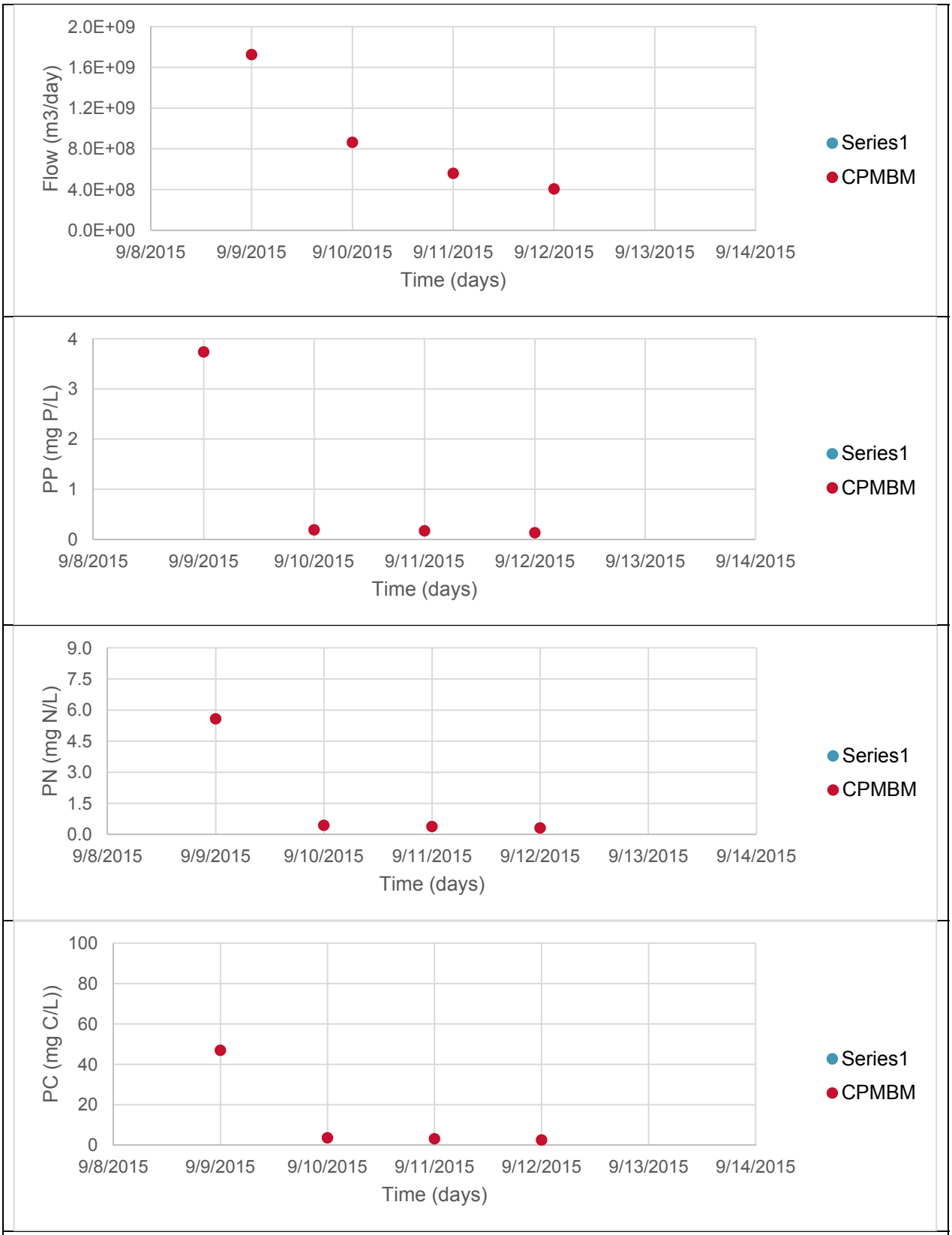

Figure 48. Comparison of USGS data and the CPMBM for flow, nitrogen, Phosphorus and carbon for Tropical Storm Lee.

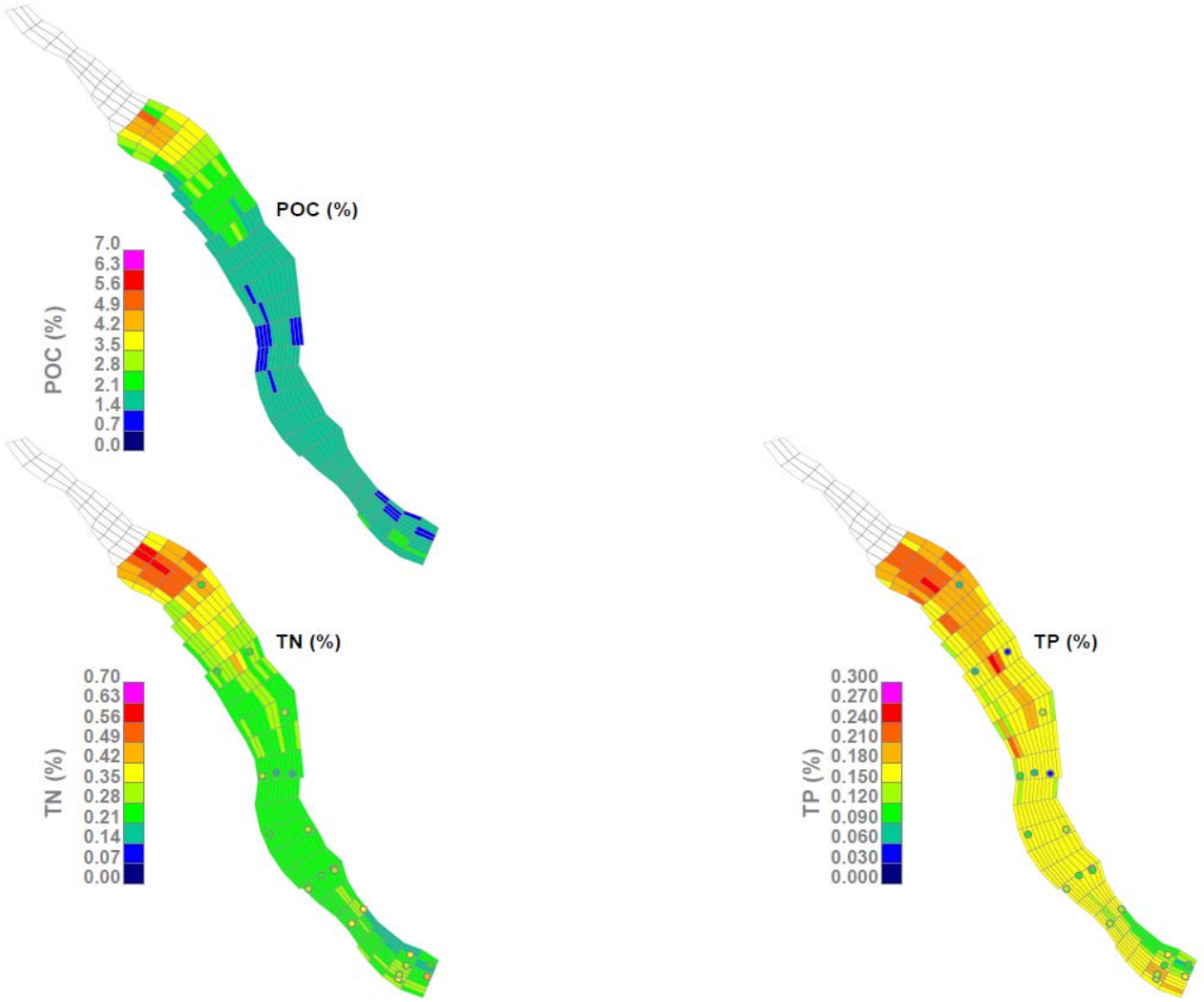

Figure 49. Calibration of surface sediment composition versus SRBC 2000 data set.

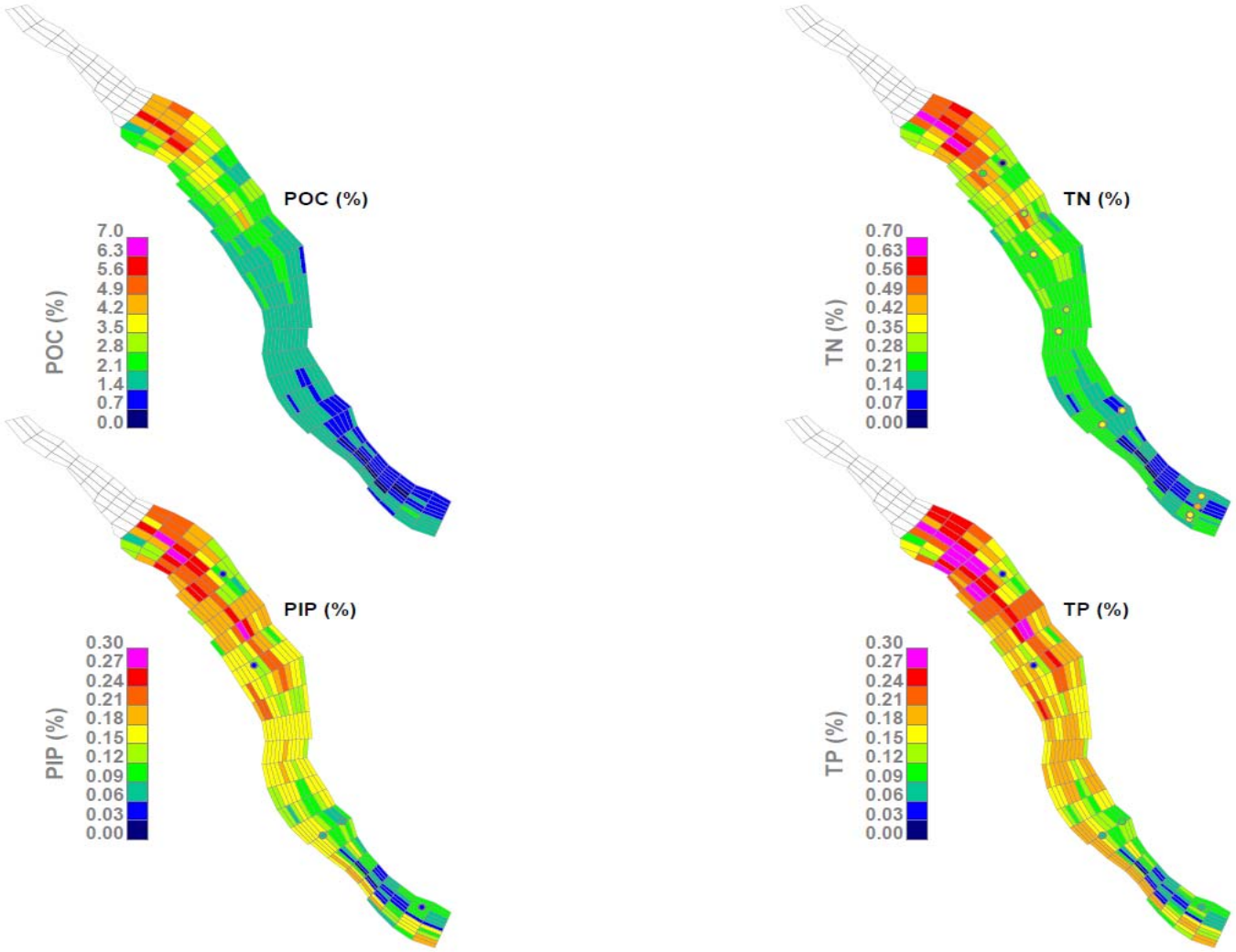

Figure 50. Calibration of surface sediment composition versus UMCES 2015 data set.

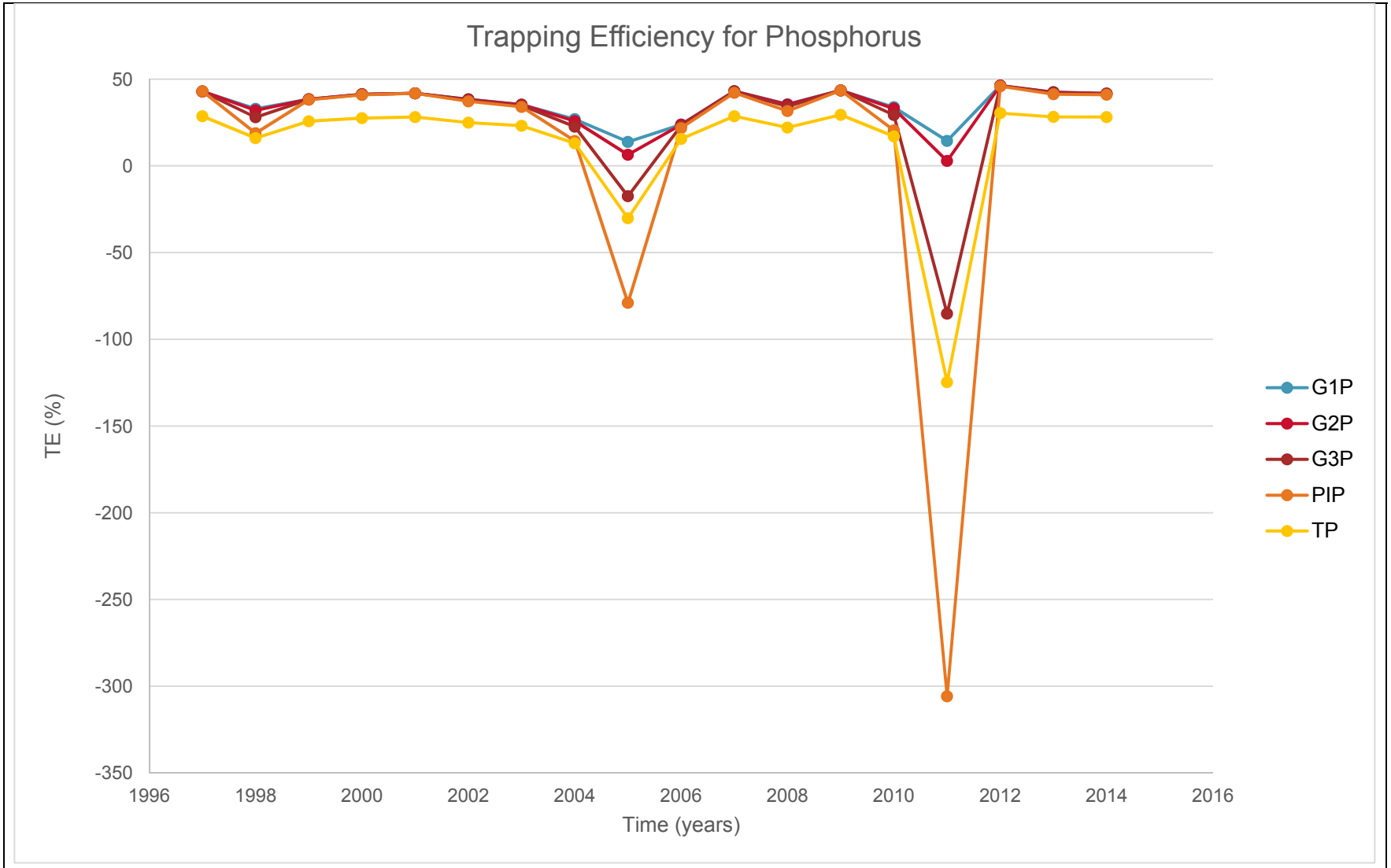

Figure 51. Trapping Efficiency for Phosphorus

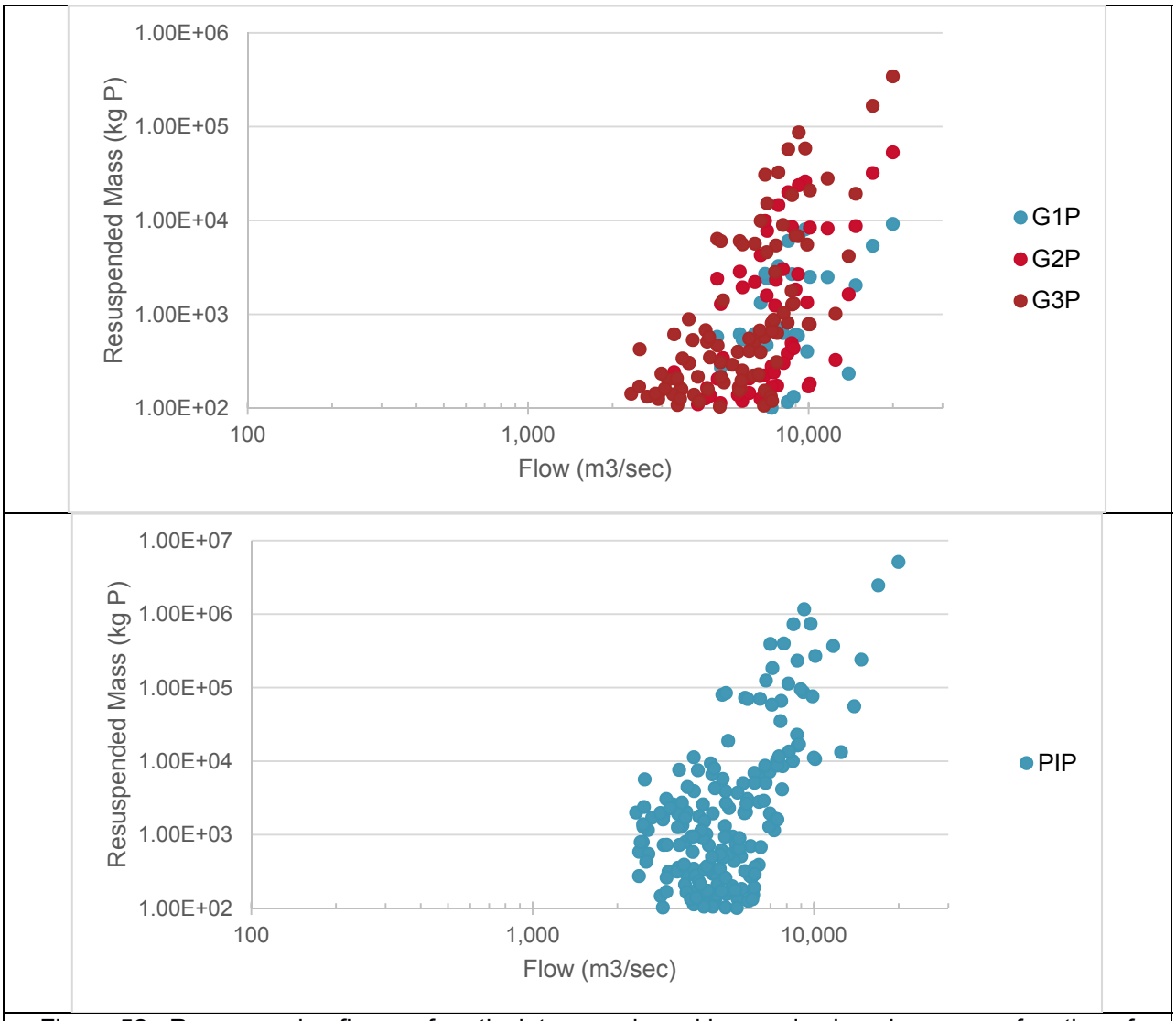

Figure 52. Resuspension fluxes of particulate organic and inorganic phosphorus as a function of flow.

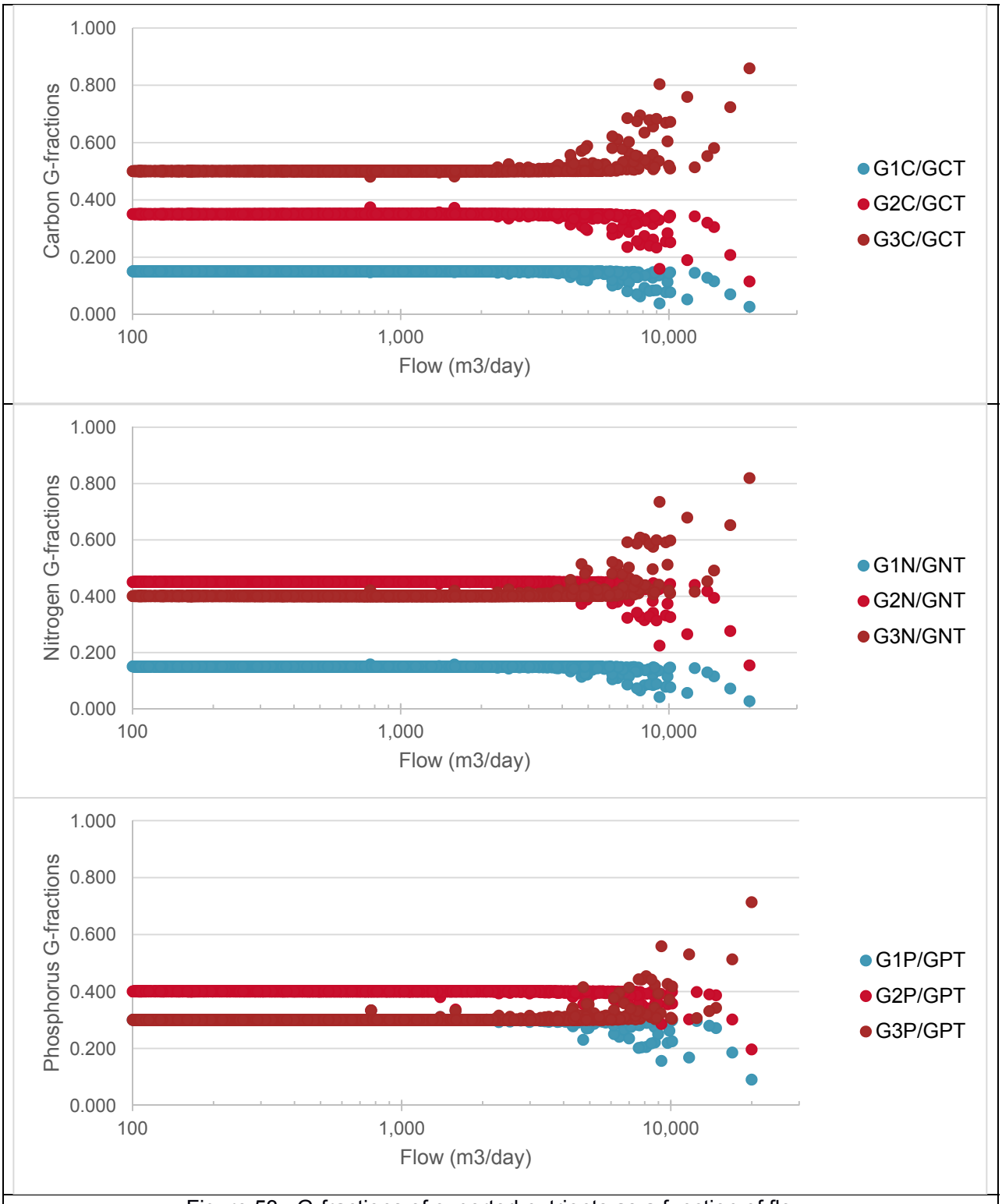

Figure 53. G-fractions of exported nutrients as a function of flow.

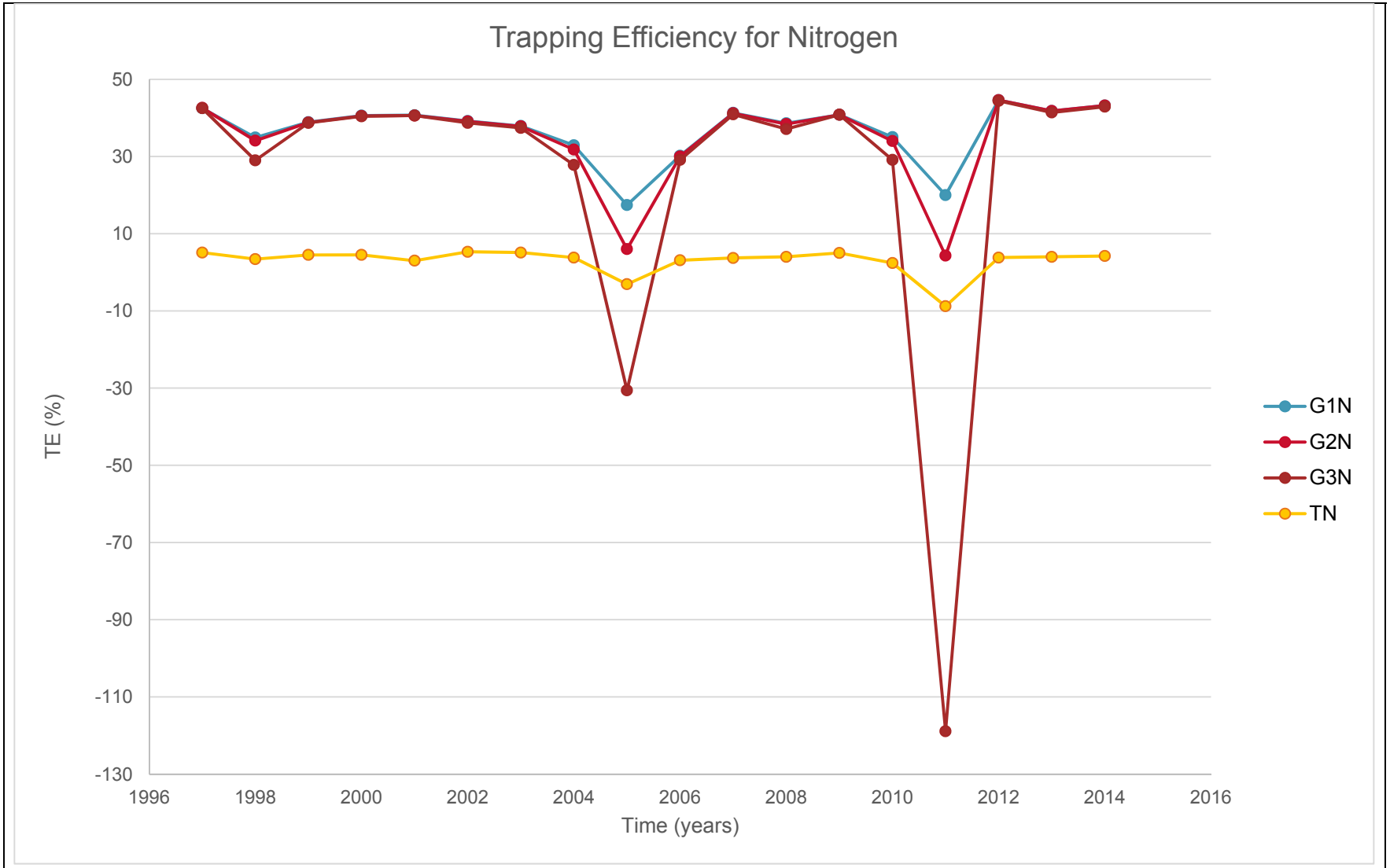

Figure 54. Trapping Efficiency for Nitrogen

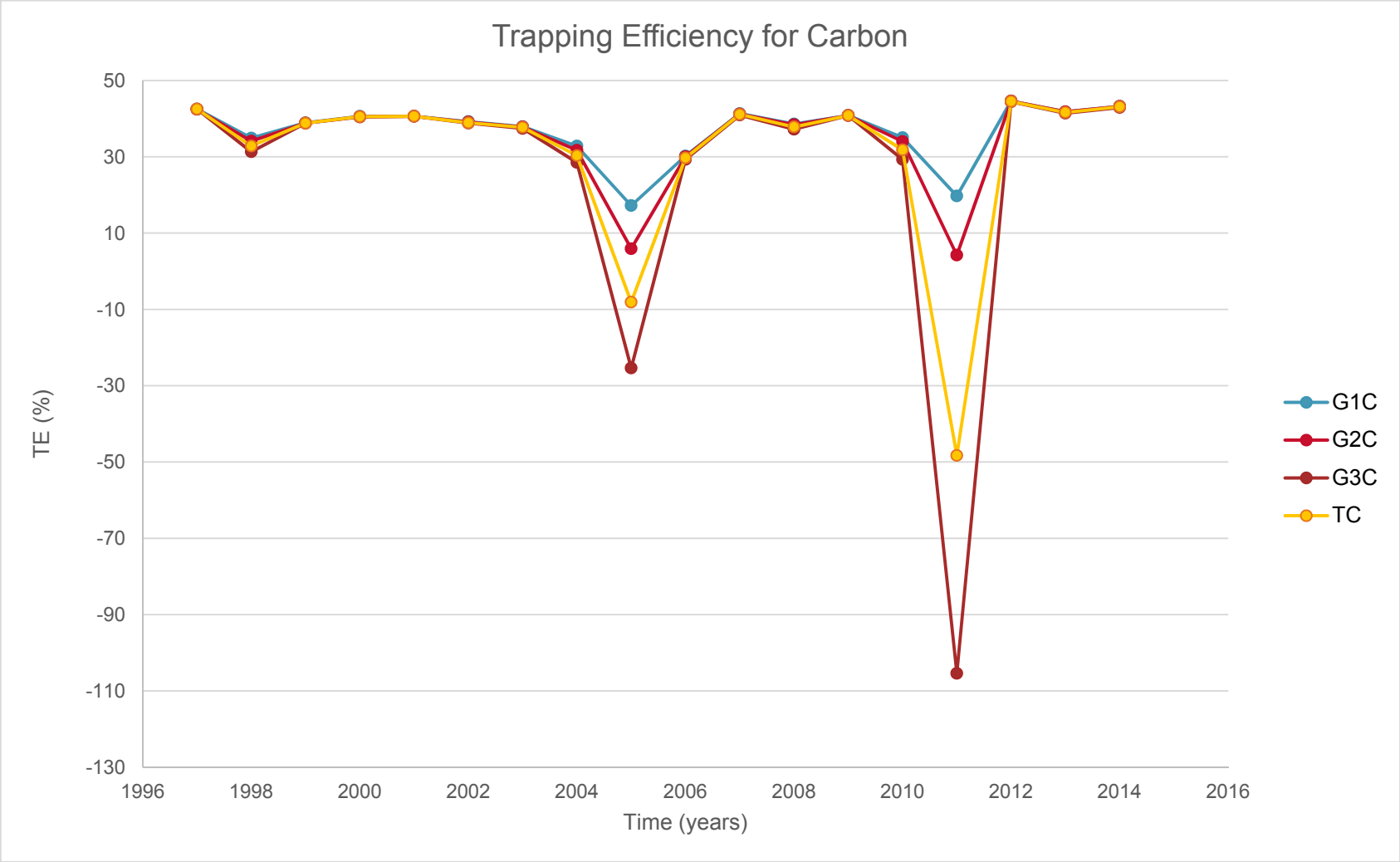

Figure 55. Trapping Efficiency for Carbon

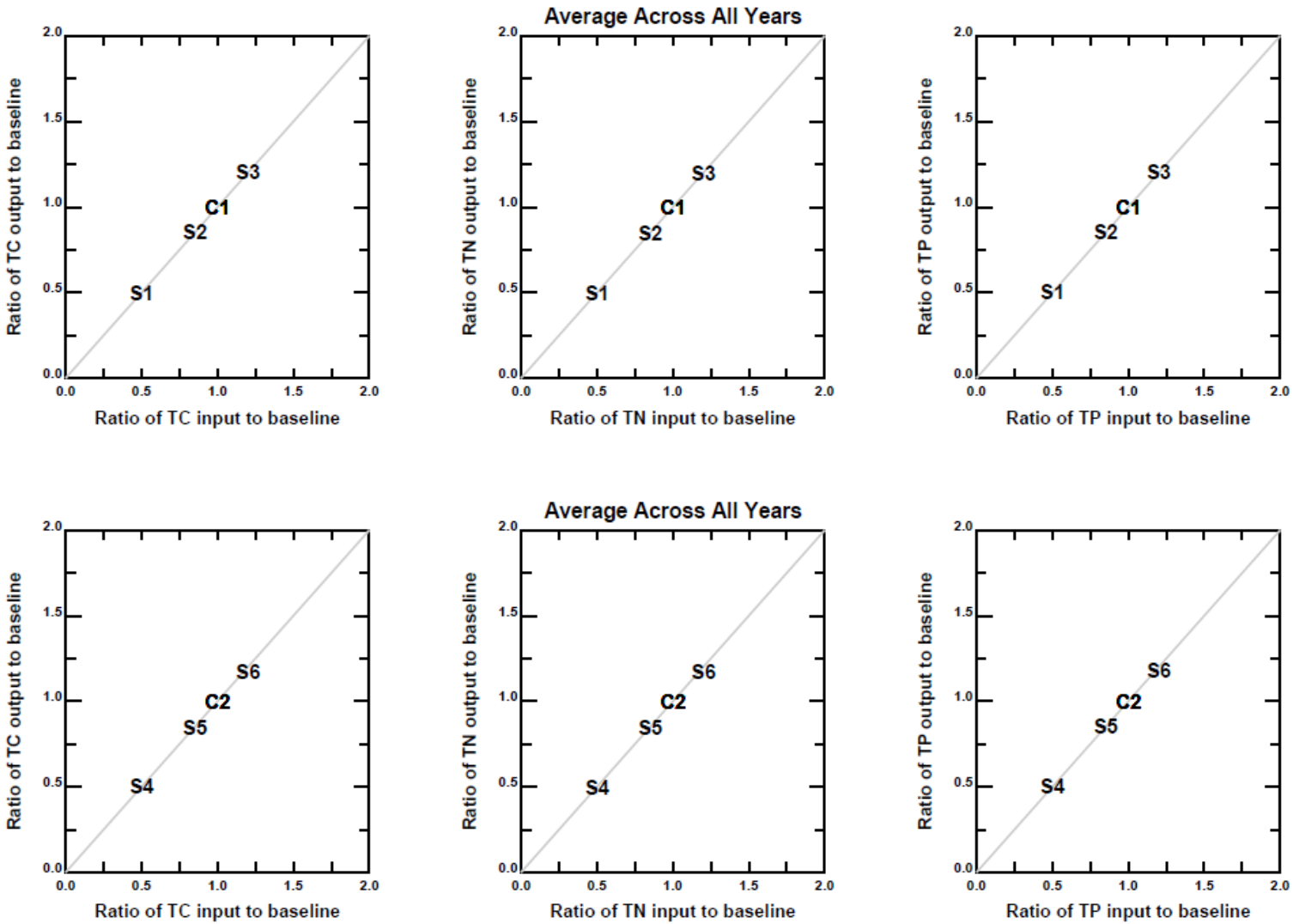

Figure 56. Linear response to nutrient management scenarios.

Appendix